

**Above and belowground biomass and net primary productivity in two
subtropical mangrove forests in Japan**

A. T. M. ZINNATUL BASSAR

2023

**Division of Forest and Biomaterials Science, Graduate School of Agriculture,
Kyoto University**

Contents

Chapter 1

General Introduction

1.1 Importance of mangrove and its production	1
---	---

Chapter 2

Site description

2.1 Study site and climate	6
2.2 Stand structure measurement	7
2.4 Soil properties analysis.....	9

Chapter 3

Development of allometric equations of *R. stylosa* and *B. gymnorhiza* in the Manko Wetland of Okinawa Island in Japan.

3.1 Introduction	18
3.2 Materials and methods	18
3.3 Results	20
3.4 Discussion	21

Chapter 4

Seasonal pattern of aboveground litterfall of three Rhizophoraceae family species in two subtropical regions in Japan

4.1 Introduction	33
4.2 Material and method.....	33
Fig. 4.1.....	33
4.3 Statistical analysis	34
4.4 Results	34
4.5 Discussion	36

Chapter 5

Fine root dynamics of three *Rhizophoraceae* family species in two subtropical regions in Japan.

5.1 Introduction	43
5.2 Material and Method	44
5.3 Statistical analysis	47
5.4 Results	47

5.5 Discussions.....	51
Chapter 6	
Measuring biomass and net primary production of two subtropical mangrove forests in Japan	
6.1 Introduction	60
6.2 Material and Method	61
6.4 Results	62
6.5 Discussion	64
Chapter 7	
7. Conclusion and recommendation	81
References	84
Appendix.....	94

Figures

Fig. 1.1: Modified framework calculations of net primary production (<i>NPP</i>) from Clark et al. (2001) and Kloeppel et al. (2007) showing how aboveground <i>NPP</i> (<i>NPP</i> _{AG}) and belowground <i>NPP</i> (<i>NPP</i> _{BG}) are estimated.	2
Fig. 2.1: Map showing the location of the study areas along the Miyara River mangrove with the sampled mangrove stands.....	6
Fig. 2.2: Map showing the location of the study area in the Mamko Wetland mangrove with the sampled mangrove stands.....	6
Fig. 2.3: Average monthly temperature ($^{\circ}$ C), rainfall (mm), and wind speed (m s^{-1}) of Miyara river area and Manko wetland area during the study period.....	6
Fig. 2.4: Histogram showing the number of trees of the diameter classes of a) downstream <i>R. stylosa</i> , b) downstream <i>B. gymnorhiza</i> , and c) upstream <i>B. gymnorhiza</i> in the Miyara River mangrove.....	7
Fig. 2.5: Histogram showing the number of trees of the diameter classes of a) <i>K. obovata</i> , b) <i>R. stylosa</i> , and c) <i>B. gymnorhiza</i> in the Manko Wetland mangrove.....	8
Fig. 2.6: Stem height <i>H</i> - diameter <i>D</i> relationship of <i>R. stylosa</i> and <i>B. gymnorhiza</i> along the river.....	9
Fig. 3.1: Procedure of sample collection to data compilation for allometric equation development.	24
Fig. 3.2: Best fit allometric models for leaf biomass, stem biomass, branch biomass, total aboveground biomass, belowground biomass and total biomass of <i>R. stylosa</i> and <i>B. gymnorhiza</i>	25
Fig 3.3: Comparison of the <i>AGB</i> (kg) and <i>D</i> (cm), and <i>BGB</i> (kg) and <i>D</i> (cm) relationships of <i>R. stylosa</i> of the present allometric model with the other developed models wherever data of the sampled trees were used.....	26
Fig 3.4: Comparison of the <i>AGB</i> (kg) and <i>D</i> (cm), and <i>BGB</i> (kg) and <i>D</i> (cm) relationships of <i>B. gymnorhiza</i> of the present allometric model with the other developed models wherever data of the sampled trees were used.....	27
Fig. 4.1: Litter trap for aboveground litter collection.....	34
Fig. 4.2: Monthly litterfall of a) leaves, b) stipules, c) branches, d) flowers, e) fruits and f) propagules along the Miyara river mangrove.....	36
Fig. 4.3: Monthly litterfall of a) leaves, b) stipules, c) branches, d) flowers, e) fruits and f) propagules in the Manko Wetland.....	37
Fig. 4.4: Monthly total litterfall a) along the Miyara river mangrove and b) in the Manko Wetland mangrove.....	37
Fig. 5.1: Fine roots inside litter bags before and after decomposition.	45
Fig. 5.2 (a-f): Seasonal variation in fine root biomass (g m^{-2}) and necromass (g m^{-2}) of <i>R. stylosa</i> (a—b), downstream <i>B. gymnorhiza</i> (c—d) and upstream <i>B. gymnorhiza</i> (e—f), respectively	

wherever biomass and necromass data were collected on March 16, June 23, September 26 and December 23 in 2022, and March 27 in 2023.....	47
Fig. 5.3 (a-f): Fine root biomass and necromass of <i>K. obovata</i> (a—b), <i>R. stylosa</i> (c—d), and <i>B. gymnorhiza</i> (e—f), respectively in g m ⁻² obtained through the sequential core method wherever data were collected on March 13, May 18, October 10 in 2019 and January 24 and March 26 in 2020.....	48
Fig. 6.1: The contribution of each of the increment of each of the components to the total <i>NPP</i> of the three species at two study sites.....	63

Tables

Table 1.1: Mangrove species found in Japan	1
Table 2.1: Stand structure of upstream and downstream <i>B. gymnorrhiza</i> plots, and downstream <i>R. stylosa</i> plots of Miyara River mangrove and <i>K. obovata</i> , <i>R. stylosa</i> and <i>B. gymnorrhiza</i> plots of Manko Wetland mangrove showing mean diameter at breast height D , mean tree height H , basal area, tree density (ρ).....	8
Table 2.2: The values of coefficients H_{\max} and a in Eq. 2 for the stem diameter D - height H relationships are shown with S.E and R^2 values.....	8
Table 2.3: Soil pore water salinity, soil pH, soil nitrogen, and water level are shown for downstream <i>R. stylosa</i> plots; and upstream and downstream <i>B. gymnorrhiza</i> plots of the Miyara River of Ishigaki, and Manko Wetland of Naha mangrove.	17
Table 3.1: Height (H), diameter (D), total biomass, aboveground biomass, leaf biomass, branch biomass, stem biomass, aboveground root biomass (AGB_{roots}), and belowground root biomass (BGB_{coarse}) of six individual trees of <i>B. gymnorrhiza</i> used for allometric equations development.	28
Table 3.2: Height (H), diameter (D), total biomass, aboveground biomass, leaf biomass, branch biomass, stem biomass, aboveground root biomass (AGB_{roots}), and belowground root biomass (BGB_{coarse}) of six individual trees of <i>R. stylosa</i> used for allometric equations development...	28
Table 3.3: Selection of the best fit allometric models for leaf, branch, stem, BGB_{coarse} , AGB and total biomass of <i>B. gymnorrhiza</i> using R^2 , slope error, intercept error, RSS and AIC	21
Table 3.4: Selection of the best fit allometric models for leaf, branch, stem, BGB_{coarse} , AGB and total biomass of <i>R. stylosa</i> using R^2 , slope error, intercept error, RSS , and AIC	30
Table 3.5: Biomass of leaves, stem, branch, AGB_{roots} and BGB_{coarse} of upstream and downstream <i>B. gymnorrhiza</i> stands, and downstream <i>R. stylosa</i> stand in the Miyara River mangrove obtained during March of 2022 and 2023.	31
Table 3.6: Biomass of leaves, stem, branch, AGB_{roots} and BGB_{coarse} of <i>K. obovata</i> , <i>R. stylosa</i> and <i>B. gymnorrhiza</i> plots in Manko Wetland, Okinawa, Japan. The biomass values for <i>K. obovata</i> and <i>R. stylosa</i> were obtained in every March of 2019 to 2022 and biomass values of <i>B. gymnorrhiza</i> were obtained in every March of 2021 to 2022.	31
Table 3.7: Latitude ($^{\circ}$), D (cm) range of present allometric models and some developed models from other areas.....	24
Table 4.1: Contribution (%) of litterfall components to the total litterfall.....	38
Table 5.1: Production P and mortality m of very fine and fine roots of two species in the Miyara River mangrove and three species in the Manko Wetland mangrove during different seasons in which fine root samples were collected through sequential core method.....	49
Table 5.2: Root diameter-based residual ratio per day (r) of <i>R. stylosa</i> , upstream and downstream <i>B. gymnorrhiza</i> , respectively in the Miyara River mangrove, and of <i>K. obovata</i> , <i>R. stylosa</i> , and <i>B. gymnorrhiza</i> , respectively in the Manko Wetland mangrove conducted based on the decomposition equation of Fujimoto et al. (2021).	59
Table 6.1: Aboveground biomass AGB , belowground coarse root biomass BGB_{coarse} and fine root mass of upstream and downstream <i>B. gymnorrhiza</i> plots, and downstream <i>R. stylosa</i> plots	

of Miyara River mangrove and <i>K. obovata</i> , <i>R. stylosa</i> and <i>B. gymnorrhiza</i> plots of Manko Wetland mangrove.....	61
Table 6.2: Increment of leaves, stems, branch, AGB_{root} and AGB ($Mg\ ha^{-1}\ y^{-1}$) of upstream and downstream <i>B. gymnorrhiza</i> plots, downstream <i>R. stylosa</i> plots in the Miyara River mangrove, and <i>K. obovata</i> , <i>R. stylosa</i> and <i>B. gymnorrhiza</i> plots in the Manko Wetland of Japan..	62
Table 6.3: Increment of AGB , total litterfall, tree dead mass increment, and NPP_{AG} ($Mg\ ha^{-1}\ y^{-1}$) of upstream and downstream <i>B. gymnorrhiza</i> stands, downstream <i>R. stylosa</i> stand along the Miyara River, and <i>K. obovata</i> , <i>R. stylosa</i> and <i>B. gymnorrhiza</i> plots in the Manko Wetland of Japan.....	62
Table 6.4: $\Delta BGB_{coarse-living}$, $\Delta BGB_{coarse-dead}$, fine root production, NPP_{BG} ($Mg\ ha^{-1}\ y^{-1}$) of upstream and downstream <i>B. gymnorrhiza</i> plots, downstream <i>R. stylosa</i> plots in Miyara river mangrove, and <i>K. obovata</i> , <i>R. stylosa</i> and <i>B. gymnorrhiza</i> plots in Manko Wetland of Japan... ..	63
Table 6.5: Aboveground biomass increment (AGB), belowground biomass (BGB_{coarse}) increment, fine root production, total litterfall, tree dead mass increment, and net primary production (NPP) of upstream and downstream <i>B. gymnorrhiza</i> plots, downstream <i>R. stylosa</i> plots in Miyara river mangrove, and <i>K. obovata</i> , <i>R. stylosa</i> and <i>B. gymnorrhiza</i> plots in Manko Wetland of Japan.	63
Table 6.6: Locations, forest types, dominant species, latitude, aboveground biomass AGB , tree density ρ (ha^{-1}), basal area ($m^2\ ha^{-1}$) and mean H (m) at different mangroves.	64
Table 6.7: The changed total basal area ($m^2\ ha^{-1}$) of upstream and downstream <i>B. gymnorrhiza</i> and downstream <i>R. stylosa</i> stands along with the changed contribution (%) of trees of $D \leq 5$ cm and $D > 5$ cm avoiding the trees at the 7 m from the center.....	65
Table 6.8: Locations, dominant species, latitude, total belowground biomass BGB_{total} including coarse and fine roots mass, fine roots mass percentage in BGB_{total} , and root shoot ratio RSR are shown for different mangroves.	66
Table 6.9: Comparison of BGB_{coarse} ($Mg\ ha^{-1}$) of the present study with other studies	66

Chapter 1

General Introduction

1.1 Importance of mangrove and its production

Mangrove, the most productive ecosystems in the tropical and subtropical regions, along with other coastal ecosystems (tidal salt marsh and seagrass) sequester huge amounts of carbon in the aboveground and belowground part known as “blue carbon” (McLeod et al. 2011). The carbon stock in mangroves (965 Mg ha^{-1}) (UNEP 2014) is relatively higher than in other coastal ecosystems. The relevant blue carbon pool in the mangrove environment includes the living aboveground and belowground biomass (roots and rhizomes); as well as dead aboveground (litter, downed wood, dead trees) and belowground mass (Lovelock et al. 2017). Mangrove tree species are well-adapted to living in saline and brackish environments, which is one of the reasons that they are unique (Kauffman et al. 2016). Mangroves in Japan grow from Kagoshima to Okinawa and they are the most northerly across the Indo-West Pacific biogeographical region. The northern limit of mangroves is located in Kiire, a town in Kagoshima ($31^{\circ}20' \text{ N}$), where a *Kandelia obovata* community is designated as a natural monument. The total mangrove area in Japan is only 553 ha and the mangroves on Iriomote Island account for 80% of the total (Minagawa 2000).

Kandelia obovata, *Bruguiera gymnorrhiza* and *Rhizophora stylosa* are three very common mangrove species of Rhizophoraceae family found in Japan and these are locally called Mehirugi, Ohirugi and Yaeyamahirugi, respectively (Minagawa 2000)

Some common characteristics of these three species are shown in Table 1.1.

Table 1.1

Mangroves have complex root systems that extend above and below the water line which possess a number of adaptations to facilitate survival in these unique environments. Mangrove soil contains limited amount of oxygen which necessitates the mangrove root system to take up oxygen from the atmosphere (Atwood et al. 2017). For this purpose, mangrove species adapt to the environment by producing specialized aboveground roots (e.g., stilt roots for *Rhizophora stylosa* and pneumatophores for *Kandelia obovata*, knee roots for *Bruguiera gymnorrhiza*), which allow gas exchange for belowground root tissues.

Net primary production (*NPP*) is defined as the organic matter production within an area over time and it is an important index for the evaluation of carbon dynamics in the case of forest

ecosystems (Luo et al. 2002). The proper quantification of all the materials that contribute to *NPP* is necessary for the accurate estimation of *NPP* which affect evaluation of the ecosystem function (Mooney 1996; Chapin et al. 2000). Most of the previous studies in mangrove forest ecosystems that have estimated aboveground *NPP* (NPP_{AG}) restricted their measurement summing the increment in aboveground biomass (*AGB*) and litterfall (Chambers et al. 2001; Khan et al. 2009; Wang et al. 2011), some included increment of belowground coarse roots (BGB_{coarse}) (Kira and Ogawa 1971; Shvidenko et al. 2008). Recently, some studies started to include fine root production (Yashiro et al. 2010; Baishya and Barik 2011; Ohtsuka et al. 2013; Kihara et al. 2021). Fine root production is an important part of *NPP* because of its high rate of turnover. Furthermore, as the part of aboveground litter of mangroves will be washed to the ocean, the belowground decomposition is likely to remain as soil carbon to the Mangrove ecosystems. In the present study, belowground carbon dynamics was measured with the estimation of *NPP*. To assess the difference in relation to climate and species, two sites from Okinawa Island and Ishigaki Island were selected. The species in the study were common on each island. For *NPP* estimation, a modified framework from Clark et al. (2001) and Kloeppel et al. (2007) was used.

Fig. 1.1

1.2 Chapter description

In Chapter 2, the study sites along with climatic variables (temperature, rainfall and wind speed) during the study period are presented. Furthermore, stand structure (stem diameter, height, basal area, tree density) of the study sites are presented.

In Chapter 3, the procedure of the development of biomass allometric equations of different plant parts of *R. stylosa* and *B. gymnorrhiza* is presented., with emphasis on the significance of species and site-specific allometric models.

In Chapter 4, the aboveground litterfall of two sites is presented. To show the seasonal variation, litterfall for the Miyara River mangrove from March 2020 to March 2021, and for the Manko Wetland mangrove from March 2019 to March 2020 are presented.

In this chapter I ask the follows. Does litter production exhibit seasonal variations? Does the seasonality vary among species? How litterfall is correlated with temperature, rainfall, and windspeed variation?

In Chapter 5, the fine root dynamics and the fluctuations in fine root production within the mangrove forest stands were discussed, focusing on both seasonal and species-specific variations. To illustrate the seasonal fluctuation, fine roots for the Miyara River mangrove from

March 2020 to March 2021 and the Manko Wetland mangrove from March 2019 to March 2020 are provided.

In this chapter I ask the follows. What is the effect of different stress factors, such as salinity and pH, on the production of fine roots along the gradient of a river? How variable is seasonal pattern of fine root production? How do fine root mortality and decomposition in mangrove environments vary among species? Do these factors contribute to the production of fine roots?

In Chapter 6, The above- and belowground biomass of the mangrove forests found within the Miyara River in Ishigaki, Japan, as well as the Manko Wetland located in Naha, Japan are discussed. The *AGB* and *BGB_{coarse}* of *R. stylosa* and *B. gymnorrhiza* stands are estimated using the allometric equations in Chapter 3 whereas these of *K. obovata* are estimated using allometric equations developed by others (Khan et al., 2009 and Hoque et al., 2011). Then, *NPP* of the two sites were estimated by the increment of *AGB*, *BGB_{coarse}*, dead mass due to tree mortality, and fine root and aboveground litterfall production.

The addressed questions in this chapter are as follows: How do the *NPP* components (litterfall, biomass increment, root production) contribute to the total *NPP*? Which are the major parameters for *NPP*? Does *NPP* vary along the river stands and in different species stands in the same environment?

Figures

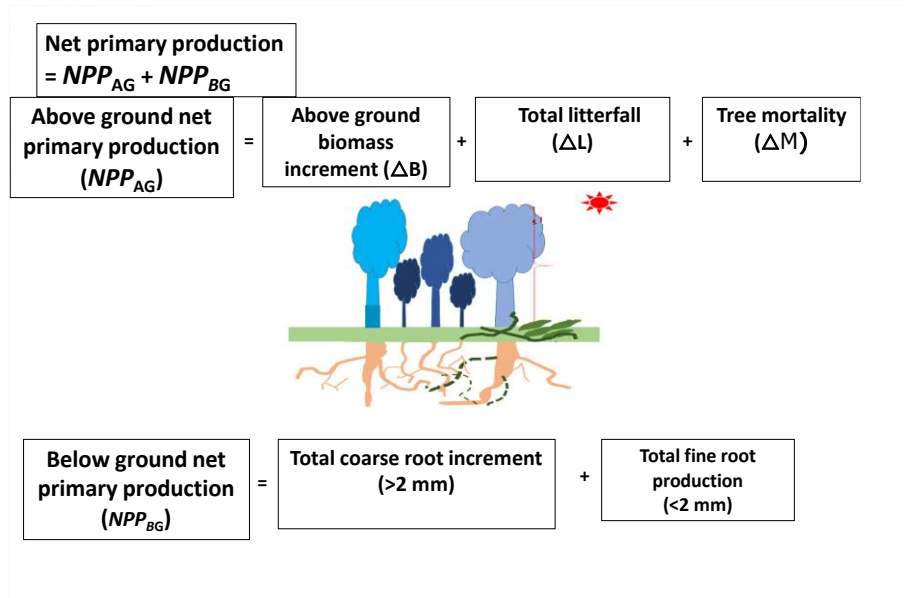











Fig. 1.1: Modified framework calculations of net primary production (NPP) from Clark et al. (2001) and Kloeppel et al. (2007) showing how aboveground NPP (NPP_{AG}) and belowground NPP (NPP_{BG}) are estimated.

Tables

Table 1.1: Mangrove species found in Japan

<i>K. obovata</i>	<i>R. stylosa</i>	<i>B. gymnorrhiza</i>
Height can reach up to 8 m.	Height can reach up to 30 m.	Height may reach 30–35 m.
Leaves are obovate to obovate-elliptic shaped.	Leathery leaves, elliptic. The upper side is smooth and dark green, the bottom is waxy.	Leaves are elliptical, aggregated at the tips of apical shoots in clusters.
		
Flowers are white and like star.	Flowers are composed of cream colored.	The flower has notched and hairy petals and pink to red.
		
Lateral root system is available.	Prop/ Stilt roots reaches up to 3 m long.	Knee roots emerge from the underground and moves horizontally.
		

Chapter 2

Site description

2.1 Study site and climate

a) Miyara River site

The study was conducted in two subtropical regions; one of these was along the Miyara River (24°21' N, 124°12' E) on Ishigaki Island, Japan (Fig. 2.1). Three true mangrove species were observed along the river: *Bruguiera gymnorrhiza* (L.) Lamk., *Rhizophora stylosa* Griff., and *Kandelia obovata* (S., L.) Yong. *K. obovata* was observed only in small patches scattered along the bank of the river. In this study, we focused on downstream *R. stylosa* and *B. gymnorrhiza* plots for comparisons among different species, and *B. gymnorrhiza* plots in the upstream and downstream for comparisons among different locations along the river. In Miyara River mangrove site, the annual mean temperature was 24.9° C, annual mean rain fall was 236 mm, and annual mean wind speed was 5.3 m s⁻¹ during study period between February, 2022 and March, 2023. Monthly average values were shown in Figure 2.1.

Fig 2.1

b) Manko Wetland site

Another study area was Manko Wetland (26°11'N, 127°40'E) of Okinawa Island, Japan which is located at the junction of the Nuha and Kokuba rivers and is described as brackish tidal flat, covering an extensive area at low tide (Hoque et al. 2011) within a subtropical (Khan et al. 2009) climatic region.

Fig 2.2

Manko Wetland mangrove is dominated by *K. obovata*, *R. stylosa*, and *B. gymnorrhiza*. The colonization of *R. stylosa* and *B. gymnorrhiza* has become stabilized and pure stands are grown at a distance of 690 m from the *K. obovata* stand. The annual mean temperature of the study period from January 2019 to March 2022 was 23.7° C, average mean rainfall was 212.5 mm, annual mean windspeed was 5.1 m s⁻¹, showing similar wind speeds all over the months.

Fig 2.3

2.2 Stand structure measurement

a) Miyara River site

A total, of 12 plots were established in the Miyara River mangrove; each plot had a 7 m radius and 153.9 m² area, of which four *B. gymnorrhiza* plots in the upstream area; and four *B. gymnorrhiza* and four *R. stylosa* plots were established in the downstream area along the Miyara River of Ishigaki during March 4 to March 19, 2022 and conducted tree census. A minimum distance of 25 m from the center of one plot to another was maintained. The distance of each of the trees from the center of each plot was recorded and each tree was given a number marked on the tree by permanent marker. The stem diameter at 1.3 m (D) of the trees with $D > 5$ cm within a 7 m radius plot was recorded with a measuring tape, and trees with $D < 5$ cm were recorded within a 2 m radius from the center of the plot (Kauffman and Donato 2012). Tree height (H) was measured using a 15 m-height fiberglass pole (AT-15, Myzox Co., Ltd., Aichi) or a laser range finder (TruPulse360, Laser Technology, Inc., Colorado). D of *R. stylosa* trees was measured 0.1 m above the highest prop root (Clough et al. 1997). Again, tree census was conducted during March 13 to March 21, 2023. I measured the D of all the recorded tree individuals.

Fig. 2.4

Most of the trees ranged between diameter class 6 cm to 12 cm for downstream *R. stylosa* whereas most of the trees ranged between 9 to 18 cm for upstream and downstream *B. gymnorrhiza* stands (Fig. 2.4).

The water level of each plot was measured near the center of the plot during 10 June to 17 June, 2022. To measure the water level of each stand (four plots of the same species along the position of the river is termed as stand), I used 2 m long PVC pipes. Initially, PVC pipes were rubbed with white powder. The water level was continuously monitored over a week between 10 and 17 June, 2022 by observing the clear marks of the water on the pipes. The high tide time varied from 2.30 pm to 4 pm during the day. We assumed the lowest mark of the water level among the stands as “0” m and then calculated the comparative elevation of all other stands respective to that stand. In the present study, the elevation of stand 3 of upstream *B. gymnorrhiza* was found to be the lowest and considered as “0” m (actual value of 47 cm).

(b) Manko Wetland

Three monospecific stands of *K. obovata*, *R. stylosa*, and *B. gymnorrhiza* from the Manko Wetland mangrove of Naha, Okinawa, Japan were also considered as study plots in the present study. One 20 m × 20 m plot in *K. obovata* dominated stand and two 10 m × 10 m plots, one in

R. stylosa dominated stand and another in *B. gymnorrhiza* dominated stand were established. Tree height (*H*) and stem diameter at breast height (*D*) were measured in the *K. obovata* and *R. stylosa* plots from March 12 to March 21 in 2019, from March 13 to March 19 in 2020, from March 21 to March 26 in 2021 and March 17 to March 24 in 2022. In the *B. gymnorrhiza* plot, *H* and *D* were measured from March 26 to March 30 in 2021 and March 24 to March 29 in 2022.

Fig. 2.5

Most of trees of the *K. obovata* plot ranged between diameter class 6 cm to 9 cm whereas the diameter of *R. stylosa* and *B. gymnorrhiza* ranged from 3 cm to 9 cm and 3 to 6 cm, respectively. The observed *D*, *H* of the mangrove stands of the two study sites along with basal area and ρ are shown in Table 2.1.

Table 2.1

The variation of the *H* - *D* relationship is an important element for describing forest stands which provides clues on how trees compete for resources (Canham et al. 2006; Mugasha et al. 2013). It has been proposed that variability in the *H* - *D* relationships within and among different habitats reflect responses to environmental gradients of light, elevation, slope, aspect, or proximity to the coast (Schmidt et al. 2011).

The following function was used to evaluate the tree *H* - *D* relationships of the stands in the Miyara River mangrove.

$$H = \frac{1}{\left(\frac{1}{H_{max}}\right) + \left(\frac{1}{aD}\right)} \dots\dots\dots(2)$$

where, H_{max} is the asymptotic maximal tree height; and ‘*a*’ is a coefficient. Eq. 7 corresponds to a special case of a generalized allometric function when the value of the exponent for *D* is assumed as one (Ogawa et al. 1965; Kira and Ogawa 1971). We performed *F*-test to examine differences in the *H* - *D* relationships among sites within a species as well as between two species within a site. In each case, the pooled data as well as the data of each site position (downstream or upstream) were regressed separately. The resulting residual sums of squares (RSS) values were used for the *F*-test (Aiba and Kohyama 1997; Suwa et al. 2009). We could not perform statistics of the *H* - *D* relationship in the Manko Wetland because there was not a sufficient number of plots of the same species.

Table 2.2

According to the analysis of the $H - D$ relationship (Fig. 2.6) based on Eq.2, it did not differ between the downstream and upstream *B. gymnorhiza* plots ($F_{(2, 331)} = 1.05, p = 0.32$); and between the downstream *B. gymnorhiza* and *R. stylosa* plots ($F_{(2, 527)} = 1.06, p = 0.24$). The a and H_{\max} in Eq. 2 were estimated as 2.20 m cm⁻¹ and 9.30 m for *R. stylosa* plots, 1.78 m cm⁻¹ and 12.26 m for the downstream *B. gymnorhiza* plots, and 1.25 m cm⁻¹ and 13.07 m for the upstream *B. gymnorhiza* plots, respectively (Table 2.2) (see Fig. S4.1 for details).

Fig. 2.6

2.3 Soil properties analysis

Total soil N was analyzed from oven-dried soil samples with a CN-analyzer (JM Macro Corder-1000, J-Science Co, Ltd., Kyoto, Japan). Soil water was collected from three different positions in each plot by digging holes. A 15 ml cylinder syringe with a filter was used for soil water extraction to remove soil from the water. A standard pH meter (LAQUAtwin, HORIBA Advanced Techno Co., Ltd., Japan) was calibrated using buffer solutions (pH 4 and 7) to measure the pH of soil pore water. Soil salinity was measured using a salinity meter (Atago ES-421, Tokyo, Japan).

In the Miyara River mangrove, soil salinity and pH were measured seasonally (every three months interval) from March 4 to March 13, from 12 June to 18 June, from September 11 to September 21 in 2022, and from December 28, 2022 to January 6, 2023 and from March 13 to March 21, 2023. Soil water was collected during day time, atleast 1 hour after the low tide started. In the Manko Wetland mangrove, soil salinity and pH were measured on 14 March, May 15, October 21 in 2019, and January 13 and March 17 in 2020.

The difference in salinity along the Miyara River mangrove was significant ($p < 0.01$, Table 2.3) and the soil salinity of upstream *B. gymnorhiza* stands was significantly lower than that of downstream *B. gymnorhiza* stands ($p < 0.01$), and *R. stylosa* stands ($p < 0.01$), respectively. The difference in pH was significant ($p < 0.01$, Table 2.3) and the pH of upstream *B. gymnorhiza* stands was significantly higher than that of downstream *B. gymnorhiza* stands ($p < 0.01$), and *R. stylosa* stands ($p < 0.05$), respectively. The effect of stands on soil N (%) was significant ($p < 0.05$) and the soil N at the downstream *B. gymnorhiza* stands was higher than that in upstream *B. gymnorhiza* stands ($p < 0.05$, Bonferroni post-hoc test). There was significant difference of water level along the Miyaraeffect of stands on comparative elevation was suggested ($p < 0.01$, Table 2.3) and the comparative elevation was higher at *R. stylosa* stands than that at upstream *B. gymnorhiza* stands ($p < 0.01$).

In the Manko Wetland mangrove, a significant variation in soil salinity was observed between the three plots ($p < 0.01$) and the soil salinity of the *R. stylosa* plot was significantly lower than the *K. obovata* plot ($p < 0.01$) and the *B. gymnorrhiza* plot ($p < 0.01$), respectively (Table 2.3). Significant variation of soil *N* was also found between the three plots ($p < 0.01$) and the soil *N* content of *R. stylosa* was significantly lower than that of *K. obovata* plot ($p < 0.01$) and the *B. gymnorrhiza* plot ($p < 0.01$), respectively. Also, the variation of soil pH between the three species plots was found significant ($p < 0.05$) and soil pH in the *K. obovata* plot was significantly lower than that found in the *R. stylosa* ($p < 0.05$) and the *B. gymnorrhiza* plots ($p < 0.05$), respectively.

Figures

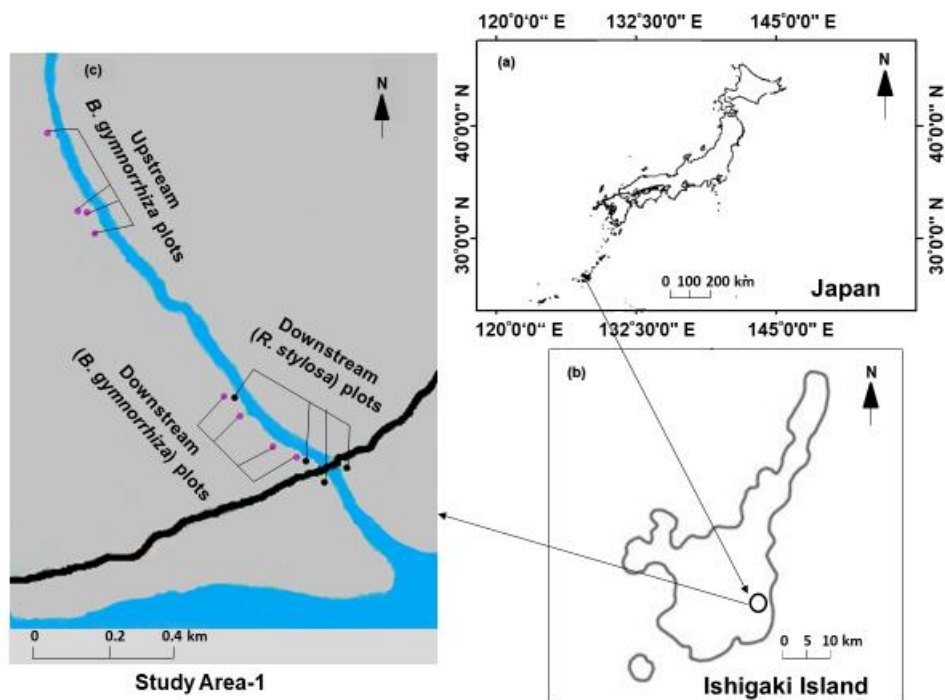


Fig. 2.1: Map showing the location of the study areas along the Miyara River mangrove with the sampled mangrove stands.

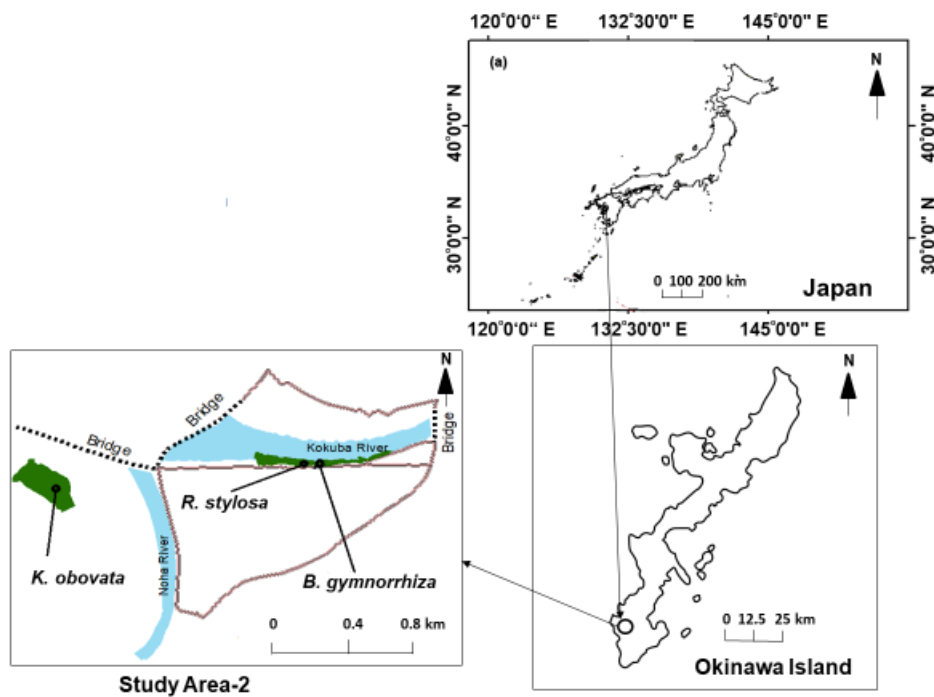


Fig. 2.2: Map showing the location of the study area in the Mamko Wetland mangrove with the sampled mangrove stands.

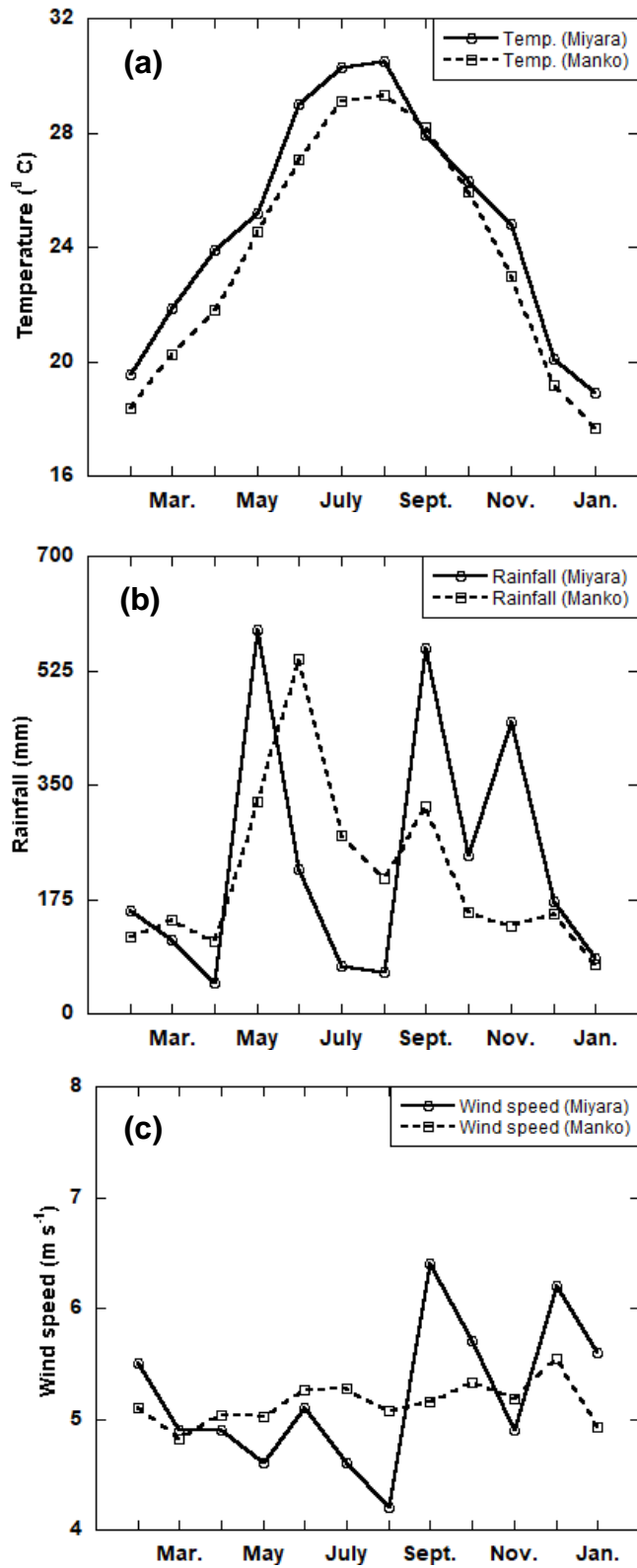


Fig. 2.3: Average monthly temperature ($^{\circ}\text{C}$), rainfall (mm), and wind speed (m s^{-1}) of Miyara river area and Manko wetland area during the study period. Here filled line and dotted line were used to represent the Miyara River mangrove and the Manko Wetland mangrove.

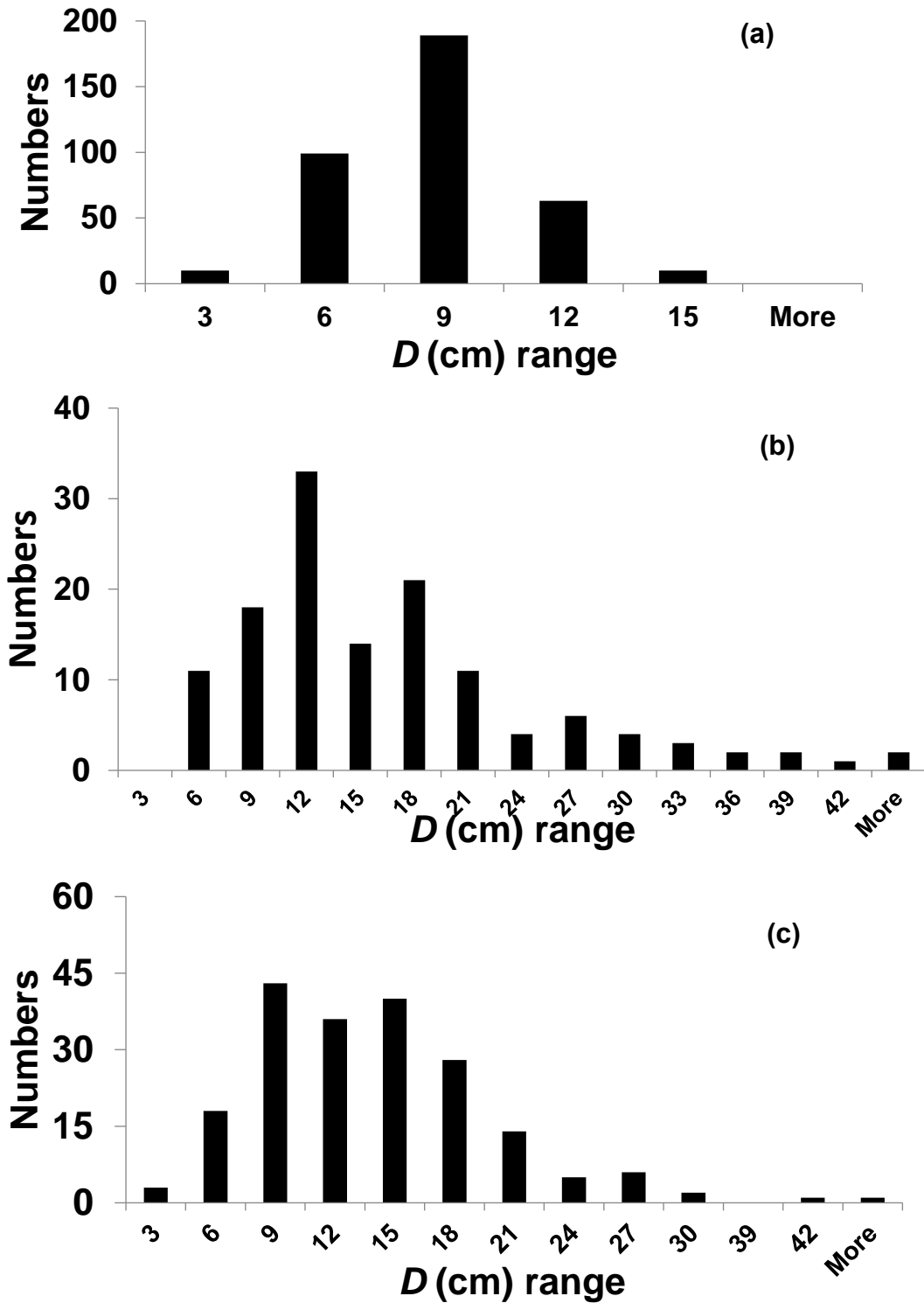


Fig. 2.4: Histogram showing the number of trees of the diameter classes of a) downstream *R. stylosa*, b) downstream *B. gymnorrhiza*, and c) upstream *B. gymnorrhiza* in the Miyara River mangrove. Here, the range is shown as 0-3 cm, 3-6 cm, 6-9 cm, 9-12 cm, 12-15 cm, and above. The upper limit of each range is the maximum limit and the lower limit of the next range starts after that value.

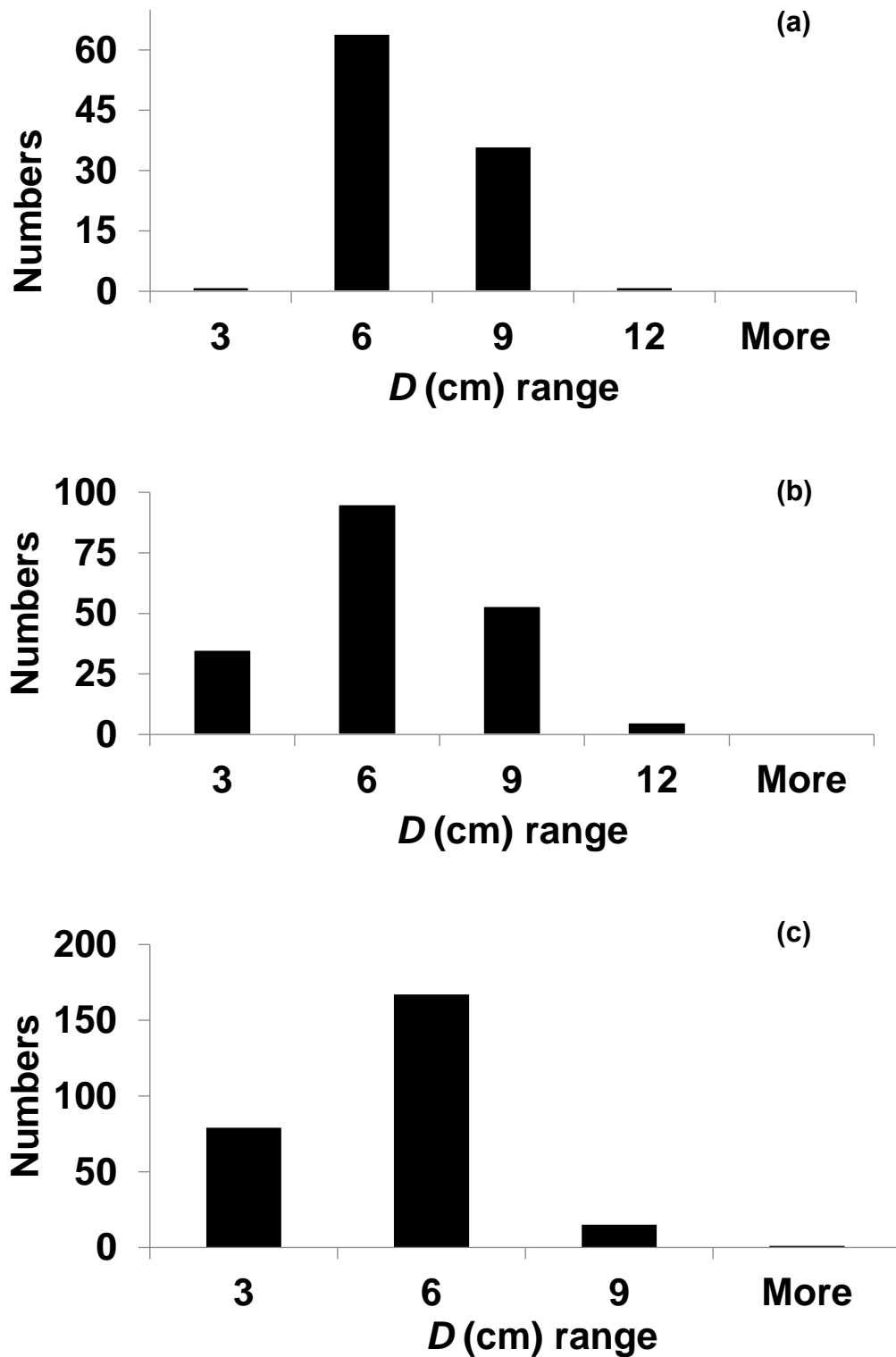


Fig. 2.5: Histogram showing the number of trees of the diameter classes of a) *K. obovata*, b) *R. stylosa*, and c) *B. gymnorrhiza* in the Manko Wetland mangrove. Here, the range is shown as 0-3 cm, 3-6 cm, 6-9 cm, 9-12 cm, and above. The upper limit of each range is the maximum limit and the lower limit of the next range starts after that value.

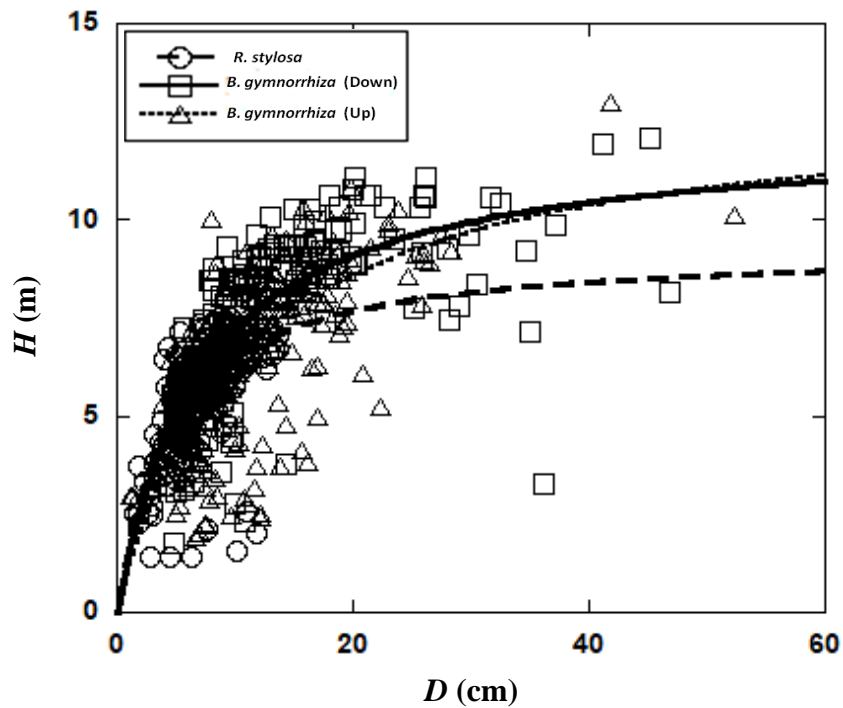


Fig. 2.6: Stem height H - diameter D relationship of *R. stylosa* and *B. gymnorrhiza* along the river. Here, open circle, open square, and closed triangle indicate *R. stylosa*, downstream *B. gymnorrhiza*, and upstream *B. gymnorrhiza* plots, respectively. The solid, dashed, and dotted lines mean the regression analysis results respectively for *R. stylosa*, downstream *B. gymnorrhiza*, and upstream *B. gymnorrhiza* plots, based on Eq. 2 (R^2 of 0.49, 0.46, and 0.45, respectively).

Tables

Table 2.1: Stand structure of upstream and downstream *B. gymnorrhiza* plots, and downstream *R. stylosa* plots of Miyara River mangrove and *K. obovata*, *R. stylosa* and *B. gymnorrhiza* plots of Manko Wetland mangrove showing mean diameter at breast height *D*, mean tree height *H*, basal area, tree density (ρ). We used the mean data of each plot for making comparisons among stands in the Miyara River area but used the actual value for comparing among the species plots in Manko Wetland. Mean values are shown with S.D. Here, values matched with the different letters were significantly different ($p < 0.05$) between stands for Miyara River mangrove and between plots for the Manko Wetland mangrove.

Species	<i>D</i> (cm) ± S.D	<i>H</i> (m) ± S.D	Basal area (m ² ha ⁻¹)	ρ (ha ⁻¹)
<i>B. gymnorrhiza</i> (upstream)	12.94 ± 0.86 ^{ab}	6.70 ± 0.85 ^a	50.58 ± 4.99 ^a	4109 ± 1543 ^a
<i>B. gymnorrhiza</i> (downstream)	16.77 ± 4.75 ^b	8.15 ± 0.86 ^b	53.36 ± 14.68 ^a	2572 ± 1492 ^a
<i>R. stylosa</i> (downstream)	7.86 ± 1.37 ^a	5.80 ± 0.09 ^a	32.41 ± 14.09 ^a	11306 ± 9603 ^a
<i>K. obovata</i> (Manko Wetland)	6.21 ± 1.6 ^a	5.11 ± 1.11 ^a	17.6	5800
<i>R. stylosa</i> (Manko Wetland)	5.18 ± 1.92 ^a	5.18 ± 1.08 ^a	46	18700
<i>B. gymnorrhiza</i> (Manko Wetland)	4.07 ± 1.36 ^b	3.92 ± 0.88 ^b	36	26300

Table 2.2: The values of coefficients H_{\max} and a in Eq. 2 for the stem diameter D - height H relationships are shown with S.E and R^2 values.

Plots	$H - D$ relationship		R^2
	$H_{\max} \pm \text{S.E}$	$a \pm \text{S.E}$	
<i>B. gymnorrhiza</i> (upstream)	13.07 ± 1	1.25 ± 0.1	0.45
<i>B. gymnorrhiza</i> (downstream)	12.26 ± 0.7	1.78 ± 0.2	0.46
<i>R. stylosa</i> (downstream)	9.30 ± 0.4	2.20 ± 0.1	0.49

Furthermore, the RSR of the *R. stylosa* stand was significantly higher than that of upstream *B. gymnorrhiza* stand ($p < 0.01$, Table 4.5) with relatively lower H although the variation of H was not significant.

Table 2.3: Soil salinity, soil pH, soil nitrogen, and water level are shown for downstream *R. stylosa* plots; and upstream and downstream *B. gymnorrhiza* plots of the Miyara River of Ishigaki, and Manko Wetland of Naha mangrove. Mean values are shown with S.D. Here, values matched with the different letters were significantly different ($p < 0.05$). We compared within the Miyara River, Ishigaki mangrove, and within the Manko Wetland, Naha mangrove. No comparison was conducted between the Miyara River, Ishigaki mangrove and the Manko Wetland, Naha mangrove.

Plots	Salinity % \pm S.D	pH \pm S.D	Soil N%	Water level (cm)
<i>R. stylosa</i> (Downstream)	1.09 ± 0.60^a	7.13 ± 0.34^a	0.16 ± 0.02^a	51.75 ± 18.93^a
<i>B. gymnorrhiza</i> (Downstream)	0.75 ± 0.29^a	6.94 ± 0.28^b	0.17 ± 0.02^a	23.25 ± 13.39^{ab}
<i>B. gymnorrhiza</i> (Upstream)	0.31 ± 0.25^b	7.34 ± 0.25^a	0.12 ± 0.02^b	4.25 ± 4.63^b
<i>K. obovata</i> (Manko Wetland)	2.35 ± 0.06^a	7.58 ± 0.06^b	0.17 ± 0.04^a	-
<i>R. stylosa</i> (Manko Wetland)	1.68 ± 0.20^b	7.72 ± 0.05^a	0.07 ± 0.02^c	-
<i>B. gymnorrhiza</i> (Manko Wetland)	2.41 ± 0.32^a	7.66 ± 0.04^a	0.14 ± 0.01^b	-

Chapter 3

Development of allometric equations of *Rhizophora stylosa* and *Bruguiera gymnorrhiza* in the Manko Wetland of Okinawa Island in Japan.

3.1 Introduction

The allometric method is used for biomass estimation in which the whole or partial mass of trees is estimated from measurable tree dimensions like stem diameter and height (Clough and Scott 1989; Ketterings et al. 2001; Hossain 2004; Komiyama et al. 2005, 2008; Hossain et al. 2012; Picard et al. 2015). The basic theory of allometric relationship is based on that the growth rate of one part of the organism is proportional to that of another. For example, tree diameter is highly correlated with tree mass and so regression equation can be developed for predicting tree mass if a range of tree diameter is measured (Komiyama et al. 2008). Moreover, it is difficult to harvest all trees destructively from the forest every time to measure biomass because the total mass of individual trees reaches several tons in matured mangrove forests (Komiyama et al. 2008). Researchers tried to develop generalized allometric models for different mangrove forests of the world (Clough and Scott 1989; Nelson et al. 1999; Komiyama et al. 2002, 2005; Hossain 2004; Chave et al. 2005; Návar 2009; Basuki et al. 2009). The biomass allometric equations for *K. obovata* were developed in the Manko Wetland area ($AGB = 3.203 \times 10^{-2} (D_{0.1} H)^{1.058}$, Khan et al., 2005 and $BGB = 0.0483 (D_{0.1}^2 H)^{0.834}$, Hoque et al., 2011). However, species and site-specific allometric models are preferred for estimation of biomass and net primary productivity *NPP* (Ketterings et al. 2001; Khan et al. 2005; Smith and Whelan 2006; Kairo et al. 2009) because species-specific allometric models provide a greater level of accuracy at a given location for measuring biomass and *NPP* (Ngomanda et al. 2014; Imam Maulana et al. 2016).

This study aimed to develop biomass allometric models for *R. stylosa* and *B. gymnorrhiza*, and to test the performance of models with different independent variables (diameter at breast height, total height) for estimating aboveground and belowground biomass of *R. stylosa* and *B. gymnorrhiza* as well as biomass of each plant organs.

3.2 Materials and methods

Six trees of each species from the Manko Wetland were selected to cover the entire diameter range of trees of each species.

3.2.1 Biomass data collection from sample trees

Six individuals of *B. gymnorrhiza* and six from *R. stylosa* were selected from the Manko Wetland mangrove avoiding the insect and disease-infected and deformed trees. The *R. stylosa* trees were and *B. gymnorrhiza*. The selected individuals were felled at the ground level after measuring the Diameter at Breast Height (D in cm). Total height (H in m) was measured from the felled trees as it is more convenient and less erroneous than the standing trees.

The aboveground parts of each individual were separated into leaves, branches, stems, and aboveground roots. The trees were sectioned every 1 meter for the flexibility of measurement to get the precise total mass value and total height of the stem. After digging the soil, all the belowground roots were collected, washed, and gathered. Then, roots having more than 2 mm in diameter were separated as coarse roots. Aboveground roots were collected only for *R. stylosa*. The fresh mass of all the components including leaves, branches, stems, aboveground roots, and belowground coarse roots were taken separately in the field immediately after felling using either a portable digital hanging balance of 100 kg capacity or a 30 kg stable balance, and recorded in a data sheet. Then subsamples of each part, which was 20% of the total mass, were separated and fresh mass was taken in the field. For the stem, subsamples were taken from the base and the top of every 1 m sectioned bole. The subsamples were kept in bags, taken to the laboratory, and oven-dried at 65° C for 72 hours to 96 hours to reach constant mass. The mass of the dried subsamples was taken and the conversion ratio (oven dry weight in kg / Fresh weight in kg) was measured. The oven-dried mass of different parts of the individuals was calculated from the resulting conversion ratio and fresh mass of the respective plant parts.

Fig. 3.1

3.2.2 Selection of the best-fit models

A power equation was used to get the best-fit allometric models for biomass estimation. Allometric relationships between independent variables (D and H) and oven-dried biomass of plants (leaf, branch, stem, aboveground roots, AGB_{roots} , AGB , BGB_{coarse} , total biomass) were examined. Power equation was tested with only D , only H , or a combination of D and H (DH , D^2H) for each part. Leaf, stem, branch, AGB_{roots} (for *R. stylosa* only), AGB , BGB , and total biomass were the dependent variables for biomass measurement.

The simple allometric equation is written in the form,

$$Y = aX^b \dots\dots\dots(1)$$

Where Y is the dependent variable, X is the dependent variable, a is the coefficient and b is the allometric constant. The equation is then linearized by taking logarithms, as the form,

$$\ln Y = \ln a + b \ln X \dots \dots \dots (2)$$

Then, the models were selected based on the highest coefficient of determination (R^2) values. In the case of similar R^2 values, the models were selected based on least Residual sum of square error (RSS), and akaike information criteria (AIC) (Chave et al. 2005; Basuki et al. 2009; Siddique et al. 2012; Picard et al. 2015).

3.3 Results

3.3.1 Biomass allocation and $H - D$ relationship

For *B. gymnorrhiza*, the diameter ranged from 1.6 cm to 6.7 cm and height ranged from 2.7 m to 4.7 m (Table 3.1); and D ranged from 1.3 cm to 10.2 cm and H ranged from 2 m to 6.9 m for *R. stylosa* (Table 3.2), respectively.

Table 3.1

Again, the biomass distribution of above and belowground parts of six *R. stylosa* trees including different components is shown in Table 3.2.

Table 3.2

Significantly higher leaf biomass of *R. stylosa* was observed than *B. gymnorrhiza*, and most importantly the significant variation between these two species was the AGB_{roots} in *R. stylosa* which was absent in *B. gymnorrhiza*.

3.3.2 Allometric model development

The independent variable D showed higher R^2 values than other independent variables and in such cases the models with the independent variable D were selected as the best-fitted allometric models.

The derived equations for *B. gymnorrhiza* and *R. stylosa* using all the independent variables are shown in Table 3.4 and Table 3.5 respectively

Table 3.3

Table 3.4

The finally selected allometric models of *B. gymnorrhiza* were as follows-

$$\text{Leaf biomass} = 0.1225(D)^{1.54} \dots \dots \dots (3)$$

$$\text{Stem biomass} = 0.1682 (D)^{2.03} \dots \dots \dots (4)$$

$$\text{Branch biomass} = 0.0271 (D)^{2.64} \dots \dots \dots (5)$$

$$AGB = 0.2943 (D)^{2.04} \dots \dots \dots (6)$$

$$BGB_{\text{coarse}} = 0.0895 (D)^{2.21} \dots \dots \dots (7)$$

$$\text{Total biomass} = 0.3844 (D)^{2.09} \dots\dots\dots(8)$$

The selected allometric models of *R. stylosa* were as follows-

$$\text{Leaf biomass} = 0.0262(D)^{1.95} \dots\dots\dots(9)$$

$$\text{Stem biomass} = 0.1295 (D)^{2.34} \dots\dots\dots(10)$$

$$\text{Branch biomass} = 0.0311 (D)^{2.63} \dots\dots\dots(11)$$

$$AGB_{\text{roots}} = 0.002 (D)^{3.82} \dots\dots\dots(12)$$

$$AGB = 0.2039 (D)^{2.41} \dots\dots\dots(13)$$

$$BGB_{\text{coarse}} = 0.0759 (D)^{2.23} \dots\dots\dots(14)$$

$$\text{Total biomass} = 0.2823 (D)^{2.37} \dots\dots\dots(15)$$

Fig. 3.2

3.3.3 Estimation of biomass of different tree parts using present developed equations

The contribution of the estimated leaf biomass to the total aboveground biomass (*AGB*) for upstream and downstream *B. gymnorrhiza* stands, and downstream *R. stylosa* stand in the Miyara River mangrove were 8.4%, 7.1% and 5.2%, respectively; wherever stem biomass were 45.9%, 43.4% and 54%, respectively, and branch biomass contributed 45.7%, 49.5% and 23.7%, respectively (Table 3.5). For *R. stylosa*, aboveground root (*AGB_{roots}*) contributed 17.1% to the *AGB* (Table 3.5).

Table 3.5

Biomass contribution of leaves, stem and branch to *AGB* for *K. obovata* in the Manko Wetland area were 6%, 55% and 39%, respectively; whereas for *R. stylosa* were 6%, 57% and 24% respectively, and for *B. gymnorrhiza* were 20%, 57% and 24%, respectively (Table 3.6). In addition, *AGB_{coarse}* of *R. stylosa* contributed 14% to *AGB* (Table 3.6).

Table 3.6

3.4 Discussion

3.4.1 Allometric model development

D and *H* are commonly used physical parameters in the allometric models to estimate the biomass of tree species (Saintilan 1997; Komiyama et al. 2002; Xiao and Ceulemans 2004; Cienciala et al. 2006). The present study tested linear regression equations of independent (*D* and *H*) and dependent (biomass of different components) variables to get best-fitted model for biomass

estimation. The selection of the best regression equation is the key to allometric modeling in biomass estimation (Steinke et al. 1995; Tam et al. 1995). So, the present study has applied DBH (shown as D) along with height (H) as independent variables which are easily measurable physical parameters (Komiyama et al. 2002; Ong et al. 2004; Comley and McGuinness 2005). Research conducted in several mangrove environments demonstrates that the power curve accurately depicts the relationship between biomass and tree girth, or D , such as *Rhizophora apiculata* and *Bruguiera parviflora* at the Matang Mangrove Reserve, Malaysia (Gong and Ong 1990; Ong et al. 2004), *R. apiculata* at Palau Kecil, Malaysia (Putz and Chan 1986), *Bruguiera-Rhizophora* species dominated mangrove in Northern Australia (Clough and Scott 1989), *R. stylosa* in northwestern Australia (Clough et al. 1997) and for the *B. parviflora* at Kuala Selangor, Malaysia (Hossain 2004).

Although the use of R^2 value provides a general idea for selecting the best-fit models (Parresol 1999; Zar 2010). In this research, the R^2 value using independent variable D was much higher than the other independent variables and so the selection of models was easier considering the higher R^2 values of D than the other independent variables. This study showed the best-fitted allometric model with high R^2 values which has a similarity to Suwa et al. (2008), Khan et al. (2005) ($R^2 = 0.96$), and Hoque et al. (2011) ($R^2 = 0.98$). The forest structure of the study site in Japan (Khan et al. 2005; Suwa et al. 2008; Hoque et al. 2011), including the present study, was monospecific to closed canopy, plantation (Manko Wetland mangrove) and natural (Miyara river mangrove), respectively. Therefore, the variation in independent variables and R^2 values of the allometric models varied between the two species (Komiyama et al. 2008; Alemayehu et al. 2014).

3.4.2 Biomass partitioning between the plant parts

The present study was consistent with several previous studies, as a higher proportion of biomass in the stem was observed in lower D classes of *Rhizophora apiculata* and *R. stylosa* in Australia (Clough and Scott 1989), and *Bruguiera Parviflora* in Malaysia (Hossain 2004). The biomass proportions for branches in the present study were found at higher D classes which was consistent with Hossain et al. (2012). However, similar findings of higher biomass proportion of branch were observed with lower D classes of *R. apicuata* and *R. stylosa* in Australia (Clough and Scott 1989) and *B. parviflora* in Malaysia (Hossain 2004). Again, a difference in the biomass partitioning between *R. stylosa* and *B. gymnorhiza* was observed in the present study. Previous studies showed that variations in the proportion of biomass between their parts in different mangrove species were not only affected by the geographical location and microclimates but also

depended on species-specific architecture at different stages and forest stand structure (Tam et al. 1995; Hossain 2004). Moreover, plant size (H and D) and age have significant influence on partitioning biomass into various parts of a species (Clough et al. 1997; Peichl and Arain 2007).

3.4.3 Model validation

The difference in the allometric equations between the two species in the present study may be due to the variation in the diameter and height classes as well as coefficients in allometric models (Mahmood et al. 2004). Even the coefficient value of the same species may vary with localities and depend on site quality, tree density, and species composition (Clough and Scott 1989; Steinke et al. 1995).

Fig. 3.3

The relationship between AGB (kg) and D (cm) of *R. stylosa* of the presently developed model was between the general allometric equations of Komiyama et al. (2005) and Chave et al. (2005) although neither of the models was too Close. Also, the AGB of the present model deviated from Clough and Scott (1989), Comley and McGuinness. (2005) and Fromard et al. (1998) which resulted due to variation of the study areas. Again, the present model of BGB_{coarse} of *R. stylosa* was far from Komiyama et al. (2005) and Comley and McGuinness (2005).

Fig. 3.4

The AGB (kg) of the present developed model of *B. gymnorrhiza* was between the general allometric models of Chave et al.(2005) and Komiyama et al. (2005) but far from Clough and Scott. (1989). Again, the BGB_{coarse} model of the present study results in a substantially lower estimation (51%) of BGB_{coarse} from the model of Komiyama et al. (2005). The D range was lower in the present study than D (> 5 to 55 cm) reported by Komiyama et al. (2005), D (\geq 5 to 156 cm) for Chave et al. (2005), D (< 5 to 25 cm) for Clough and Scott (1989), D (5 to 25 cm) for Comley and McGuinness. (2005) and D (2 to 45 cm) reported by Fromard et al. (1998) (Table 3.7). None of these models prepared within or near the present study areas (Table 3.7).

Table 3.7

Figures

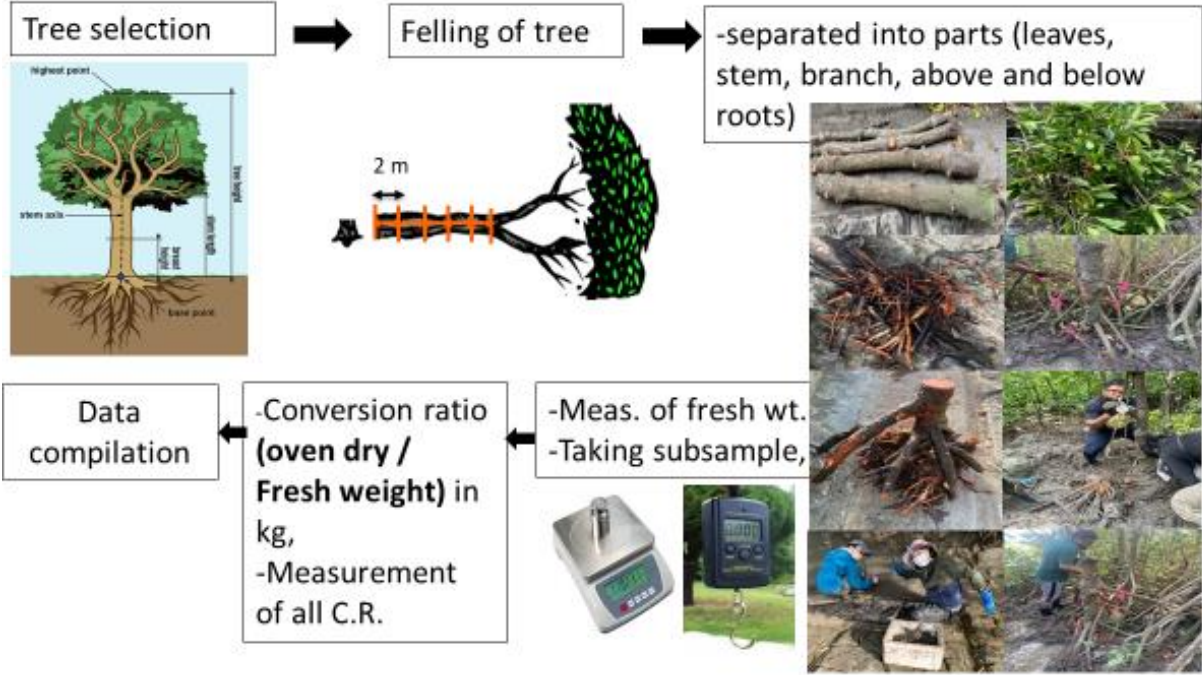


Fig. 3.1: Procedure of sample collection to data compilation for allometric equation development.

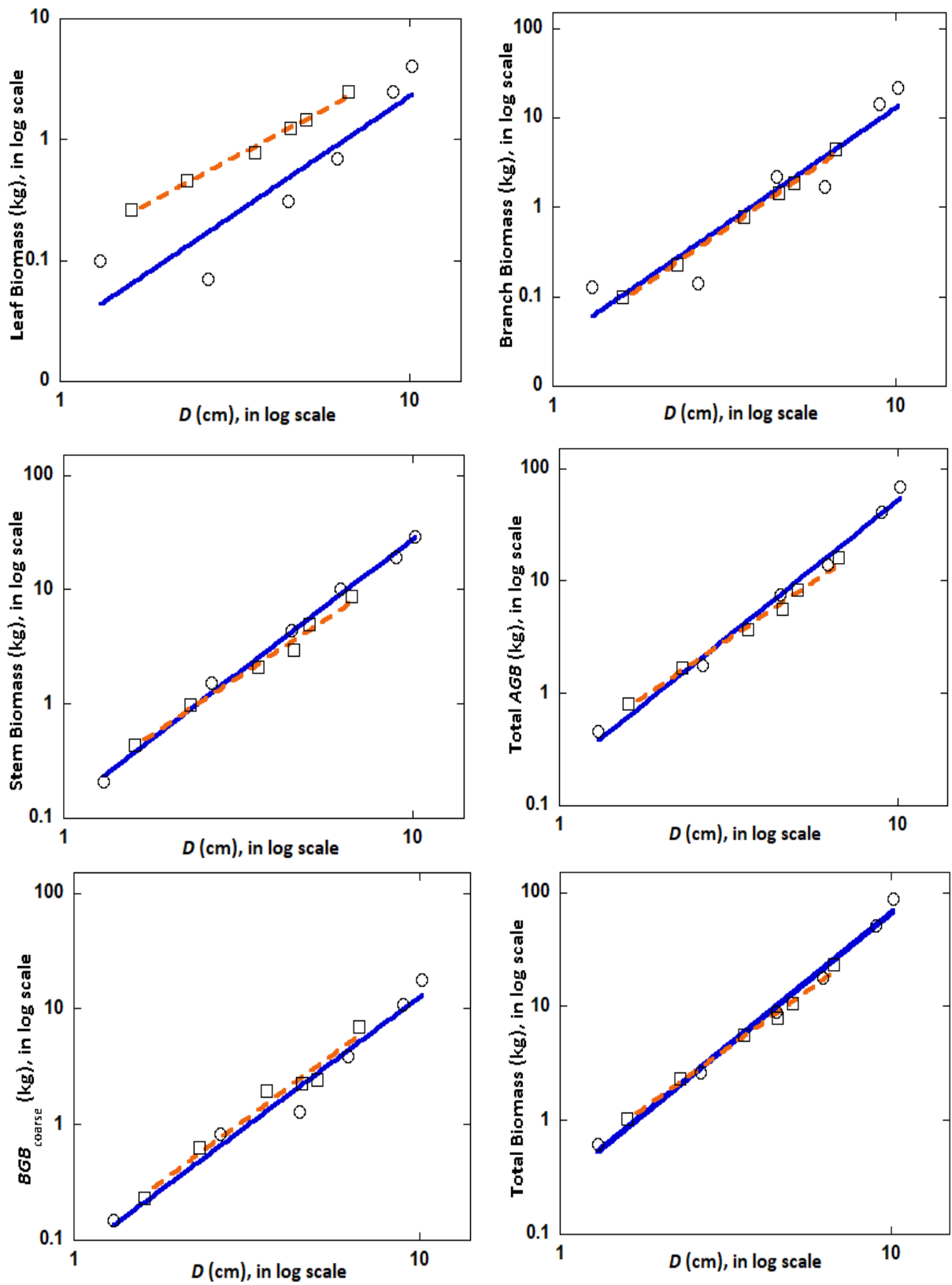
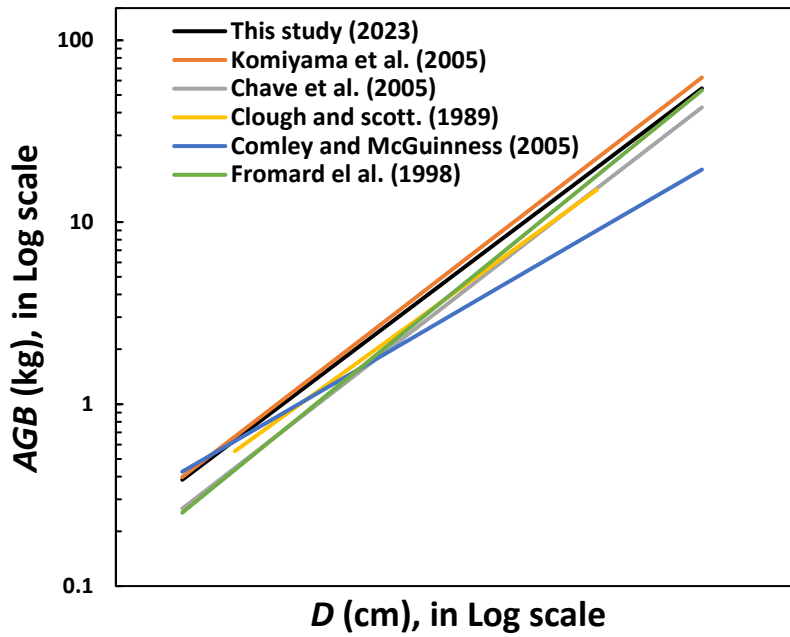
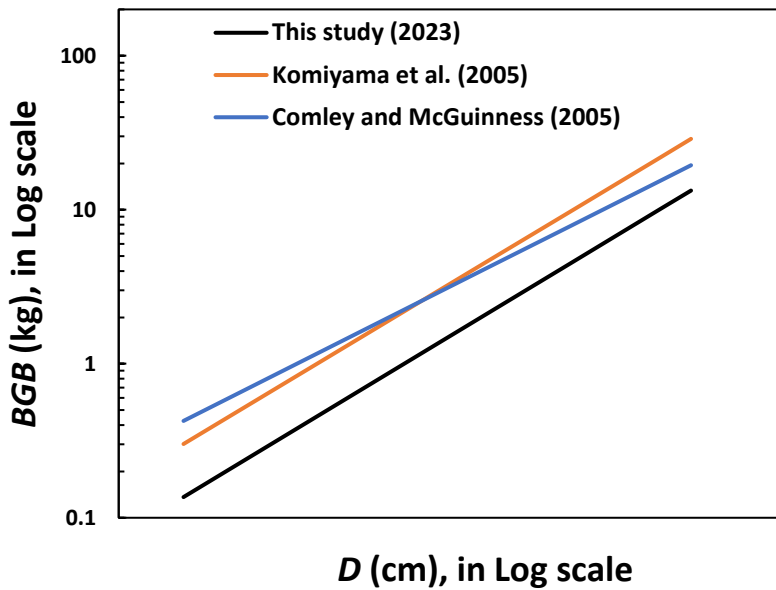


Fig. 3.2: Best fit allometric models for leaf biomass, stem biomass, branch biomass, total aboveground biomass, belowground biomass and total biomass of *R. stylosa* and *B. gymnorhiza*. Here blue lines with circle points indicate *R. stylosa* and orange line with square points indicates *B. gymnorhiza*.



Allometric equations:
 $AGB = 0.2039 (D)^{2.41}$ (This study, 2023)
 $AGB = 0.251 \times WD \times D^{2.46}$ (Komiya et al. 2005)
 $AGB = 0.168 \times WD \times D^{2.47}$ (Chave et al., 2005)
 $AGB = 0.105 \times D^{2.68}$ (Clough and Scott, 1989)
 $AGB = 0.261 \times D^{1.86}$ (Comley and McGuinness., 2005)
 $AGB = 0.128 \times D^{2.60}$ (Fromard et al., 1998)
 Where, WD = wood density,
 D = diameter at breast height.
 Here, WD of *R. stylosa* for this region is 0.86 which is extracted



Allometric equations:
 $BGB = 0.0759 (D)^{2.23}$ (This study, 2023)
 $BGB = 0.199 \times (WD^{0.899}) \times D^{2.422}$ (Komiya et al. 2005)
 $BGB = 10^{(-0.583 + 1.86 \times D)}$ (Comley and McGuinness, 2005)

Fig 3.3: Comparison of the *AGB* (kg) and *D* (cm), and *BGB* (kg) and *D* (cm) relationships of *R. stylosa* of the present allometric model with the other developed models wherever data of the sampled trees were used.

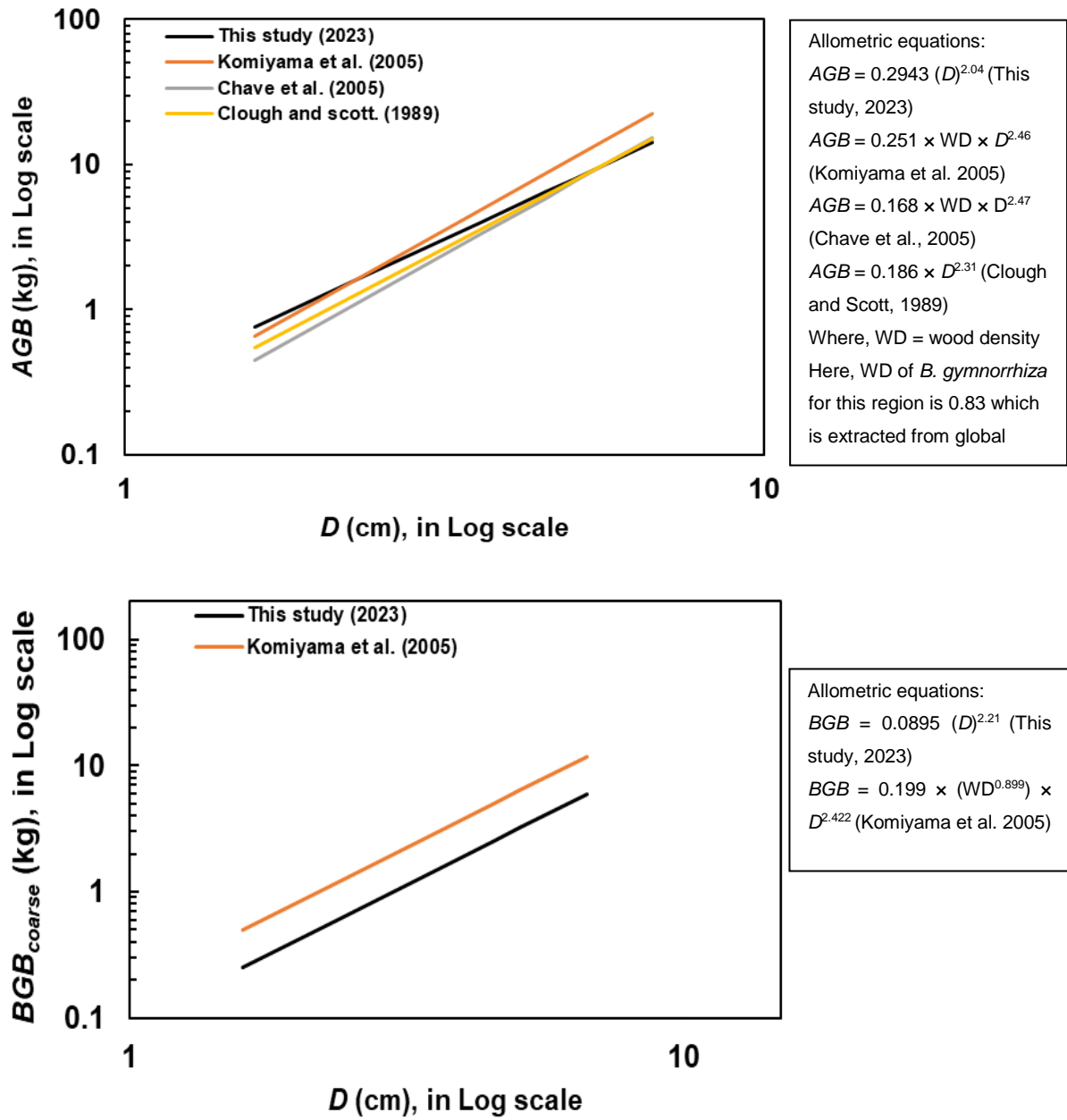


Fig 3.4: Comparison of the AGB (kg) and D (cm), and BGB (kg) and D (cm) relationships of *B. gymnorrhiza* of the present allometric model with the other developed models wherever data of the sampled trees were used.

Tables

Table 3.1: Height (H), diameter (D), total biomass, aboveground biomass, leaf biomass, branch biomass, stem biomass, aboveground root biomass (AGB_{roots}), and belowground root biomass (BGB_{coarse}) of six individual trees of *B. gymnorhiza* used for allometric equations development.

Tree No.	H (m)	D (cm)	Total biomass (kg)	AGB (kg)	Leaf biomass (kg)	Branch biomass (kg)	Stem biomass (kg)	BGB_{coarse} (kg)
B1	2.7	2.3	2.3	1.7	0.5	0.2	1	0.6
B2	2.9	1.6	1	0.8	0.3	0.1	0.4	0.2
B3	4.7	5.1	10.7	8.3	1.5	1.9	4.9	2.4
B4	4	4.6	7.9	5.6	1.3	1.4	3	2.3
B5	4.6	6.7	23	16	2.5	4.4	8.7	7.1
B6	3.2	3.6	5.6	3.7	0.8	0.8	2.1	2

Table 3.2: Height (H), diameter (D), total biomass, aboveground biomass, leaf biomass, branch biomass, stem biomass, aboveground root biomass (AGB_{roots}), and belowground root biomass (BGB_{coarse}) of six individual trees of *R. stylosa* used for allometric equations development.

Tree No.	H (m)	D (cm)	Total biomass (kg)	AGB (kg)	Leaf biomass (kg)	Branch biomass (kg)	Stem biomass (kg)	AGB_{roots} (kg)	BGB_{coarse} (kg)
T1	6.8	6.2	17.9	14	0.7	1.7	10.1	1.5	3.9
T2	3.8	2.7	2.6	1.8	0.1	0.1	1.5	0.04	0.8
T3	6.4	9	50.5	40.5	2.5	14.1	19	4.9	10.8
T4	6.9	10.2	86.5	68.8	4.1	22	29.2	13.6	17.7
T5	2	1.3	0.6	0.5	0.1	0.1	0.2	0.02	0.2
T6	4.2	4.5	8.9	7.6	0.3	2.2	4.3	0.8	1.3

Table 3.3: Selection of the best fit allometric models for leaf, branch, stem, BGB_{coarse} , AGB and total biomass of *B. gymnorhiza* using R^2 , slope error, intercept error, RSS and AIC .

Plant part	Equation	R^2	Slope error	Intercept error	RSS	AIC
Leaf	$y = 0.122 (D)^{1.54}$	0.992	0.012	0.073	0.013	-23.99
Leaf	$y = 0.041 (D \times H)^{1.18}$	0.975	0.017	0.133	0.08	-10.93
Leaf	$y = 0.055 (D^2 \times H)^{0.71}$	0.988	0.015	0.054	0.04	-13.31
Leaf	$y = 0.020 (H)^{2.99}$	0.817	0.029	0.98	0.60	-1.03
Branch	$y = 0.027 (D)^{2.64}$	0.996	0.014	0.252	0.19	-8.00
Branch	$y = 0.038 (D \times H)^{1.33}$	0.901	0.047	0.379	1.27	5.44
Branch	$y = 0.060 (D^2 \times H)^{0.78}$	0.913	0.06	0.201	1.12	6.69
Branch	$y = 0.014 (H)^{3.47}$	0.705	0.042	1.924	3.80	10.01
Stem	$y = 0.168 (D)^{2.03}$	0.982	0.036	0.187	0.60	-1.12
Stem	$y = 0.055 (D \times H)^{2.66}$	0.974	0.031	0.308	1.20	5.11
Stem	$y = 0.046 (D^2 \times H)^{0.98}$	0.989	0.018	0.077	0.51	1.94
Stem	$y = 0.015 (H)^{3.98}$	0.821	0.034	1.529	8.34	14.73
BGB_{coarse}	$y = 0.090 (D)^{2.21}$	0.943	0.025	0.409	1.20	3.09
BGB_{coarse}	$y = 0.008 (D \times H)^{1.95}$	0.890	0.014	0.545	3.30	11.16
BGB_{coarse}	$y = 0.040 (D^2 \times H)^{0.93}$	0.894	0.055	0.268	3.17	12.92
BGB_{coarse}	$y = 0.015 (H)^{3.73}$	0.595	0.055	2.403	12.11	16.96
AGB	$y = 0.294 (D)^{2.04}$	0.988	0.036	0.189	1.55	4.64
AGB	$y = 0.086 (D \times H)^{1.49}$	0.968	0.063	0.223	5.06	13.73
AGB	$y = 0.096 (D^2 \times H)^{0.95}$	0.988	0.039	0.079	1.82	9.59
AGB	$y = 0.033 (H)^{3.84}$	0.786	0.08	1.636	33.30	23.03
Total Biomass	$y = 0.384 (D)^{2.09}$	0.983	0.048	0.227	4.15	10.53
Total Biomass	$y = 0.103 (D \times H)^{1.54}$	0.948	0.099	0.294	16.44	20.80
Total Biomass	$y = 0.112 (D^2 \times H)^{0.99}$	0.976	0.067	0.118	7.60	18.17
Total Biomass	$y = 0.047 (H)^{3.82}$	0.732	0.131	1.861	85.40	28.68

Table 3.4: Selection of the best fit allometric models for leaf, branch, stem, BGB_{coarse} , AGB and total biomass of *R. stylosa* using R^2 , slope error, intercept error, RSS , and AIC .

Plant part	Equation	R^2	Slope error	Intercept error	RSS	AIC
Leaf	$y = 0.026 (D)^{1.95}$	0.948	0.040	0.541	0.84	0.96
Leaf	$y = 0.005 (D \times H)^{1.57}$	0.914	0.010	0.534	1.16	4.91
Leaf	$y = 0.014 (D^2 \times H)^{1.15}$	0.916	0.024	0.271	1.15	6.84
Leaf	$y = 0.026 (H)^{2.37}$	0.545	0.114	2.353	6.19	12.94
Branch	$y = 0.031 (D)^{2.63}$	0.966	0.091	0.639	22.50	20.68
Branch	$y = 0.002 (D \times H)^{2.16}$	0.925	0.010	0.724	31.50	24.70
Branch	$y = 0.023 (D^2 \times H)^{1.03}$	0.919	0.049	0.338	34.06	27.17
Branch	$y = 0.104 (H)^{2.50}$	0.477	0.567	2.880	219.88	34.36
Stem	$y = 0.130 (D)^{2.34}$	0.989	0.054	0.281	8.37	14.75
Stem	$y = 0.096 (D \times H)^{1.31}$	0.956	0.120	0.307	28.18	24.03
Stem	$y = 0.110 (D^2 \times H)^{0.83}$	0.982	0.079	0.114	11.35	20.58
Stem	$y = 0.049 (H)^{3.13}$	0.731	0.206	2.201	173.54	32.94
AGB_{root}	$y = 0.002 (D)^{3.82}$	0.932	0.005	1.230	9.46	15.48
AGB_{root}	$y = 0.001 (D \times H)^{2.73}$	0.926	0.010	0.905	10.03	17.83
AGB_{root}	$y = 0.001 (D^2 \times H)^{1.57}$	0.930	0.001	0.523	9.70	19.63
AGB_{root}	$y = 0.040 (H)^{2.68}$	0.461	0.257	3.406	74.89	27.90
BGB_{coarse}	$y = 0.076 (D)^{2.23}$	0.974	0.041	0.395	5.02	11.68
BGB_{coarse}	$y = 0.044 (D \times H)^{1.37}$	0.911	0.090	0.466	21.89	22.52
BGB_{coarse}	$y = 0.101 (D^2 \times H)^{0.76}$	0.917	0.151	0.239	20.58	24.15
BGB_{coarse}	$y = 0.097 (H)^{2.46}$	0.598	0.402	2.21	99.12	33.58
AGB	$y = 0.204 (D)^{2.42}$	0.976	0.067	0.355	47.73	25.19
AGB	$y = 0.002 (D \times H)^{2.48}$	0.958	0.004	0.627	156.27	34.31
AGB	$y = 0.148 (D^2 \times H)^{0.92}$	0.946	0.219	0.232	200.11	37.79
AGB	$y = 0.071 (H)^{3.33}$	0.606	0.445	3.312	1450.30	45.68
Total Biomass	$y = 0.282 (D)^{2.37}$	0.976	0.026	0.320	42.98	26.56
Total Biomass	$y = 0.139 (D \times H)^{1.48}$	0.919	0.275	0.479	471.30	40.93
Total Biomass	$y = 0.096 (D^2 \times H)^{1.01}$	0.956	0.150	0.245	254.05	42.93
Total Biomass	$y = 0.076 (H)^{3.42}$	0.612	0.492	3.395	2263.10	50.35

Table 3.5: Biomass of leaves, stem, branch, AGB_{roots} and BGB_{coarse} of upstream and downstream *B. gymnorrhiza* stands, and downstream *R. stylosa* stand in the Miyara River mangrove obtained during March 4 to March 19, 2022 and March 13 to March 21, 2023.

Plots	Leaves (Mg ha ⁻¹)		Stem (Mg ha ⁻¹)		Branch (Mg ha ⁻¹)		AGB_{roots} (Mg ha ⁻¹)		BGB_{coarse} (Mg ha ⁻¹)	
	2022	2023	2022	2023	2022	2023	2022	2023	2022	2023
<i>B. gymnorrhiza</i> (upstream)	22.0 ± 2	22.1 ± 3	118.1 ± 12	119.9 ± 13	115.8 ± 27	119.5 ± 27	-	-	105.9	110.5
<i>B. gymnorrhiza</i> (downstream)	20.7 ± 4	21.2 ± 4	125.6 ± 36	129.6 ± 35	141.9 ± 62	147.8 ± 63	-	-	117.6	122.1
<i>R. stylosa</i> (downstream)	9.9 ± 5	10.6 ± 5	103.4 ± 37	109.8 ± 42	46.0 ± 15	48.2 ± 16	32.3 ± 3	34.8 ± 4	49.6	52.3

Table 3.6: Biomass of leaves, stem, branch, AGB_{roots} and BGB_{coarse} of *K. obovata*, *R. stylosa* and *B. gymnorrhiza* plots in the Manko Wetland, Okinawa, Japan. The biomass values for *K. obovata* and *R. stylosa* plots from March 12 to March 21 in 2019, from March 13 to March 19 in 2020, from March 21 to March 26 in 2021 and March 17 to March 24 in 2022. and biomass values of *B. gymnorrhiza* were obtained from March 26 to March 30 in 2021 and March 24 to March 29 in 2022.

Plots	Leaves (Mg ha ⁻¹)	Stem (Mg ha ⁻¹)	Branch (Mg ha ⁻¹)	AGB_{roots} (Mg ha ⁻¹)	BGB_{coarse} (Mg ha ⁻¹)
<i>K. obovata</i>	3.7 ± 0.2	31.9 ± 1	22.7 ± 1	-	24.6 ± 1
<i>R. stylosa</i>	13.7 ± 1	139.2 ± 7	57.6 ± 3	33.1 ± 3	66.5 ± 3
<i>B. gymnorrhiza</i>	29.1 ± 1	84.2 ± 5	35.5 ± 3	-	59.3 ± 4

Table 3.7: Latitude ($^{\circ}$), D (cm) range of present allometric models and some developed models from other areas.

Latitude ($^{\circ}$)	D (cm) range	Study area	Reference
24 $^{\circ}$	1–10	Japan	Present study
1 $^{\circ}$ to 12 $^{\circ}$	>5–55	Thailand and Indonesia	Komiyama et al (2005)
1 $^{\circ}$ to 25 $^{\circ}$	\geq 5–156	Australia, Brazil, Cambodia, India, Indonesia, Malaysia, Venezuela, Mexico, Jamaica, Colombia, Costa Rica	Chave et al (2005)
18 $^{\circ}$ 16'	<5–25	Australia	Clough and Scott, 1989
12 $^{\circ}$ 24'	5–25	Australia	Comley and McGuinness (2005)
5 $^{\circ}$ 23' to 5 $^{\circ}$ 28'	2–45	French Guiana	Fromard et al (1998)

Chapter 4

Seasonal pattern of aboveground litterfall of three Rhizophoraceae family species in two subtropical regions in Japan

4.1 Introduction

Litterfall forms the uppermost layer of the forest floor and becomes a primary source of available organic matter (Lee 1989; Bouillon et al. 2002) It is therefore one of the most important sources of carbon and nutrients (Wafar et al. 1997) and an important primary source of net primary production (Bunt 1995). More specifically, the dynamics of carbon and other nutrient cycling of forest ecosystems is a function of the seasonal pattern of litterfall (Das and Ramakrishnan 1985). The seasonal pattern of mangrove litterfall is influenced by rainfall, temperature, and high winds (Twilley et al. 1997; Cox and Allen 1999). The seasonal patterns of litterfall vary within environmental gradient and even for different tree species in the same environment (Scheer et al. 2009; Zhang et al. 2014).

This chapter aimed to explore the seasonality and species variation in litter production in two dominant mangrove species- *R. stylosa* and *B. gymnorrhiza* in the Miyara River of Ishigaki, Japan, and three mangrove species in the Manko Wetland of Naha, Japan namely *K. obovata*, *R. stylosa* and *B. gymnorrhiza*. I hypothesized that seasonality in weather patterns, especially temperature, rainfall, and wind speed determine seasonality in litterfall production. We also hypothesize that there is variation in seasonal dynamics of litterfall among species depending on the variation in phenological characters.

4.2 Material and method

4.2.1 Litterfall collection

Three litter traps having 1 mm mesh with a collection area of 0.21 m² of each litter trap were established in each plot along the Miyara River of Ishigaki, Japan in February, 2022. These were placed 1 m above the ground to avoid casualties through tidal water, insects etc. In the Miyara River mangrove, litterfall were collected every 26th and 27th of each month from March 2022 to February 2023. In this region, I focused on downstream *R. stylosa* and *B. gymnorrhiza* plots for comparison of litterfalls among different species, and *B. gymnorrhiza* plots in the upstream and downstream for comparison among litterfalls of different locations along the river.

Fig. 4.1

Twelve litter traps were placed in *K. obovata* plot and six were placed in both *R. stylosa* and *B. gymnorrhiza* plots in the Manko Wetland mangrove on March 16, 2019. Litterfalls of *K. obovata*, *R. stylosa* and *B. gymnorrhiza* were collected for two years, between March 2019 and March 2020, and between March 2021 and March 2022. Between March 2019 and March 2020, litterfall were collected on May 18, October 10 in 2019 and January 24 and March 26 in 2020. All the litter traps were emptied on 2nd March, 2021 and then took litterfall on March 30, August 25, December 26 in 2021 and March 23 in 2022. One of the aims of collecting litterfall was to observe the seasonal pattern and so for the Manko Wetland, the seasonal data of spring, summer, autumn, and winter were considered between March 2019 and March 2020 as spanning from 3rd March to 4th May, 5th May to 8th October, 9th October to 22nd January, 23th January to 26th March, respectively. The litters were collected and carried to the laboratory and kept in a cotton bag and then these were separated into leaves, stipules, branches, fruits, flowers, and propagules. After separating, the components were kept for 3 to 5 days for air drying. Then the individual litter components were dried in an oven at 65°C for 72 h and then finally weights were taken using a digital balance.

4.3 Statistical analysis

Repeated measure ANOVA (analysis of variance) was performed to observe difference in litter production among the species. Tukey HSD post-hoc test was performed to examine the variations of focal parameters within, and among species plots. The Pearson correlation test was performed for the Miyara river plots using IBM SPSS statistics 28.0 software to check the correlation between average monthly air temperature, rainfall, and wind speed with litter production.

4.4 Results

4.4.1 Aboveground litterfall along Miyara river, Ishigaki

Higher total litterfall was collected for downstream *R. stylosa* stand than upstream and downstream *B. gymnorrhiza* stands (Fig. 4.2, 4.4). Leaf litters of the three species collected in January, February and March were lower than other months whereas (Fig. 4.2 and Fig S4.2) with high amount from April to September. Higher amount of leaf litters was collected for *R. stylosa* followed by downstream *B. gymnorrhiza* and upstream *B. gymnorrhiza* stands. Stipule litters collected in June, July, August and September were higher than the samples collected in other seasons (Fig. 4.2 and Fig S4.2). Branch and flower litters of downstream *B. gymnorrhiza* stand were higher than downstream *R. stylosa* and upstream *B. gymnorrhiza* stands. Flower litters

produced from June to October were higher than those of the litters of other months (Fig. 4.2 and Fig S4.2). Fruit litters of June, July, November and December were higher than other months (Fig. 4.2 and Fig S4.2). Also, higher propagule litters were also found in June and July than other months (Fig. 4.2 and Fig S4.2).

In the upstream and downstream *B. gymnorhiza* stands, the leaf litters collected from June to September were higher than those collected from November and onwards till March (Fig. 4.2 and Fig S4.2). Flower litters found during July and August were also higher than the litters of other months (Fig. 4.2 and Fig S4.2). Propagule litters of June and July were higher than those measured in other months (Fig. 4.2 and Fig S4.2).

In the downstream *R. stylosa* stand, leaf litters of different months. Branch litters found during July was higher than measured from October to February (Fig. 4.2 and Fig S4.2). Higher amount of flower litters was observed from June to August than in other months (Fig. 4.2 and Fig S4.2). Again, fruit litters collected in May (Fig. 4.2) and October (Fig. 4.2) were higher than other months.

Fig. 4.2

4.4.2 Aboveground litterfall in the Manko Wetland, Okinawa

In the Manko Wetland, total litterfall of *B. gymnorhiza* was the highest followed by *R. stylosa* and *K. obovata*. Leaf litterfall was the maximum in all three species among the litter components. Litterfall of flowers was observed highest during spring (March-May) for *K. obovata* and *R. stylosa* but peaked in summer (May-October) for *B. gymnorhiza* (Fig. 4.3 and 4.4). Fruit litterfall was observed maximum during summer for *K. obovata* and *R. stylosa* but peaked in autumn for *B. gymnorhiza* (Fig. 4.3 and Fig S4.3).

Leaf, stipule, branch and fruit litterfall of *K. obovata* collected during summer was higher than those collected in spring and winter. Flower litters were found highest in autumn. Propagule litters collected in winter was higher than those collected in spring, autumn and summer (Fig. 4.3 and Fig S4.3).

Leaf, branch and fruit litters of *R. stylosa* collected in summer were higher than those collected in spring, autumn and winter. Stipule litters collected in autumn were higher than those collected in spring, summer, and winter. Moreover, the stipule litters of summer were higher than that collected in winter. Flower litters collected in spring were higher than those of summer, autumn and winter (Fig. 4.3 and Fig S4.3).

Leaf, Stipule, branch, flower and propagule litters of *B. gymnorrhiza* collected in summer were higher than those collected in spring, autumn and winter, respectively (Fig. 4.3 and Fig S4.3).

Fig. 4.3

The total monthly litterfall of the two species along the Miyara River mangrove and three species in the Manko Wetland are shown in Fig. 4.4.

Fig. 4.4

4.4.3 Impact of temperature, rainfall, and wind speed on litter production

In the Miyara River mangrove, a strong correlation was found between mean monthly air temperature with the total monthly litter production of upstream *B. gymnorrhiza* ($r = 0.92$, $p < 0.01$), with downstream *B. gymnorrhiza* ($r = 0.92$, $p < 0.01$), and with *R. stylosa* stand ($r = 0.92$, $p < 0.01$). Also, the correlation between average monthly rainfall with the total monthly litter production of upstream *B. gymnorrhiza* ($r = 0.56$, $p < 0.05$), with downstream *B. gymnorrhiza* ($r = 0.54$, $p < 0.05$), and with *R. stylosa* stand ($r = 0.61$, $p < 0.05$).

4.5 Discussion

4.5.1 Seasonality in litterfall

The increase of litterfall during summer than other months may be due to the typhoons occurred during the season which not only made the leaves fall but also caused branches and twigs to break off; about 85.9 % of the mean annual branch litters for *K. obovata*, 96.3 % for *R. stylosa* and 50% for *B. gymnorrhiza* were produced in these months. The peak of the flower litterfall was found during summer due to the phenological pattern of flowering during that time although flowers of *R. stylosa* in both the sites were available almost throughout the year. Maximum flower litterfall of *K. obovata* during summer (May to October) was supported as flowers bloom from May to September, with a peak in August, after which their abundance dramatically reduces (Kamruzzaman et al. 2013). Moreover, the availability of fruit litter during summer was due to the phenological pattern which shows that the greatest abundance of mature fruits of *K. obovata*, *R. stylosa*, and *B. gymnorrhiza* are generally observed in September and July. *K. obovata* propagule litters were found during winter and spring whereas propagules of *R. stylosa* and *B. gymnorrhiza* were found during summer because most of the mature propagules drop during this period (Kamruzzaman et al. 2013, 2017). The seasonal patterns of leaf litterfall for the three

species are almost similar but *R. stylosa* produced a much higher amount of leaf litters than the other species in the Manko Wetland, and also in the Miyara River mangrove.

The result was consistent with previous studies as in a sub-tropical mangrove forest, the highest litterfall production occurred during summer and autumn and slowed down during the winter season (Mfilinge et al. 2005) and in a tropical mangrove forest litter production occurred throughout the year having peaks during the rainy and dry seasons (Wang'ondou et al. 2014).

4.5.2 Contribution of litter components to total litterfall

The contribution of leaf, branch and flower litterfall to the total litterfall in the present study (Table 4.1) is supported by other researchers as Aké-Castillo et al (2006) showed that among the total annual litter productions in the different mangroves of the world, leaf litters contribute 70%, followed by flower litters at 15%, branch 10%.

Table 4.1

The mean yearly litterfall of *K. obovata* in this study (8.2 Mg ha^{-1}) having the highest amount of leaf litters in all cases shows similarity with the litterfall of *K. obovata* in Ohura Bay, Japan (8.7 Mg ha^{-1} , (Hardiwinoto et al. 1989), Manko Wetland (9.0 and 9.9 Mg ha^{-1} , (Kamruzzaman et al. 2012, 2013, 2017) but less than *K. obovata* dominated mangrove in Manko Wetland (10.6 Mg ha^{-1} , Khan et al. 2009), *K. candel* (10.07 Mg ha^{-1}) dominated mangrove in Hong Kong (Lee 1989). The litterfall production of *R. stylosa* of the present study (11.3 - 15.4 Mg ha^{-1}) is quite similar to the *R. mangle* dominated mangrove in Florida, USA (11.3 Mg ha^{-1} , Dawes et al. 1999), *R. mangle*, and *L. racemosa* dominated mangrove in Dominican Republic (11.40 Mg ha^{-1} , Sherman et al. 2003); *R. stylosa* dominated mangrove in Manko Wetland, Japan (10.57 and 11.20 Mg ha^{-1} , Kamruzzaman et al. 2012), pure *R. stylosa* (14 Mgha^{-1}) mangrove of Australia (Alongi 2011), pure *R. mangle* (12.3 Mg ha^{-1} , Ramos E Silva et al. 2007) dominated mangrove of Brazil, *Rhizophora spp.* (15.8 Mg ha^{-1} , Srisunont et al. 2017) dominated mangrove forest in Thailand, *R. stylosa* (14.3 Mg ha^{-1}) dominated mangroves in Papua New Guinea (Leach and Burgin 1985). The mean total litterfall of *B. gymnorrhiza* in both the sites in the present study was higher than that recorded in Ohura Bay, Okinawa Island (7.73 Mg ha^{-1} ; Hardiwinoto et al. 1989) and in Manko Wetland (9.90 Mg ha^{-1} , Kamruzzaman et al. 2012).

4.5.3 Impact of temperature, rainfall, and wind speed on litter production

A strong correlation of litter production with temperature and rainfall determines that the factors affect litter production. It is noticeable that the relationship was extracted whenever monthly

litters were withdrawn. We could not find the relationship between weather patterns and litter production in the Manko Wetland mangrove.

Figures:



Fig. 4.1: Litter trap for aboveground litter collection

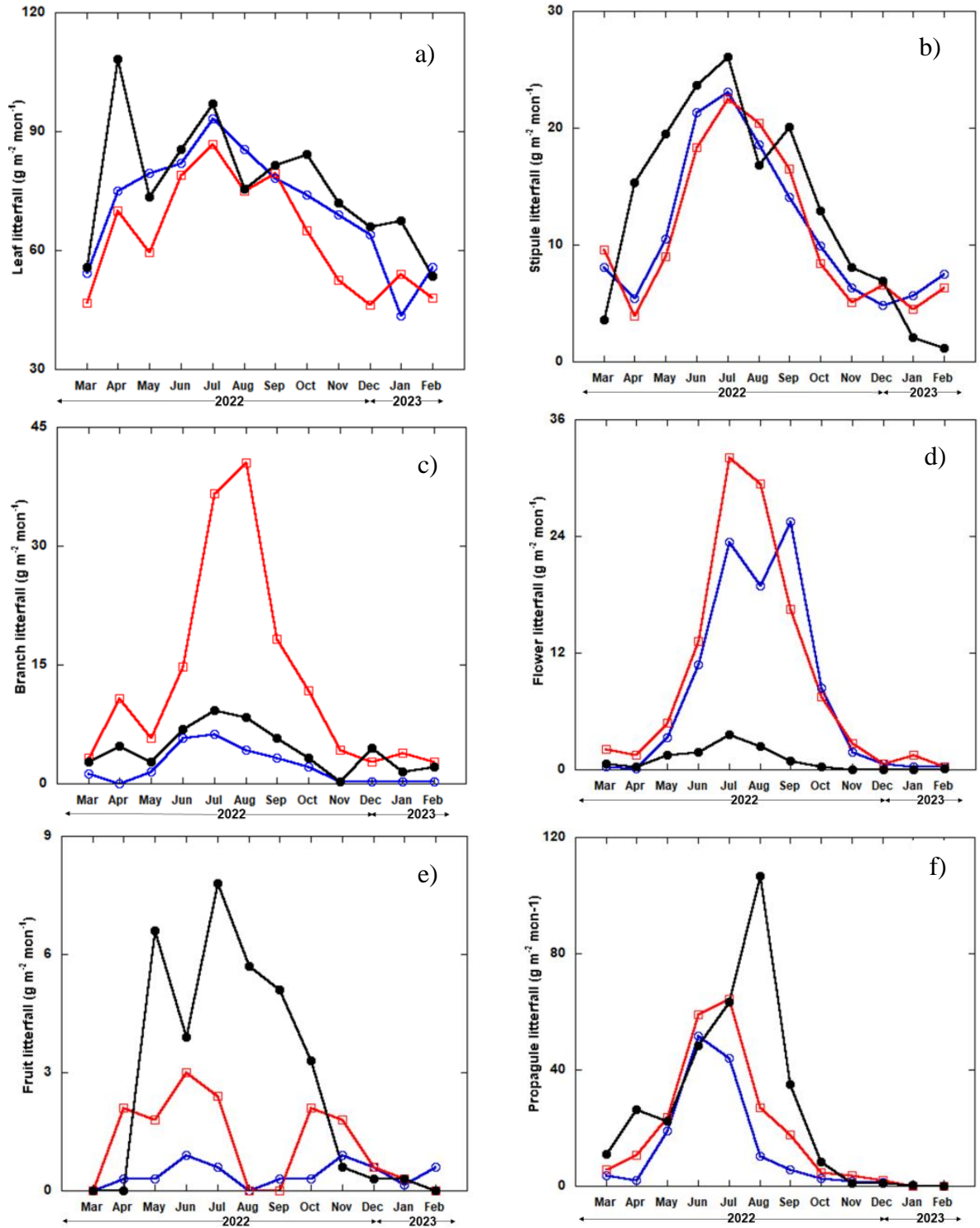


Fig. 4.2: Monthly litterfall of a) leaves, b) stipules, c) branches, d) flowers, e) fruits and f) propagules along the Miyara river mangrove. Here blue, red and black lines represent upstream *B. gymnorrhiza*, downstream *B. gymnorrhiza* and downstream *R. stylosa* stands, respectively. Litterfall were collected every 26th and 27th of each month from March 2022 to February 2023.

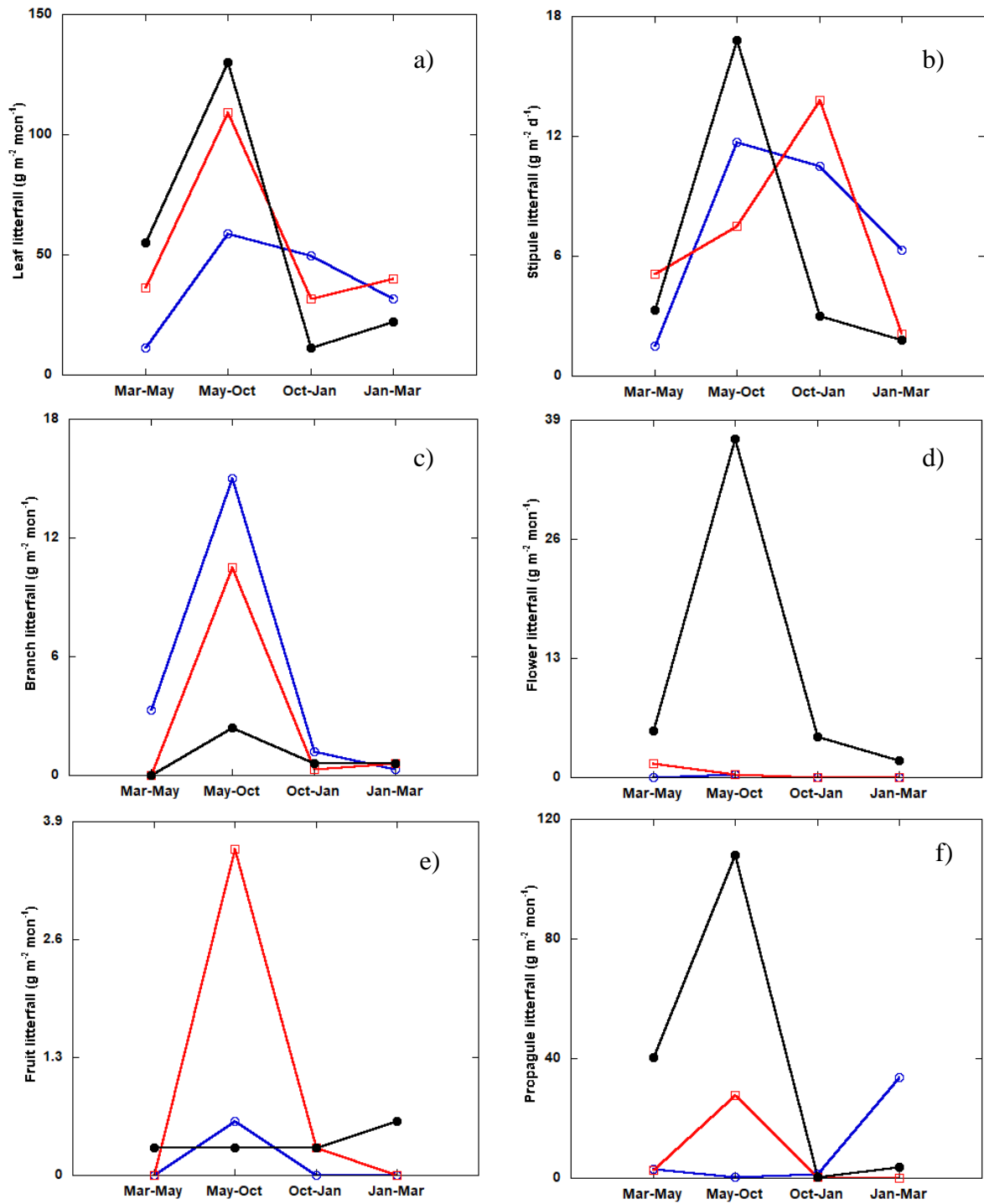


Fig. 4.3: Monthly litterfall of a) leaves, b) stipules, c) branches, d) flowers, e) fruits and f) propagules in the Manko Wetland. Here blue, red and black lines represent *K. obovata*, *R. stylosa* and *B. gymnorhiza* plots, respectively. Litterfall were collected on May 18, October 10 in 2019 and January 24 and March 26 in 2020.

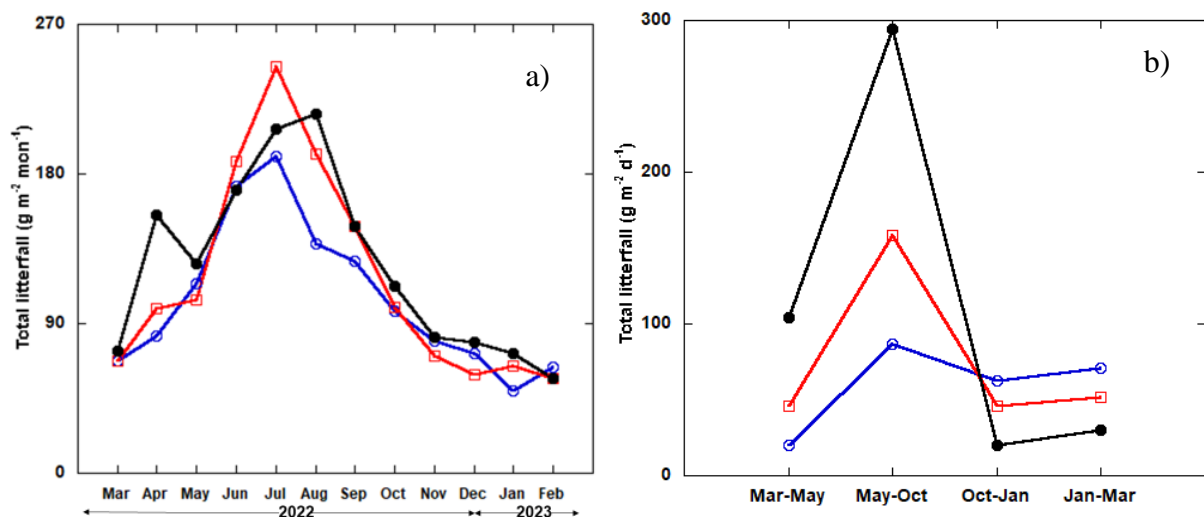


Fig. 4.4: Monthly total litterfall a) along the Miyara river mangrove and b) in the Manko Wetland mangrove. Here blue, red and black lines represent in a) upstream *B. gymnorrhiza*, downstream *B. gymnorrhiza* and downstream *R. stylosa* stands, respectively and b) *K. obovata*, *R. stylosa* and *B. gymnorrhiza* plots, respectively.

Tables

Table 4.1: Contribution (%) of litterfall components to the total litterfall.

Plots	Leaf (%)	Stipule (%)	Branch (%)	Flower (%)	Fruit (%)	Propagule (%)
<i>B. gymnorrhiza</i> (Upstream, Miyara river)	68	11	2	7	1	11
<i>B. gymnorrhiza</i> (Downstream, Miyara river)	55	9	11	8	1	16
<i>R. stylosa</i> (Downstream, Miyara river)	62	10	3	1	2	22
<i>K. obovata</i> (Manko Wetland)	63	12	15	2	1	7
<i>R. stylosa</i> (Manko Wetland)	67	13	7	1	2	10
<i>B. gymnorrhiza</i> (Manko Wetland)	52	11	6	10	1	20

Chapter 5

Fine root dynamics of three *Rhizophraceae* family species in two subtropical regions in Japan.

5.1 Introduction

Fine root production represents a large carbon cost to trees which accounts for more than 50% (Ruess et al. 2003; Finér et al. 2011) and up to 70% of *NPP* in different types of forest ecosystems (Santantonio and Grace 1987; Janssens et al. 2002). Being a productive ecosystem, mangroves accumulate huge amounts of carbon in the belowground part as compared with other forest ecosystems (Donato et al. 2011). Regardless of the important roles, fine roots have been poorly reported in the literature (Smithwick et al. 2014; Warren et al. 2015) due to relatively inadequate knowledge of how accurately measuring fine root production (Hendricks et al. 2006; Zhou et al. 2014). This may lead to unreliable estimates of carbon budgets and generate uncertainties in forest simulation models (Smithwick et al. 2014). It was suggested that decomposition value should be added for more accurate estimation of production (Santantonio and Grace 1987; Osawa and Aizawa 2012) because fine roots grow, die, and decompose simultaneously.

Production, mortality, and decomposition vary among species which appear to occur continuously and simultaneously throughout the entire year (Ostertag 2001; Valverde-Barrantes et al. 2007) and so a detailed understanding of the seasonality of fine root dynamics is needed to clarify the ecological impact of fine roots on forest carbon cycling (Brassard et al. 2009; Winterdahl et al. 2014).

High soil salinity (Feller et al. 2003) and low pH (Koch 1997) negatively affect production by increasing stress conditions for growth whereas higher available soil *N* promotes higher biomass production (Feller et al. 2003; McKee et al. 2007). Stress condition reduces *AGB* (Sherman et al. 2003). Several studies reported that fine root production is positively related to aboveground production (Nadelhoffer et al. 1985; O'Grady et al. 2006; Van Do et al. 2015) because these are controlled by the same edaphic factors (Liu et al. 2021). In addition, there are interspecific variations in production, from upstream to downstream (Enoki et al. 2014), based on salinity (Suwa et al. 2009; Sofawi 2017).

One of the objectives of this chapter was to investigate the fine root production and its seasonality of three species in two different locations. Another objective was to explore the variations of fine root production between as well as within the species.

5.2 Material and Method

5.2.1 Measurement of fine root biomass and necromass by sequential core method

The sequential core sampling method was used for assessing fine root (< 2 mm) biomass and necromass down to 30 cm soil depth from the ground surface. The core sampler used was made of a stainless-steel cylinder with a 5 cm inner diameter and 40 cm length (Zibo Baishun Stainless Steel, Zhoucun, China). Soil core sampling was carried out on sampling points along a grid line. In this study, roots with a diameter of less than 2 mm were considered as total fine roots (Vogt et al. 1983) which were grouped as very fine roots having <0.5 mm of diameter and fine roots having 0.5—2 mm of diameter. In the Miyara River mangrove area, sequential core sampling data were collected every three months, as on March 16, June 23, September 26 and December 23 in 2022, and March 27 in 2023. I collected 8 core samples from each plot, 32 samples from every stand (we have defined one stand including 4 plots). In the Manko Wetland mangrove, sequential core sampling was carried out on March 13, May 18, October 10 in 2019 and January 24 and March 26 in 2020. Further sampling was carried out on March 30, August 25, December 26 in 2021 and March 23 in 2022. In this study site, 12 core samples were collected in each survey. The sequential core data from March 16, 2022 to March 27, 2023 for the Miyara River mangrove, and from March 13, 2019 to March 26, 2020 for the Manko Wetland were used to represent the seasonality.

5.2.2 Fine root separation

The soil samples were subjected to a fine root separation process. The samples were thoroughly mixed with water in a bucket, and materials like leaves, twigs, and other fragments were removed. The remaining roots were sieved through a 2 mm mesh and then through a 0.5 mm mesh to separate fine roots (0.5—2 mm) and very fine roots (<0.5 mm). Then, the fine, living roots were separated from dead roots, based on their color and firmness (Middleton and McKee 2001) as living roots are treated as turgid, are whitish in color, and will float in water due to aerenchyma. After washing off the mud particles, the remaining roots were collected, packed in a bag, brought to the laboratory, and stored in a freezer at -20° C. Subsequently, the root samples that were taken to the laboratory were rechecked using measuring calipers and separated into four types, depending on diameter class and liveliness: i) live roots of <0.5 mm, ii) live roots of 0.5—2 mm, iii) dead roots of <0.5 mm, and iv) dead roots of 0.5 -2 mm. Finally, the samples were placed in an oven at 65° C for 72 hours and the dry masses were then measured.

5.2.3 Decomposition experiment of root litters

The decomposition experiment was carried out using a portion of the air-dried fine root samples. Samples for the experiment were prepared by mixing about 3.0 g of air-dried fine root with root-free mud and placed in litter bags (for decomposition) made of 10 cm × 10 cm RIWP (root impermeable but water permeable) sheets with fine pores of approximately 6 μm diameter. The mass of air-dried roots was converted to dry mass using the oven-dried to air-dried ratio measured in separate samples. The RIWP sheets allow water and microorganisms to pass through but not the fine roots ensuring that new roots do not grow and enter into the litter bags. Litter bags were buried at 10 cm, 20 cm, and 30 cm depth with some bags on the forest floor. Meanwhile, litter bags were tied with green rope and placed 2-3 m from the tree, for easy visibility during field surveys. The litter bags were buried in the Miyara River mangrove in March 2022.

Fig. 5.1

A total of 48 litter bags containing approximately 3 g of fine roots were buried in every stand along the Miyara River. Six litter bags from every diameter class were harvested in each survey. The incubation periods for decomposition in the Miyara River mangrove were from 13 March 2022 to 23 June 2022, 24 June 2022 to 26 September 2022, 27 September 2022 to 23 December 2022, and 24 December 2022 to 16 March 2023. The roots were washed with tap water, dried in an oven at 65 ° C for 72 hours, and weighed. Then the air-dried conversion factor was used. Afterwards, the change in root mass during the period was calculated; the change in the amount in each bag was treated as the decomposition for the period.

The litter bags for decomposition were buried in March 16, 2019 in *K. obovata*, *R. stylosa*, and *B. gymnorrhiza* plots in the Manko Wetland and the incubation periods were from March 16 to May 17, from May 18 to October 9 in 2019, from October 10, 2019 to January 23, 2020 and from January 24 to March 26 in 2020. Eight samples, four of every diameter class for *K. obovata* and six samples, three of all diameter classes for each of the other two species, were withdrawn during every collection period.

5.2.4 Calculation of root production, mortality, and decomposition

Fine root production, mortality, and missing dead roots or decomposition in our study were measured as proposed by Fujimoto et al. (2021). The production was expressed as,

$$P_n = n(b + m) \dots \dots \dots (a)$$

where, P is the production, n is denoted as the number of days, b is the change of live mass of fine roots between time interval, m is the mortality. Mortality was denoted as,

$$m = \frac{\ln r(N_j - N_i \times r^{j-i})}{r^{j-i} - 1} \dots\dots\dots(b)$$

where, N_j and N_i are dead mass of fine roots of time i and j , r^{j-i} is the residual ratio between time i and j . Missing dead roots were denoted as,

$$MDR_n = m(n - \frac{r^n - 1}{\ln(r)}) \dots\dots\dots(c)$$

where, MDR_n is missing dead roots or amount of decomposition for n days, r is the residual ratio of root litter per day which is calculated from R_n , the residual ratio of root litter after n days, as,

$$r = \sqrt[n]{R_n} \dots\dots\dots(d)$$

5.2.5 Fine root turnover

Fine root turnover (FR_{tr}) was estimated as the ratio of the total amount of fine roots produced in a year over the mean standing biomass of fine roots ($FR_{tr} = \frac{\text{Annual fine root production}}{\text{Mean fine root biomass}}$) as estimated by Aber et al. (1985).

5.2.6 Additional method used to compare with the sequential core method

Considering the controversies about which method of fine root collection is more accurate, I additionally checked the seasonality of fine root production with the ingrowth core method, only in the Manko Wetland mangrove. Cylindrical-shaped ingrowth cores with a diameter of 3.5 cm and length of 40 cm, made of flexible plastic mesh with a mesh opening of 10 mm were used for the study. After hollowing out the holes with PVC pipes, ingrowth cores were installed in the holes and refilled with soil from the site in which roots have been removed. The root-free soil was prepared by thoroughly mixing soil collected from the site with water in a container and rinsed through 0.42 mm mesh. The muddy water was preserved in a cloth bag (50 cm × 50 cm) made of a RIWP sheet, which also allowed water and microorganisms to penetrate through it. The bags were hung with the tree branch for 24 hours to release water which allow the soil to become sufficiently firm. Finally, this was used to fill the ingrowth cores. Thirty-eight ingrowth cores were installed in the *K. obovata* plot, whereas 28 cores were installed each in the *R. stylosa* and *B. gymnorhiza* plots on March 16, 2019. Eight cores from the *K. obovata* plot and six from each of the other two species plots were collected on May 18 and October 9 in 2019, and January 23 and March 26 in 2020 for estimating fine root production. A total of 32, 24 and 24 ingrowth cores were thus collected from *K. obovata*, *R. stylosa* and *B. gymnorhiza* plots, respectively. The

other ingrowth cores that could not be accounted for were lost due to destruction by cyclone and crab attack.

5.3 Statistical analysis

One-way ANOVA (analysis of variance) was performed using Kaleidagraph 4.0 software to check seasonal variation of biomass, necromass, production, mortality, and decomposition rate within the same species plot and among the species plots. Tukey HSD post-hoc test was performed to examine the variations of focal parameters within, and among species plots. The Pearson correlation test was performed using IBM SPSS statistics 28.0 software to check the correlation between production and, soil *N*, soil salinity, and pH.

5.4 Results

5.4.1 Seasonal variation of the fine root biomass and necromass

In the Miyara River mangrove, no significant difference in very fine roots and fine root biomass and necromass was observed ($p > 0.05$, Fig. 5.2) in the upstream *B. gymnorrhiza* stand. But significant difference was observed in the very fine roots biomass in the downstream *B. gymnorrhiza* stand ($p < 0.05$) and the very fine root biomass in September was significantly higher than in other survey periods ($p < 0.01$), and was significantly lower in December than in other seasons ($p < 0.01$). Again, the biomass in December was significantly lower than was in March 2022 ($p < 0.05$) and the biomass recorded in June was lower than in September ($p < 0.05$). Furthermore, the fine root biomass of December was significantly lower than that of September ($p < 0.01$), and June ($p < 0.05$). The very fine and fine root necromass samples estimated in December were lower than those collected in March 2023 ($p < 0.05$), June ($p < 0.05$), and September 2022 ($p < 0.01$). The necromass of June was higher than that of March 2023 samples ($p < 0.05$). For *R. stylosa*, very fine root biomass collected in December was less than others ($p < 0.05$) except in March 2023. Moreover, the fine root biomass in September was more than that in December and March 2023 ($p < 0.05$). Fine root biomass of September was lower than that of December ($p < 0.01$), and September ($p < 0.01$). Fine root necromass *R. stylosa* was lower in December than that of March, June, and September 2022 samples ($p < 0.01$, Fig. 5.2). Again, the necromass of March 2023 was less than that of June samples ($p < 0.05$, Fig. 5.2).

Among the species stands in the Miyara River, very fine root biomass and necromass of upstream *B. gymnorrhiza* stand was significantly lower than that of downstream *B. gymnorrhiza* and *R.*

stylosa stands ($p < 0.01$, Fig. 5.2), respectively. Fine root biomass and necromass of upstream *B. gymnorrhiza* stand were also lower than that of downstream *B. gymnorrhiza* and *R. stylosa* ($p < 0.05$, Fig. 5.2).

Fig. 5.2

In the Manko Wetland, an insignificant seasonal variation was observed in the biomass of very fine roots ($p > 0.05$, Fig. 5.3), and the fine roots of *K. obovata* ($p > 0.05$, Fig. 5.3). Insignificant variation was also observed in the necromass of very fine roots ($p > 0.05$, Fig. 5.3), and fine roots collected in different seasons roots ($p > 0.05$, Fig. 5.3), but the necromass of the very fine roots was significantly higher than that of fine roots ($p < 0.05$, Fig. 5.3). An insignificant variation was observed in the biomass of *R. stylosa* in different seasons ($p > 0.05$). A significant variation in fine root necromass was observed ($p < 0.05$) and the fine root necromass collected from March 2019 to January 2020 were significantly lower than those collected in March 2020 ($p < 0.05$, Fig. 5.3). Furthermore, all the very fine root necromass collected throughout the survey times were significantly higher than that of fine root necromass ($p < 0.05$, Fig. 5.3). Significant differences in fine root biomass of *B. gymnorrhiza* at different sampling time was observed ($p < 0.05$, Fig. 5.3) and the fine root biomass collected in March 2019 ($p < 0.01$, Fig. 5.3) and May 2019 ($p < 0.05$, Fig. 5.3) was significantly lower than those collected in the other seasons. Moreover, the biomass of very fine roots throughout the year was significantly higher than that of fine roots ($p < 0.05$, Fig. 5.3). A significant variation in fine root necromass was observed ($p < 0.01$) and the fine root necromass collected in March 2019 ($p < 0.01$, Fig. 5.3) and May 2019 ($p < 0.05$, Fig. 5.3) were significantly lower than those collected in other seasons. Furthermore, the necromass of very fine roots throughout the year was significantly higher than those of fine roots ($p < 0.05$, Fig. 5.3).

Fig. 5.3

In the Manko Wetland mangrove forest, insignificant variation in the biomass of very fine roots, and fine roots between three species plots were observed ($p > 0.05$) but significant variations were observed among necromass of very fine roots, and fine roots ($p < 0.01$). The very fine root necromass of *K. obovata* plot was significantly higher than that of *R. stylosa* ($p < 0.01$) and *B. gymnorrhiza* ($p < 0.01$) plots. Furthermore, fine root necromass of *R. stylosa* plots was significantly lower than that of *K. obovata* ($p < 0.01$) and *B. gymnorrhiza* plots ($p < 0.01$).

5.4.2 Fine root production, mortality, and decomposition

5.4.2.1 Fine root production and mortality

In the Miyara River mangrove, significant variation in the very fine root productions in *R. stylosa* was observed ($p < 0.01$, Table 5.1) and the very fine root production of *R. stylosa* was significantly lower during autumn than during spring, summer and winter ($p < 0.01$). Moreover, very fine roots production was higher in winter than in summer ($p < 0.05$). There was also seasonal variation in fine root production and total fine root production ($p < 0.01$). Fine root production and total fine root production were significantly lower in autumn than in summer, spring and winter ($p < 0.01$) except for total fine root in winter. In upstream *B. gymnorrhiza* stand, a significant variation was observed within very fine roots, fine roots, and total fine root production ($p < 0.01$, Table 5.1). In all cases, the very fine root, fine root, and total fine root production in autumn were significantly lower than that in spring ($p < 0.01$). A significant variation was observed in the very fine root production ($p < 0.01$, Table 5.1) in the downstream *B. gymnorrhiza* stand and the very fine root production in autumn was lower than in spring ($p < 0.01$), summer ($p < 0.05$) and winter ($p < 0.01$). There was also seasonal variation in fine root productions, with significantly lower values in autumn than in spring ($p < 0.01$), summer ($p < 0.05$), and winter ($p < 0.01$). Again, seasonal variation of total fine root production was significant and the total fine roots in autumn were lower than in spring ($p < 0.01$), summer ($p < 0.05$) and winter ($p < 0.01$).

Furthermore, seasonal differences in mortality of very fine roots of *R. stylosa* were significant ($p < 0.01$, Table 5.1) and the mortality in autumn was significantly lower than in spring ($p < 0.01$), summer ($p < 0.01$) and winter ($p < 0.01$). The variation of fine root mortality in *R. stylosa* was also significant ($p < 0.01$) and the mortality in autumn was significantly lower than in spring ($p < 0.01$) and winter ($p < 0.01$). Insignificant seasonal variation was observed in the mortality of very fine roots in upstream *B. gymnorrhiza* plots ($p > 0.05$), but seasonal variations in the fine root mortality were significant ($p < 0.05$) and the fine root mortality was higher in spring than in autumn ($p < 0.05$). Very fine root and fine root mortality in downstream *B. gymnorrhiza* plots varied seasonally ($p < 0.01$), lower in autumn than in spring ($p < 0.01$), summer ($p < 0.05$) and winter ($p < 0.01$). Again, the fine root mortality was significantly higher in winter than that in spring ($p < 0.05$).

On the other hand, insignificant seasonal difference in very fine root and fine root production was observed using the pooled data of the three species in the Manko Wetland (Table 5.1). Furthermore, the seasonal variation in mortality was observed as insignificant ($p > 0.05$, Table

5.1). In the Manko Wetland mangrove, the very fine root production of *K. obovata* was at its maximum in summer and lowest in winter (Table 5.1) whereas fine root (0.5—2 mm) production was highest in spring with no production in winter (Table 5.1). The mortality of the very fine root of *K. obovata* was found at its maximum in summer and minimum in autumn whereas fine root mortality was highest in spring and lowest in winter (Table 5.1). The maximum production of very fine roots and fine roots of *R. stylosa* plot were observed in spring and minimum in autumn; whereas the maximum mortality rate of very fine roots was found in winter and the minimum in summer. The highest fine root mortality was observed in winter (Table 5.1). For *B. gymnorrhiza*, the maximum production of very fine roots and fine roots was observed in spring and summer, respectively; and the minimum in autumn. The maximum mortality for both the root classes was found in summer and the minimum in autumn (Table 5.1).

Table 5.1

The total fine root production (in Mg ha⁻¹ y⁻¹), mortality (in Mg ha⁻¹ y⁻¹) and decomposition (in Mg ha⁻¹ y⁻¹) of the two species along the Miyara River mangrove and two species of the Manko Wetland mangrove are shown in Table S5.1.

5.4.2.2 Variation in decomposition

In the Miyara River mangrove, the decomposition of *R. stylosa*, upstream *B. gymnorrhiza*, and downstream *B. gymnorrhiza* were 0.02 g m⁻² d⁻¹, 0.01 g m⁻² d⁻¹, and 0.02 g m⁻² d⁻¹, respectively.

On the other hand, the amount of decomposition in Manko Wetland, for *K. obovata*, was 0.13 g m⁻² d⁻¹, whereas for *R. stylosa* and *B. gymnorrhiza* it was 0.02 g m⁻² d⁻¹, and 0.04 g m⁻² d⁻¹, respectively. Insignificant seasonal variations in decomposition rates were observed between very fine and fine roots ($p > 0.05$, Table 5.2).

Insignificant seasonal variation in residual ratio per day (r) was observed in different seasons, and between species plots ($p > 0.05$) in both sites. Furthermore, the r did not vary with diameter classes.

Table 5.2

5.4.2.3 Fine root turnover

Fine root turnover (FR_{tr}) was estimated 3.75 y⁻¹, 5.14 y⁻¹ and 4.30 y⁻¹ for upstream *B. gymnorrhiza*, downstream *B. gymnorrhiza* and downstream *R. stylosa* along the Miyara River mangrove area and estimated 6.86 y⁻¹, 4.37 y⁻¹ and 4.47 y⁻¹ for *K. obovata*, *R. stylosa* and *B. gymnorrhiza* in the Manko wetland mangrove area.

5.4.3 Correlation between fine root production and soil properties

Insignificant correlation was observed between salinity and fine root mass production of upstream *B. gymnorrhiza* ($r = 0.23$, $p > 0.05$), downstream *B. gymnorrhiza* ($r = 0.12$, $p > 0.05$), and *R. stylosa* ($r = 0.02$, $p > 0.05$), respectively in the Miyara River mangrove area. Also, insignificant correlation was found between soil pH and fine root mass in upstream *B. gymnorrhiza* ($r = 0.24$, $p > 0.05$), downstream *B. gymnorrhiza* ($r = 0.36$, $p > 0.05$), and *R. stylosa* ($r = 0.19$, $p > 0.05$), respectively. Furthermore, insignificant correlations were observed between fine root production in different seasons, and soil *N* ($r = 0.14$, $p > 0.05$), soil salinity ($r = 0.06$, $p > 0.05$), and pH ($r = 0.01$, $p > 0.05$) in the Manko Wetland.

A significant correlation was extracted of fine root production through the ingrowth core method with soil salinity ($r = 0.61$, $p < 0.05$) and soil pH ($r = 0.89$, $p < 0.01$)

5.5 Discussions

5.5.1 Variation in fine root production of the three species

The proportion of dead fine roots in both sites (40–75%), in the present study, was consistent with previously extracted dead fine roots (Alongi et al., 2000, 2003). One of the major reasons for getting a high amount of dead fine roots in this study might be the slow decomposition rate. The maximum amount of fine root production of all three species was found in spring–summer and the minimum in autumn–winter because roots are produced and shed during these seasons (Lucak 2012).

The fine root production of *K. obovata* in the Manko Wetland in the present study is quite similar to the production of fine roots estimated by Kihara et al. (2021) who measured fine roots in the same species stand (2.9–5.5 Mg ha⁻¹ y⁻¹). The fine root production in both sites is also consistent with some previous studies, as in Lovelock (2008) and Gleason and Ewel (2002) who estimated fine root production of *R. stylosa* and *B. gymnorrhiza* in Panama (8.5° N, 80.78° E; 3.4–4.8 Mg ha⁻¹ y⁻¹) and in the Utwe River in Micronesia (5.17° N, 162.57° E; 3.23 Mg ha⁻¹ y⁻¹). Pongparn et al. (2016) and Noguchi et al. (2020) estimated higher fine root production of *R. apiculata* in Trat, eastern Thailand (12.24°N, 102.52°E; 4.08 Mg ha⁻¹ y⁻¹) and Ranong, southern Thailand (9.97°N, 98.64°E; 7.40 Mg ha⁻¹ y⁻¹).

Fine root production of *R. stylosa* in Miyara river mangrove obtained in the present study, was higher than those of similar latitude mangroves, such as *Rhizophora spp.* dominated mangrove stands in Rookery Bay and Naples Bay, Florida, USA (Giraldo, 2005) and *Rhizophora mangle* dominated mangrove stands (22.33° N, 75.78° E; 0.82–3.25 Mg ha⁻¹ y⁻¹) of Twin Cays, Belize (McKee et al., 2007); this is because these are in different latitudinal gradient and fluctuations of

temperature and precipitation are observed at different latitudinal gradients. Xiong et al. (2017) estimated greater fine root production of *Bruguiera sexangula* (20.6 Mg ha⁻¹ y⁻¹) and *R. stylosa* (18.7 Mg ha⁻¹ y⁻¹) in an almost similar latitudinal gradient in Hainan Island, China (20.02° N, 110.34°E) because they used a different method named decision-matrix for estimating production. The present production values are expected to be more reliable than the decision-matrix model as decomposition is included in the present study which was absent in the decision-matrix model.

5.5.2 Causes of variation in fine roots

The estimated biomass and necromass using sequential core method may contain existing dead or partially decomposed fine roots. In this study, the observed changes through the sequential core method were negative in some seasons because biomass and necromass changes do not occur simultaneously. Shorter sampling intervals are always recommended because the short life cycle of fine roots can be estimated clearly, with less chance of underestimation (Van Do et al. 2015), even though there may be a change in the values over immediate days because fine root turnover is very high. In this survey, the least sampling interval was 62 days and the maximum was 144 days. Therefore, we cannot ensure the peak of biomass and necromass was in survey dates which may produce some errors. Fine root production, mortality, and decomposition might have been more accurately analyzed if we could reduce the survey interval time.

The Fujimoto et al. (2021) method, used in the present study, is a modification of the Osawa and Aizawa (2012) method. The fine root production and mortality values obtained based on Osawa and Aizawa (2012) seem to be overestimated when compared with other studies. The reason for over-estimation is attributable to the use of the over-estimated decomposition rate, which is obtained by the root-litter bag experiment (Osawa and Aizawa 2012). The production, mortality, and decomposition measured during this research through the sequential core method, following Osawa and Aizawa (2012), were for *K. obovata*- 7, 5.4, and 4.1 Mg ha⁻¹, respectively; for *R. stylosa*- 2.6, 1.9 and 0.9 Mg ha⁻¹, respectively; and for *B. gymnorrhiza*- 3.3, 2.4 and 1.3 Mg ha⁻¹, respectively. Osawa and Aizawa (2012) used the existing dead roots within the period of a root-litter bag experiment to calculate the decomposition value, although the existing dead roots included newly dead roots, which were not present at the start of the experiment and thus varied over the length of the experimental period. To improve the methodology, Fujimoto et al. (2021) proposed the use of a residual decomposition ratio (r), which they consider to be constant throughout a survey period. The results based on Fujimoto et al. (2021) seem to provide better estimates compared with other methods. However, Fujimoto et al. (2021) still include the uncertain assumption that the daily residual decomposition ratio r is constant throughout the

experimental period, yet it varies depending on factors such as temperature, and the fact that litter quality changes with decomposition. More work is needed to improve of methodology to fill the gap between observed and actual decomposition values.

High salinity was found to reduce belowground root production (Sherman et al. 2003) but in our case, the salinity (1.68—2.41%) was lower than that of the mangrove of Okukubi River (2.58—2.63%; Suwa et al. 2009), very near to our study site. This implies that the current level of salinity might not create enough stress conditions to limit fine root growth. Furthermore, the higher fine root mass where salinity was higher in this study was supported by the higher below ground mass with increasing salinity was observed for *Avicennia marina* and *Aegiceras corniculatum* dominated mangrove forests (Ball et al. 1997). Variations in soil pH may regulate decomposition processes (Tripathi et al. 2018) by controlling the activities of soil microorganisms and its effects on the soil C/N ratio by altering the utilization of carbon and nitrogen (Kemmitt et al. 2006). The lowest fine root turnover of *R. stylosa* could be the result of having less *N* in the soil than for the other two species (Nadelhoffer 2000) because plants growing in nutrient-poor environments may increase root lifespan to avoid nutrient loss (Ryser 1996). Increased fine root biomass in *K. obovata* plot might be the consequence of the uptake of more *N* and the faster turnover of fine roots (McKee 2001).

Seasonality of fine root production is not clear in the Manko Wetland mangrove in the present study which is consistent with previous research in the Manko Wetland (Kihara et al. 2021) and in Thailand (Poungparn et al. 2016). A general trend of the maximum production during summer and spring; and the minimum during winter and autumn was observed in the Manko Wetland mangrove.

5.5.3 Comparison of fine root dynamics obtained using two different methods

The observed difference in fine root production between sequential core and ingrowth core methods (See in Appendix Table S5.1 and Table S5.2) highlighted the uncertainties related to these two experimental methods. The fine root production measured by Kihara et al. (2021) using the sequential core method was 3.2 times higher than the production extracted through the ingrowth core method. Existing biomass and necromass are extracted by sequential core method wherever existing dead or partially decomposed fine roots might be present. In the ingrowth core method, production is extracted considering the initial value as zero, therefore, the extracted sampling values are always positive and thus the accumulated production was greater than with the other method. In this study, the observed changes through the sequential core method were

negative in some seasons because biomass and necromass changes do not occur simultaneously. We cannot conclude about the better method between sequential core and ingrowth core because these methods are completely different with different assumptions of production.

Figures



RIWP (Root impermeable but water permeable) sheet bags.



Decomposed litter bags.

Fig. 5.1: Fine roots inside litter bags before and after decomposition.

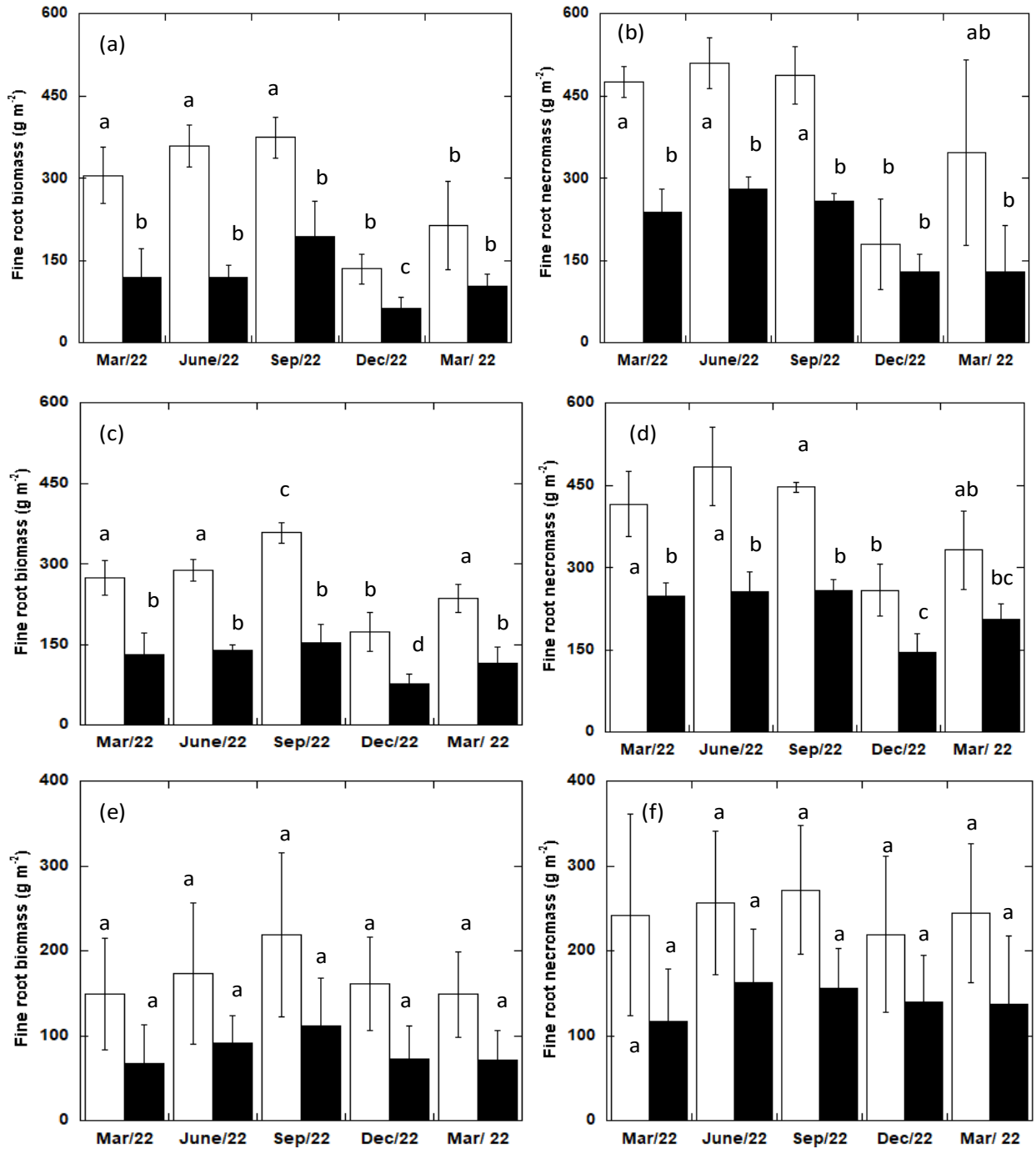


Fig. 5.2 (a-f): Seasonal variation in fine root biomass (g m^{-2}) and necromass (g m^{-2}) of *R. stylosa* (a–b), downstream *B. gymnorhiza* (c–d) and upstream *B. gymnorhiza* (e–f), respectively wherever biomass and necromass data were collected on March 16, June 23, September 26 and December 23 in 2022, and March 27 in 2023. The white and black bars represent <0.5 mm and 0.5–2 mm roots, respectively. Values matched with the different letters indicate that the difference was significant ($p < 0.05$).

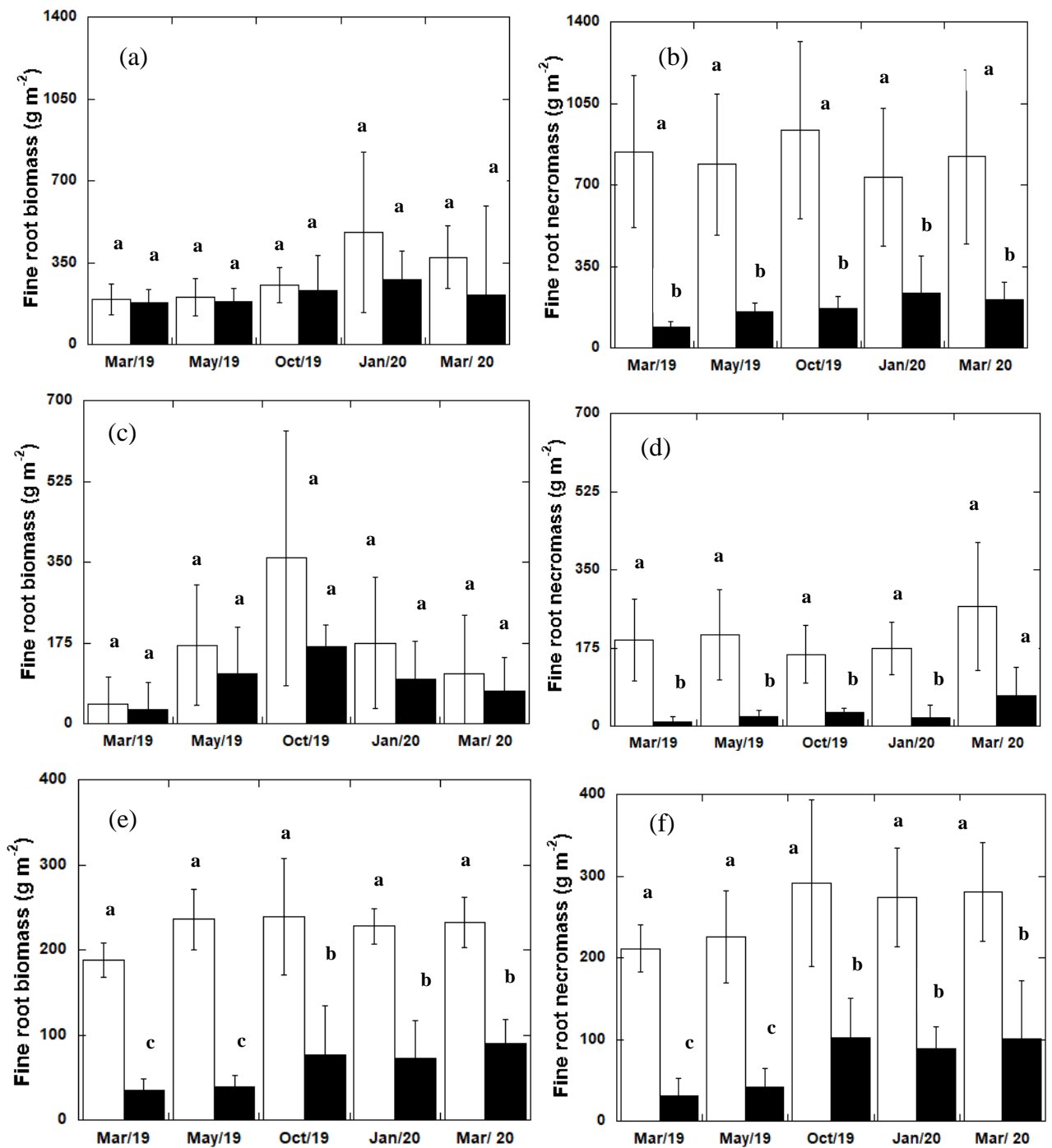


Fig. 5.3 (a-f): Fine root biomass and necromass of *K. obovata* (a–b), *R. stylosa* (c–d), and *B. gymnorhiza* (e–f), respectively in g m⁻² obtained through the sequential core method wherever data were collected on March 13, May 18, October 10 in 2019 and January 24 and March 26 in 2020. The white and black bars represent <0.5 mm and 0.5–2 mm roots, respectively. Here, variations in different sampling times among all fine root samples including both <0.5 mm root and 0.5–2 mm roots were shown. Values matched with the different alphabet indicate that the variation was significant ($p < 0.05$).

Tables

Table 5.1: Production P and mortality m of very fine and fine roots of two species in the Miyara River mangrove and three species in the Manko Wetland mangrove during different seasons in which fine root samples were collected through sequential core method. All the negative values are shown as zero (0) in this table. Here, seasonal values were compared within the site and between < 0.5 mm, and $0.5\text{--}2$ mm roots. For Manko Wetland, the seasonal values were considered by pooling data from all three species. We compared the values within the same study site.

Category	Stands	Location	Spring		Summer		Autumn		Winter	
			<0.5 mm	$0.5\text{--}2$ mm	<0.5 mm	$0.5\text{--}2$ mm	<0.5 mm	$0.5\text{--}2$ mm	<0.5 mm	$0.5\text{--}2$ mm
Production ($\text{g m}^{-2} \text{d}^{-1}$)	<i>B. gymnorrhiza</i> (upstream)	Miyara river	0.48	0.74	0.79	0.21	0	0	0.21	0
	<i>B. gymnorrhiza</i> (downstream)	Miyara river	1.12	0.06	0.68	0.31	0	0	1.98	1.10
	<i>R. Stylosa</i> (downstream)	Miyara river	1.14	0.52	0.34	0.66	0	0	2.68	0.48
	<i>K. obovata</i>	Manko wetland	0	1.30	2.53	0.59	1.04	1.26	0	0
	<i>R. stylosa</i>	Manko wetland	1.75	0.87	1.19	0.49	0	0	0.66	0.37
	<i>B. gymnorrhiza</i>	Manko wetland	1.18	0.25	1.03	0.58	0	0	0.45	0.55
Mortality ($\text{g m}^{-2} \text{d}^{-1}$)	<i>B. gymnorrhiza</i> (upstream)	Miyara river	0.23	0.50	0.32	0	0	0	0.35	0.01
	<i>B. gymnorrhiza</i> (downstream.)	Miyara river	0.97	0	0	0.16	0	0	0.92	0.71
	<i>R. Stylosa</i> (downstream.)	Miyara river	0.59	0.52	0.18	0	0	0	1.90	0.06
	<i>K. obovata</i>	Manko wetland	0	1.19	2.17	0.27	0	0.80	1.39	0.27
	<i>R. stylosa</i>	Manko wetland	0.36	0.21	0	0.09	0.27	0	1.73	0.80
	<i>B. gymnorrhiza</i>	Manko wetland	0.40	0.18	0.89	0.32	0.1	0	0.38	0.27

Table 5.2: Root diameter-based residual ratio per day (r) of *R. stylosa*, upstream and downstream *B. gymnorrhiza*, respectively in the Miyara River mangrove, and of *K. obovata*, *R. stylosa*, and *B. gymnorrhiza*, respectively in the Manko Wetland mangrove conducted based on the decomposition equation of Fujimoto et al. (2021). The incubation periods for decomposition in the Miyara River mangrove were from 13 March 2022 to 23 June 2022, 24 June 2022 to 26 September 2022, 27 September 2022 to 23 December 2022, and 24 December 2022 to 16 March 2023 and for the Manko Wetland mangrove were from March 16 to May 17, from May 18 to October 9 in 2019, from October 10, 2019 to January 23, 2020 and from January 24 to March 26 in 2020. The variation was insignificant throughout the study period ($p > 0.05$).

Stands	Location	Spring		Summer		Autumn		Winter	
		<0.5 mm	0.5-2 mm	<0.5 mm	0.5-2 mm	<0.5 mm	0.5-2 mm	<0.5 mm	0.5-2 mm
<i>B. gymnorrhiza</i> (upstream)	Miyara river	0.99966	0.99978	0.99942	0.99957	0.99956	0.99961	0.99967	0.99971
<i>B. gymnorrhiza</i> (downstream)	Miyara river	0.99951	0.99965	0.99928	0.99944	0.99944	0.99960	0.99952	0.99953
<i>R. stylosa</i> (downstream)	Miyara river	0.99954	0.99968	0.99919	0.99955	0.99967	0.99980	0.99959	0.99961
<i>K. obovata</i>	Manko wetland	0.99907	0.99930	0.99868	0.99899	0.99904	0.99915	0.99883	0.99906
<i>R. stylosa</i>	Manko wetland	0.99917	0.99951	0.99895	0.99911	0.99910	0.99926	0.99900	0.99914
<i>B. gymnorrhiza</i>	Manko wetland	0.99923	0.99940	0.99887	0.99905	0.99908	0.99921	0.99901	0.99911

Chapter 6

Measuring biomass and net primary production of two subtropical mangrove forests in Japan

6.1 Introduction

Mangrove ecosystems sequester large quantities of blue carbon (Mcleod et al. 2011) that contributes to net primary production (*NPP*). The changes in *NPP* in mangroves denote the change in ecosystem function and structure (Chapin et al. 2000; Hoque et al. 2011). Above- and belowground parts of trees play an important role in the carbon and nutrient cycles of forest ecosystems. In particular, litterfall and fine root production are major components of *NPP* (Zhou et al. 2014; Van Do et al. 2015). So, the measurement of the quantity of these components and understanding their quantitative relationships are important to understand the carbon cycle of forest ecosystems (Zak and Pregitzer 1998; Trumbore and Gaudinski 2003; Tateno et al. 2004).

Maximum biomass of a specific forest stand that can be supported by given available soil resources and light. Most of the biomass studies included only the aboveground parts while the studies on belowground parts are rare (Wang et al. 2018). The biomass of belowground coarse roots can be estimated from the *D* and *H*. However, fine roots biomass is rarely measured (Smithwick et al. 2014; Warren et al. 2015) although it can not be ignored as a component of forest ecosystems (Van Do et al. 2015) and represents a large carbon cost to trees and is an important carbon source to the soil as well (Zhou et al. 2014).

Mangrove tree biomass is sensitive to soil nitrogen (*N*) availability (Feller et al. 2003; McKee et al. 2007), salinity, and pH (Koch 1997; Feller et al. 2003). High soil salinity and low pH increase stress conditions for growth whereas higher available *N* indicates higher biomass growth. Suwa et al. (2009) showed that tree height and size decrease with increasing stress conditions, including an increase in pore water salinity and a decrease in soil *N*.

The present research will insight into the above- and belowground productions of *B. gymnorrhiza* and *Rhizophora stylosa* stands in the Miyara River mangrove and *K. obovata*, *R. stylosa*, and *B. gymnorrhiza* in the Manko Wetland of Japan as well as the contribution of the components of above- and belowground to the *NPP*.

The addressed scientific questions of this chapter are as: How do the *NPP* components (litterfall, *AGB* increment, *BGB*_{coarse} increment, fine root production, dead mass increment) contribute to the *NPP*? Which are the major parameters for *NPP*? Does *NPP* vary between the species stands along the river or between stands in the same environment?

6.2 Material and Method

The net primary production of the three species in two regions was measured as

$$NPP = NPP_{AG} + NPP_{BG}$$

with NPP_{AG} , the total aboveground net primary production and NPP_{BG} , the total belowground net primary production

Clark et al., 2001 and Kloeppel et al., 2007 proposed the NPP_{AG} ($\text{Mg ha}^{-1} \text{ yr}^{-1}$) estimation method as follows:

$$NPP_{AG} = \Delta AGB + \Delta L + \Delta M + \Delta G$$

where, ΔAGB is the aboveground biomass increment which includes biomasses of leaves, branches, and stems, and aboveground coarse root biomass (AGB_{roots} for *R. stylosa* only), ΔL is the total aboveground litter production, ΔM is the variation in the amount of dead dry matter due to tree mortality, and ΔG is the amount of biomass lost through grazing which was ignored in the current study because of the difficulty in collecting data of herbivory consumption. The AGB and tree dead mass increments, and total litterfall production from 2022 to 2023 were used for the Miyara River mangrove whereas in the Manko Wetland mangrove, the mean values from 2019 to 2020 and from 2021 to 2022 were used for *K. obovata* and *R. stylosa*, and from 2021 to 2022 were used for *B. gymnorrhiza*.

NPP_{BG} is the sum of the production of belowground fine and coarse roots where the production of fine roots (<2 mm) was conducted by the direct field method (sequential core, Chapter 6) and the increment of coarse root mass was obtained using an allometric equation (Chapter 3). To estimate coarse root production, both biomass and dead mass increments were recorded. The equation stands as

$$NPP_{BG} = \Delta BGB_{\text{coarse-living}} + \Delta BGB_{\text{coarse-dead}} + \Delta BGB_{\text{fine}}$$

Where $\Delta BGB_{\text{coarse-living}}$ is the coarse root biomass increment, $\Delta BGB_{\text{coarse-dead}}$ is the dead mass increment of coarse root and ΔBGB_{fine} is the fine root production. The $\Delta BGB_{\text{coarse-living}}$, $\Delta BGB_{\text{coarse-dead}}$, fine root production and NPP_{BG} from 2022 to 2023 were used for the Miyara River mangrove whereas mean values from 2019 to 2020 and from 2021 to 2022 were used for *K. obovata* and *R. stylosa*, and values from 2021 to 2022 were used for *B. gymnorrhiza* to show the mean increment in the Manko Wetland mangrove.

6.3 Statistical analysis

One-way analysis of variance (ANOVA) was performed using KaleidaGraph version 4.0 software (Hulinks Co., Ltd., Tokyo, Japan) to evaluate the difference between three groups of *R.*

stylosa, downstream *B. gymnorhiza*, and upstream *B. gymnorhiza* plots (defined as stands) on the focal biometrics such as *D*, *H*, *AGB*, *BGB_{coarse}*, fine root mass, soil salinity, soil pH, soil *N* and comparative elevation, and post-hoc Bonferroni test was performed to examine the difference of the focal biometrics among the plots of the Miyara river mangrove.

Again, One-way ANOVA was performed to observe difference in litter production, fine root production, *NPP_{AG}*, *NPP_{BG}*, and *NPP* between the stands along Miyara River. Tukey HSD post-hoc test was performed to examine the variations of focal parameters within stands.

6.4 Results

6.4.1 Aboveground biomass estimation

A significant difference of *AGB* between stands was observed in the Miyara River mangrove ($p < 0.05$, Table 6.1) and observed that the *AGB* of *R. stylosa* stand was significantly lower than downstream *B. gymnorhiza* stand.

Table 6.1

6.4.2 Belowground coarse root and fine root estimation

The variation of *BGB_{coarse}* (belowground coarse root biomass) between stands in the Miyara River mangrove was significant ($p < 0.01$, Table 6.1) and the *BGB_{coarse}* of the *R. stylosa* stand was significantly lower than that of the downstream *B. gymnorhiza* stand ($p < 0.01$); and that of the upstream *B. gymnorhiza* stands ($p < 0.01$), respectively. The difference of fine root biomass was significant ($p < 0.01$, Table 6.1) and the fine root biomass of *R. stylosa* stand was significantly higher than that of the upstream *B. gymnorhiza* stand ($p < 0.01$); and the downstream *B. gymnorhiza* stands showed significantly higher fine root biomass than that of the upstream *B. gymnorhiza* stands ($p < 0.05$). The effect of stands on *BGB_{total}* (summation of coarse roots and fine roots) was significant ($p < 0.01$) and the estimated *BGB_{total}* for the *R. stylosa* stands was significantly higher than that in the downstream *B. gymnorhiza* stands ($p < 0.01$), and that in the upstream *B. gymnorhiza* stands ($p < 0.05$).

Significant variation was observed among the fine root biomass of three species in Manko Wetland ($p < 0.05$), and it was observed that the fine root biomass of *R. stylosa* was significantly lower than that of *K. obovata* ($p < 0.05$, Table 6.1).

6.4.3 Aboveground biomass increment

At the Miyara River mangrove site, insignificant differences in the biomass increments of leaves, stems and branches were observed between the upstream and downstream *B. gymnorrhiza* stands ($p > 0.05$ for all, Table 6.2).

Branch biomass increment contributed highest to the total *AGB* increment for upstream and downstream *B. gymnorrhiza* stands but for *R. stylosa*, stem biomass contributed highest to the total *AGB* increment (Table 6.2).

In the Manko Wetland mangrove, stem biomass contributed highest for *K. obovata*, *R. stylosa* and *B. gymnorrhiza* plots to total *AGB* increment (Table 6.2). *AGB_{root}* increment of *R. stylosa* along the Miyara River mangrove and in the Manko wetland contributed 21% and 19% to the *AGB* increment.

Table 6.2

6.4.4 Contribution of *AGB* increment, total litterfall, and tree mortality to *NPP_{AG}*

In the Miyara river mangrove, an insignificant difference was found in the *AGB* increment, tree dead mass increment and *NPP_{AG}* between the species stands ($p > 0.5$, Table 6.3). Furthermore, insignificant difference was observed between upstream and downstream *B. gymnorrhiza* stands ($p > 0.5$, Table 6.3) but significant difference was found between upstream *B. gymnorrhiza* and downstream *R. stylosa* stands ($p < 0.5$, Table 6.3). In both the Miyara River and the Manko Wetland, litterfall production made up the largest portion of the *NPP_{AG}*, followed by *AGB* increment. The distribution of the dead mass increment due to mortality was higher in the Miyara river area than in the Manko Wetland (Table 6.3).

Table 6.3

6.4.5 Contribution of *BGB_{coarse}* and fine roots to *NPP_{BG}*

In the Miyara River mangrove site, an insignificant difference in belowground coarse roots biomass increment were observed for upstream *B. gymnorrhiza*, downstream *B. gymnorrhiza*, and *R. stylosa* stands ($p > 0.05$, Table 6.4) but total fine root production was lower in the upstream *B. gymnorrhiza* stand than in downstream *B. gymnorrhiza* and *R. stylosa* stands ($p < 0.05$, Table 6.4). For upstream *B. gymnorrhiza* stand, the contribution of *BGB_{coarse}* increment was higher to the total belowground net primary production (*NPP_{BG}*) than fine root production; whereas for downstream *B. gymnorrhiza*, these were equal. For downstream *R. stylosa*, the contribution of fine root production was higher than *BGB_{coarse}* increment (Table 6.4). In the Manko Wetland mangrove, the *BGB_{coarse}* increment contributed less to *NPP_{BG}* than fine roots for *K. obovata* but

for *R. stylosa*, and *B. gymnorrhiza* plots, the contribution of fine roots biomass increments was lower than BGB_{coarse} increment (Table 6.4).

Table 6.4

6.4.6 Contribution of the components to *NPP*

The contribution of *AGB* increment to the *NPP* was lower for upstream *B. gymnorrhiza* than downstream *B. gymnorrhiza* and *R. stylosa* stands along the Miyara River mangrove area; and was lower for *K. obovata* than *R. stylosa*, and *B. gymnorrhiza* plots, respectively in the Manko Wetland (Fig. 6.1 and Table 6.5). Litterfall production contributed highest as 38-41% to the *NPP* in the Miyara River mangrove whereas for Manko Wetland mangrove, the contribution ranged 30-47% (Fig. 6.1 and Table 6.5). Aboveground dead mass production contributed higher for upstream *B. gymnorrhiza* stand than downstream *B. gymnorrhiza*, and *R. stylosa* stands along the Miyara River area; and contributed in similar pattern for the three species in the Manko Wetland (Fig. 6.1 and Table 6.5).

Table 6.5

In the Miyara River, upstream *B. gymnorrhiza* stand had a higher total BGB_{coarse} (belowground coarse root biomass and dead mass increment) proportion to the *NPP* than downstream *B. gymnorrhiza* and *R. stylosa* stands. In contrast, upstream *B. gymnorrhiza* stand had a lower proportion for fine root production than other stands. In the Manko Wetland, the *B. gymnorrhiza* plot contributed more to the increment of BGB_{coarse} than did the *K. obovata* and *R. stylosa* plots, although the *K. obovata* plot contributed more to the fine roots than did the other two species plots. (Fig. 6.1 and Table 6.5). In the Miyara River, the contribution of NPP_{AG} of *NPP* was 70-76% while in the Manko Wetland, it was 61-81%.

Fig. 6.1

6.5 Discussion

6.5.1 Forest structural feature and above-ground biomass distribution

Dominant mangrove species in the Miyara River mangrove found in the present study site was *Bruguiera gymnorrhiza* around the upstream area, while the downstream area was occupied mostly by *R. stylosa* and *B. gymnorrhiza* with some *K. obovata* trees scattered along the banks of the river which is a typical species zonation pattern for mangroves around the Ryukyu archipelago as reported in Enoki et al. (2009) and Suwa et al. (2009). In the present study, a higher *D* class in *B. gymnorrhiza* stands than *R. stylosa* stand was found in the Miyara River mangrove which resulted in a higher cumulative basal area in the *B. gymnorrhiza* stands than that in *R. stylosa*

stand. *B. gymnorrhiza* has more shade-tolerant characteristics when grown in almost the same habitat with *Rhizophora* species (Putz and Chan 1986). The relatively high canopy height (H) and shade-tolerant characteristics of *B. gymnorrhiza* imply a greater potential for them to be dominant than *R. stylosa* at our present study site, similar reported by Enoki et al. (2009) for mangroves in Iriomote Island near the present study site.

The range of estimated AGB as 203.4-298.6 Mg ha⁻¹ in the Miyara River mangrove, and 59.4-255.6 Mg ha⁻¹ in the Manko Wetland mangrove in the present study sites were higher than 97.6-108.1 Mg ha⁻¹ reported for mangroves in Ishigaki Island by Suzuki and Tagawa (1983) that have a mean H of 6 m as opposed to 5.8-8.15 m for the trees in the present study. The AGB and mean H decreased gradually with increasing latitude (Saenger and Snedaker 1993; Khan et al. 2009). The present study site is located in a subtropical zone at a high latitude, and the AGB was relatively high compared to other mangroves in high latitude areas as previously reported in the Ryukyu Islands of Japan (Table 6.6), but similar to some mangroves in low latitude areas.

Table 6.6

On the contrary, mean H remained consistent with that of the other high-latitude mangroves. Although mean H is causally responsible for biomass accumulation (Saenger and Snedaker 1993), other factors, such as basal area and ρ affect AGB . We suspect that the relatively higher cumulative basal area for *R. stylosa* and *B. gymnorrhiza* of the present study (32.9 m² ha⁻¹ in *R. stylosa* and 51.0-53.4 m² ha⁻¹ in *B. gymnorrhiza*) than those in the other high latitude mangroves could contribute to their higher AGB estimation in Miyara river mangrove (Table 6.6). Lower basal area and H in Manko Wetland indicate that the mangrove has not reached its maturity (Table 6.6).

The basal area measured for *B. gymnorrhiza* in the Miyara River mangrove area was higher compared to other studies. The analysis showed that the $D \leq 5$ cm contributes 19% to the total basal area for the downstream *R. stylosa* stand whereas 5% for both downstream and upstream *B. gymnorrhiza* stands. The $D > 5$ cm contributes 81% for *R. stylosa*, and 95% for both downstream and upstream *B. gymnorrhiza* stands. Then, I reanalyzed avoiding the boundary trees exactly at a 7 m distance from the center of each plot (to overcome any error during field measurement). If the boundary trees are avoided to avoid potential overestimation, the values in the basal area do not change much. In the changed condition, the total basal area is reduced to 4 m² ha⁻¹, 5 m² ha⁻¹ and 2 m² ha⁻¹ for downstream *R. stylosa*, downstream *B. gymnorrhiza* and upstream *B.*

gymnorrhiza, respectively. The changed diameter >5 cm comprises 78% for downstream *R. stylosa*, and 99% for both downstream and upstream *B. gymnorrhiza* stands.

Table 6.7

The present study site in the Ishigaki is a riverine mangrove but the study site reported by Suzuki and Tagawa (1983) was the mangrove very close to the sea. Generally, mangroves close to the sea face more stressful conditions than the riverine mangroves. The salinity in this region might not create stress conditions to resist the increase in *D* and *H*.

The present basal area has similarity to the basal area reported by Kamruzzaman et al. (2019) (40-47 m² ha⁻¹) in Okinawa Island, Japan. Again, the basal area in the Miyara River area (1-6.2 m² ha⁻¹) occupied by ≤ 5 cm *D* has similarity with the basal area (1.2-4 m² ha⁻¹) reported by Trettin et al (2015). Kusmana et al (1992) reported lower basal area (2.5 m² ha⁻¹ for *Rhizophora* spp. and 1.2-20.9 for *Bruguiera* spp.) with higher *D* (31.8 cm for *Rhizophora* spp. and 14.8-29.7 cm for *Bruguiera* spp.) than the present study. The stand density reported in his research (32 ha⁻¹ for *R. stylosa* and 52-300 ha⁻¹ for *Bruguiera* spp.) was lower than the present study. So, it is shown that the high mean *D* can show a low basal area if the stand density is low. Describing the singular cause behind the high basal area in the Miyara River mangrove area presents a challenge due to its complexity. In our sites, extremely high stand density contributes to a higher basal area compared to the mangrove forest reported by Suzuki and Tagawa (1983) in Ishigaki Island, even if *D* is smaller.

6.5.2 Belowground coarse and fine root distribution

Stress condition like high salinity reduces *AGB* (Sherman et al. 2003); and *BGB*_{coarse} allocation is positively correlated with that of aboveground parts because these are controlled by the same edaphic factors (Liu et al. 2021). But in our case, the salinity downstream (0.75-1.09‰) was quite lower compared to the salinity of the downstream sites of the Okukubi River (2.58-2.63‰; Suwa et al. 2009) and the Fukido River (2.97-3.30‰; Yoshikai et al. 2022) which implies that the salinity level in the present study stands might not be enough to limit *BGB*_{coarse}. It denotes that the insufficiency of salinity to limit *AGB* allocation also affects on *BGB*_{coarse}. The higher *BGB*_{coarse} in the downstream stands than in the upstream stands was found in the present study site, which was similar to a previous report for *Avicennia marina* and *Aegiceras corniculatum* dominated mangroves (Ball et al. 1997) where they found higher *BGB*_{coarse} with increasing salinity. In addition, a linear trend of increasing *BGB*_{coarse} with increasing soil pore water salinity was observed in *Rhizophora mangle* and *Laguncularia racemosa* dominated mangrove forest at

Samana Bay, Dominican Republic (Sherman et al. 2003). Moreover, the higher BGB_{coarse} in the downstream stands might be a consequence of the higher soil N in this area than in the upstream stands. Also, the root shoot ratio (RSR) has implications for BGB_{coarse} allocation, which generally correlates negatively with H (Wang et al. 2018). In the present study in the Miyara River mangrove, RSR was significantly higher in the *R. stylosa* stands than in the downstream *B. gymnorrhiza* stands ($p < 0.01$, One-way ANOVA, Bonferroni post-hoc test, Table 4.5) where H decreased significantly.

One of the causes of higher RSR in the *R. stylosa* stand than in *B. gymnorrhiza* stands was that a significant part of the root mass was allocated to AGB_{root} in *R. stylosa* whereas most of the root mass was allocated to BGB_{coarse} in *B. gymnorrhiza* (Kamruzzaman et al. 2019).

Table 6.8

Komiyama et al. (1987) observed the higher root biomass within a denser *Rhizophora* spp. forest compared to that of less dense *Bruguiera* spp. and *Sonneratia* spp. forests. In the present study, we also found higher BGB_{coarse} in dense *R. stylosa* stands (11306 ha^{-1}) than in less dense *B. gymnorrhiza* stand ($2572\text{-}4109 \text{ ha}^{-1}$) although the variation in tree density was not significant (Table 4.1).

The mean BGB_{coarse} of *B. gymnorrhiza* plot (56.8 Mg ha^{-1}) in Manko Wetland in the present study was lower; and *B. gymnorrhiza* stands along Miyara river ($231.5\text{-}294.2 \text{ Mg ha}^{-1}$) was higher than that of *B. gymnorrhiza* dominated stand ($106.6\text{-}173.3 \text{ Mg ha}^{-1}$) in southern Thailand (Komiyama et al. 1987). The mean BGB_{coarse} of the present study was consistent with BGB_{coarse} found in the Sundarban mangrove forest in Bangladesh (Table 6.9). BGB_{coarse} of the present study lies in the range of BGB_{coarse} of Hawkesbury river, Australia, Rookery bay and Naples bay, Florida, USA, Mayaguez, Puerto Rico, Samana bay, Dominican Republic and Manko Wetland, Japan (Table 6.8), higher than that of mangroves in Western Australia and Thailand (Table 6.9), and lower than that of mangroves in Indonesia, Brisbane River, Australia, Thailand and Pacific coast, Panama (Table 6.8).

Table 6.9

The significantly lower fine root mass in the downstream *B. gymnorrhiza* stands than in the *R. stylosa* stands in the present study was consistent with a fine root study on Iriomote Island, Japan near the present study site (Fujimoto et al. 2021). The fine root contribution to the total belowground biomass in the present study ($7.3\text{-}29.1\%$) was consistent with that of mangroves in the Dominican Republic (12% , Sherman et al. 2003), Taylor River (14% , Castañeda-Moya et al. 2011) and Shark River (18% , Castañeda-Moya et al. 2011) in the USA; and Micronesia ($13\text{-}22\%$, Cormier et al. 2015); and lower than that in Thailand ($46.3\text{-}56.8\%$, Chalermchatwilai et al. 2011,

Komiyama et al. 1987) (Table 6.7). Lower fine root masses were observed in the low latitudes (Table 6.7) with some exceptions as high fine root mass was observed in low latitude in southern Thailand (137.5-236.4 Mg ha⁻¹, Komiyama et al. 1987) where they used the trench method, and low fine root biomass was observed in high latitude in Mexico (1.8 Mg ha⁻¹, Adame et al. 2014) where they applied ingrowth core method. It should be noted that these previous studies (Komiyama et al. 1987, Adame et al. 2014) applied different sampling methods from the method used in the present study.

6.5.3 Growth conditions at both the study sites

The relatively high soil salinity observed in the downstream stands compared to that in the upstream stands (Table 4.2) in the Miyara River area, was similar to the results of previous studies on mangroves in Japan (Suwa et al. 2009; Enoki et al. 2009; Yoshikai et al. 2022). These studies reported lower canopy heights (Suwa et al. 2009; Enoki et al. 2009) and lower *AGB* (Yoshikai et al. 2022) at downstream sites than at the upstream. In contrast, the present study found that *H* of *B. gymnorhiza* was significantly higher at the downstream stand than at the upstream stand, even though the downstream stands had higher soil salinity and pH than the upstream stands. Furthermore, both *D* and *AGB* in the *B. gymnorhiza* stands showed insignificant variation between downstream and upstream stands. Thus, the results in the present study were not similar to those of previous studies (Suwa et al. 2009; Enoki et al. 2009; Yoshikai et al. 2022), which may be partly due to the difference in soil salinity between the present study site and other mangroves reported by the previous studies, that is, the soil salinity in the downstream stands in the present study site ranged from 0.76-0.91% which was apparently lower than 2.58-2.63% at the downstream site in the Okukubi River (Suwa et al. 2009) and 2.97-3.30% at the downstream site in the Fukido River (Yoshikai et al. 2022). Therefore, we concluded that the salinity conditions at the downstream site in the present study may not be sufficient to limit the growth of mangrove trees. On the other hand, soil *N* was significantly higher at the downstream stands than at upstream stands in the present study site, which can partly explain the reason why the downstream *B. gymnorhiza* stands showed higher mean values in *D*, *H*, *AGB*, *BGB_{coarse}*, and fine roots mass than the upstream *B. gymnorhiza* stands (Table 2.1 of Chapter 2 and Table 6.1). In the Manko Wetland, the *K. ovotata* plot showed the lowest tree density among the species plots having w_t (individual phytomass) of 39.2 kg which is followed by *R. stylosa* and *B. gymnorhiza* with w_t as 10.8 kg and 5.6 kg, respectively. This denotes *K. ovotata* as the pioneer in this region because stand density decreases with the increase of w_t according to self-thinning theory. The lowest *H* and *D* of *B. gymnorhiza* also support that it is in the growing stage.

6.5.4 Above and belowground biomass increment

Stem and branch biomass increment were two major components contributing to the total *AGB* of all the species in the two sites. Leaf biomass increment of *B. gymnorrhiza* in the Manko Wetland ($2 \text{ Mg ha}^{-1} \text{ y}^{-1}$) was quite higher than in Miyara River ($0.1\text{-}0.7 \text{ Mg ha}^{-1} \text{ y}^{-1}$) while the biomass increments were not significantly different between the two study sites. The mangrove forest along the Miyara River was old-growth and *B. gymnorrhiza* was a pioneer species with a higher diameter (13-17 cm) and height (6.7-8.2 m) class but *B. gymnorrhiza* in the Manko Wetland was a young stand with a low diameter (4.1 cm) and height (3.9 m) class (Table 2.1, Chapter 2). The growing stage of *B. gymnorrhiza* in Manko Wetland might be one reason for producing more leaves. The aboveground root contributed to the *AGB* as well as total biomass of *R. stylosa* which was absent in other species. *R. stylosa* produces aboveground roots which contribute to the aboveground biomass but the root system is mainly belowground for *B. gymnorrhiza* and *K. obovata* although they produce aboveground roots (Kamruzzaman et al. 2019), which were not included in this study. AGB_{roots} contributed 18-19% to the *AGB* of *R. stylosa* in the present study which is slightly higher to the contribution reported for *Rhizophora* species found in the Matang mangrove forest in Malaysia (13%, Ong et al. 2004) and mangrove forest in East Sumatra, Indonesia (13%, Kusmana et al. 1992). The *AGB* increment of *R. stylosa* in the present study ($11\text{-}13 \text{ Mg ha}^{-1} \text{ yr}^{-1}$) was higher than *R. mangle* dominated mangrove forests at Laguna de Términos, Mexico ($8\text{-}12 \text{ Mg ha}^{-1} \text{ y}^{-1}$; Day et al. 1987) and $6 \text{ Mg ha}^{-1} \text{ yr}^{-1}$ recorded for *R. stylosa* at Missionary Bay, Australia (Clough 1998) and but is consistent with the value measured in Manko Wetland ($16 \text{ Mg ha}^{-1} \text{ yr}^{-1}$, Kamruzzaman et al. 2019). Kangkuso et al. (2016) showed that the *AGB* of mangrove forest differs depending on tree age, stand structure and environmental characteristics.

6.5.5 Aboveground net primary production

Total litterfall is an important component playing a major role to the NPP_{AG} . The contribution of litterfall to the NPP_{AG} in the present study (41-75%) showed similarity with mixed species stands of Dominican Republic (42%, 19.7 Mg ha^{-1} , Sherman et al. 2003). The litterfall were higher in the present study than that of the *K. obovata* dominated mangrove patch of Manko Wetland ($29.9\text{-}32.1 \text{ Mg ha}^{-1}$, Khan et al. 2009) and *K. obovata*-*R. stylosa*-*B. gymnorrhiza* dominated forest in Manko Wetland (28.6 Mg ha^{-1} , Kamruzzaman et al. 2017), which for both litterfall contributed 35% of NPP_{AG} . NPP_{AG} of *R. stylosa* in the present study was similar to the *R. mangle* (28 Mg ha^{-1}) dominated mangrove forest in Florida, USA (Ross et al. 2001) having 19-21% biomass increment as AGB_{root} , *R. stylosa* in the Manko Wetland (49 Mg ha^{-1} , Kamruzzaman et al. 2017)

having 6% AGB_{root} increment, but more than the *R. apiculata* mangrove of Malaysia (12-22 Mg ha⁻¹, Ong et al. 1981). NPP_{AG} in the present study was lower than that in the *Rhizophora-Bruguiera* spp. dominated mangroves of Sawi Bay and Florida, USA having 19% AGB_{root} increment in both cases (49 Mg ha⁻¹, Alongi et al. 2000 and 55 Mg ha⁻¹, Carter 1973).

6.5.6 Contribution of BGB_{coarse} and fine roots to NPP_{BG}

Total BGB_{coarse} increment and fine roots production of *B. gymnorrhiza* and *R. stylosa* were relatively higher in the Miyara River mangrove than that in the Manko Wetland mangrove. Belowground biomass is positively correlated with that of aboveground parts because these are controlled by the same edaphic factors (Liu et al. 2021). Moreover, higher soil *N* in the downstream part (0.16-0.17%, Table 3.2, Chapter 3) of the Miyara River than that in the upstream (0.12%, Table 3.2, Chapter 3) supports the higher belowground production in the downstream. BGB_{coarse} increment in the present study (1-6 Mg ha⁻¹) are in a similar range to the mangroves of mixed species in Panama, Australia, and New Zealand (3-5 Mg ha⁻¹, Lovelock 2008), *Rhizophora mangle* dominated mangrove of Twin Cays, Belize (1-5 Mg ha⁻¹, McKee et al. 2007). The total fine root production in the present study (2-7 Mg ha⁻¹) was lower than that of *Sonneratia alba* dominated mangrove in Okat River, Micronesia (8 Mg ha⁻¹, Gleason and Ewel 2002) and mixed species mangrove in Shark river and Tylor River, Florida, USA (4-7 Mg ha⁻¹, Castaneda-Moya et al. 2011) and more than the mixed species mangrove of Yela river and Sapwalap river, Micronesia (1-5 Mg ha⁻¹, Cormier et al. 2015) but has similarities with *Rhizophora mangle* dominated mangrove in Rokey bay and Naples bay, Florida, USA (3-4 Mg ha⁻¹, Giraldo Sánchez 2005), Ryzophoracea family dominated mangroves in Windstar and Henderson Creek, Florida, USA (1-3 Mg ha⁻¹, McKee and Faulkner 2000).

6.5.7 NPP in the Miyara River mangrove and the Manko Wetland mangrove

The total NPP of *B. gymnorrhiza* stand was higher in the downstream plots than in upstream plots at the Miyara River sites although the differences were insignificant. Soil pore water salinity was higher in the downstream stand than in the upstream stand. The salinity was quite lower in the downstream (0.75-1.09%, Table 2.3, Chapter 2) compared to that in the downstream sites of Okukubi River (2.58-2.63%; Suwa et al. 2009) and in the Fukido river (2.97-3.30%; Yoshikai et al. 2022) which implies that the salinity level in the present study might not be enough to limit productivity. The higher soil *N* content could promote higher productivity in the downstream stand than in the upstream stand. The total belowground root production was lower in *R. stylosa* than that of downstream *B. gymnorrhiza* which was due to the fact that a significant part of AGB

was allocated for the aboveground aerial root of *R. stylosa* which was considered negligible for *B. gymnorrhiza*. The mean temperature was higher along the Miyara River, Ishigaki Island, than in the Manko Wetland, Okinawa Island, which may explain the higher productivity along the Miyara River than in the Manko Wetland. Total *NPP* of all the species of the present study is more than Rhizophora forest, *Xylocarpus-Bruguiera* forest and Avicinnia-Sonneratia forest (12.4, 10 and 12 Mg ha⁻¹) of Eastern Thailand (Poungparn et al. 2012) and mixed forest of Sundarban, Bangladesh (21 Mg ha⁻¹, Kamruzzaman et al. 2017). Both of the present study sites occupy river-oriented mangroves and located near the sea. Thus, the sites are flushed recurrently by tides which may cause higher *NPP* due to being exposed to high nutrient concentrations. Similar findings were noticed in Kandellia-Rhizophora-Bruguiera dominated (43 Mg ha⁻¹) mangrove of Okukubi River, Japan (Kamruzzaman et al. 2019) which has high *NPP* which is flushed frequently by tides. The value of RSR (root shoot ratio) is lower (0.35-0.52, Table 4.5) in the present study than the terrestrial inland forest of tropical areas (5–11, Ogawa et al. 1965). It indicates that a major portion of biomass in the mangrove is allocated to the belowground than in terrestrial plants which makes RSR in mangroves lower than terrestrial plants. Another reason for large biomass allocation in the belowground may be adapt to the harsh environment as cope with the stress of the saline and high-water tables environment.

Figures

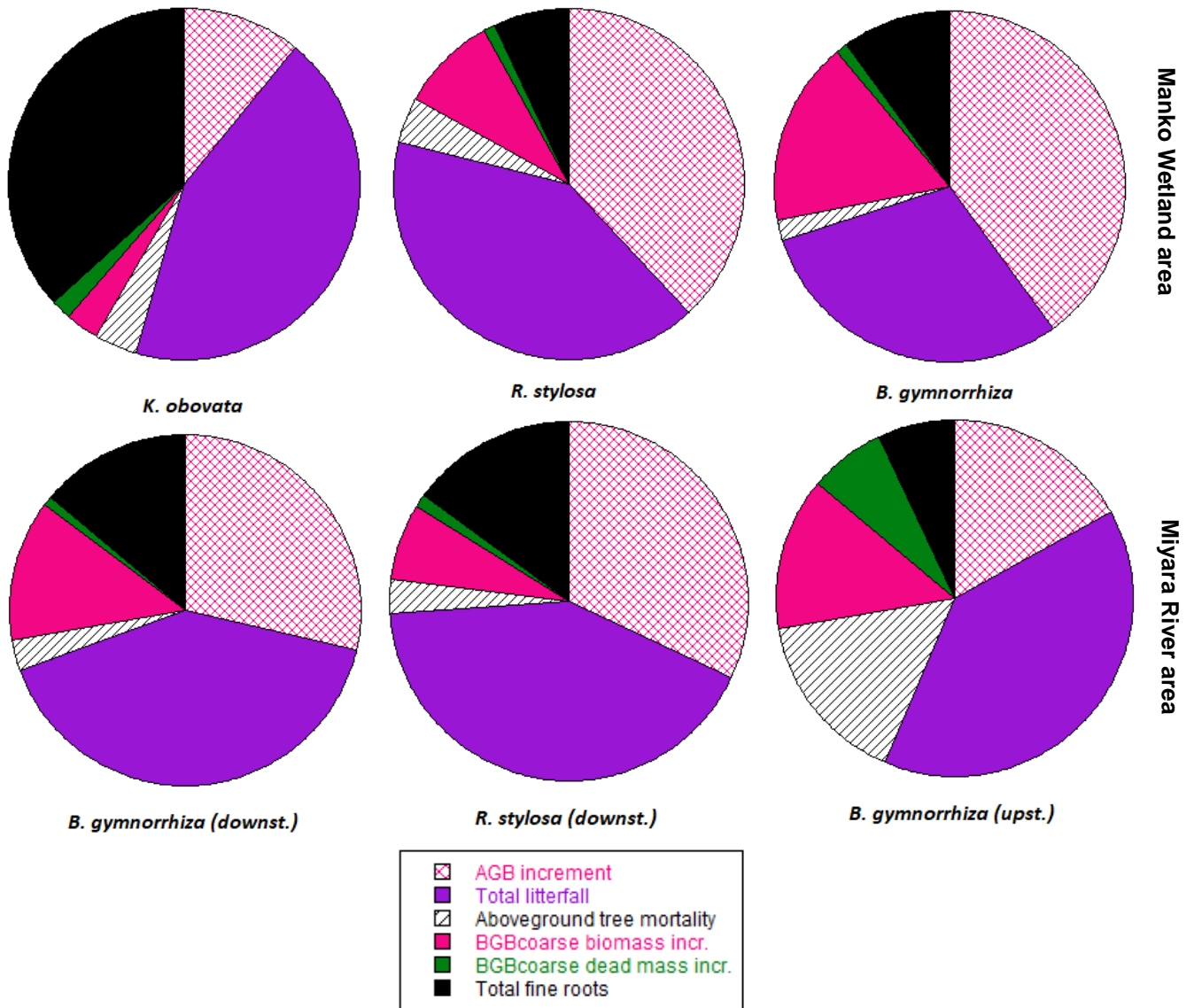


Fig. 6.1: The contribution of each of the increment of each of the components to the total *NPP* of the three species at two study sites.

Tables

Table 6.1: Aboveground biomass *AGB*, belowground coarse root biomass *BGB_{coarse}* and fine root mass of upstream and downstream *B. gymnorrhiza* plots, and downstream *R. stylosa* plots of Miyara River mangrove and *K. obovata*, *R. stylosa* and *B. gymnorrhiza* plots of Manko Wetland mangrove. The *AGB*, *BGB_{coarse}* data of 2023 were used for the Miyara River mangrove and data of 2022 were used for the Manko Wetland mangrove. The fine roots collected during March, 2021 to March, 2022 were used for the Miyara River mangrove and the mean of the fine roots collected from March, 2019 to March, 2020 and from March, 2021 to March, 2022 were used for the Manko Wetland mangrove. We used the mean data of each plot for making comparisons among stands in the Miyara River area but used the actual value for comparing among the species plots in Manko Wetland. Mean values are shown with S.D. Here, values matched with the different letters were significantly different ($p < 0.05$).

Species	<i>AGB</i> (Mg ha ⁻¹)	<i>BGB_{coarse}</i> (Mg ha ⁻¹)	Fine root mass (Mg ha ⁻¹)
<i>B. gymnorrhiza</i> (upstream)	261.4 ± 35.9 ^{ab}	110.5 ± 15.6 ^b	8.95 ± 3.26 ^b
<i>B. gymnorrhiza</i> (downstream)	298.6 ± 100 ^b	122 ± 39 ^b	12.13 ± 1.21 ^a
<i>R. stylosa</i> (downstream)	203.4 ± 66.3 ^a	52.3 ± 21 ^a	15.61 ± 1.16 ^a
<i>K. obovata</i> (Manko Wetland)	58.3	24.6	11.37
<i>R. stylosa</i> (Manko Wetland)	243.6	66.5	7.42
<i>B. gymnorrhiza</i> (Manko Wetland)	148.8	59.3	8.85

Table 6.2: Increment of leaves, stems, branch, AGB_{root} and AGB ($\text{Mg ha}^{-1} \text{y}^{-1}$) of upstream and downstream *B. gymnorrhiza* plots, downstream *R. stylosa* plots in the Miyara River mangrove, and *K. obovata*, *R. stylosa* and *B. gymnorrhiza* plots in the Manko Wetland of Japan. The biomass increments of leaf, stem, branch, AGB_{root} and AGB from 2022 to 2023 were used for the Miyara River mangrove whereas the mean of the biomass increments from 2019 to 2020 and from 2021 to 2022 were used for *K. obovata* and *R. stylosa*, and biomass increment from 2021 to 2022 were used for *B. gymnorrhiza* to show the mean increment in the Manko Wetland mangrove. The For, Miyara River mangrove, (mean \pm S.E) error bar shows the standard error of the plots. Proportion of biomass (%) to the total AGB increment is shown in parenthesis.

Plots	Leaf biomass increment in $\text{Mg ha}^{-1} \text{y}^{-1}$	Stem biomass increment in $\text{Mg ha}^{-1} \text{y}^{-1}$	Branch biomass increment in $\text{Mg ha}^{-1} \text{y}^{-1}$	AGB_{root} biomass increment in $\text{Mg ha}^{-1} \text{y}^{-1}$	Total AGB increment ($\text{Mg ha}^{-1} \text{y}^{-1}$)
<i>B. gymnorrhiza</i> (upstream, Miyara river)	0.1 ± 0.8 (1%)	1.7 ± 4 (32%)	3.7 ± 3 (67%)	-	5.4 ± 8
<i>B. gymnorrhiza</i> (downstream, Miyara river)	0.5 ± 0.5 (5%)	4.1 ± 2 (39%)	5.8 ± 2 (56%)	-	10.4 ± 5
<i>R. stylosa</i> (downstream, Miyara river)	0.7 ± 0.6 (6%)	6.4 ± 5 (55%)	2.1 ± 2 (18%)	2.5 ± 1 (21%)	11.7 ± 8
<i>K. obovata</i> (Manko Wetland)	0.1 (5%)	1 (49%)	1 (46%)	-	2.1
<i>R. stylosa</i> (Manko Wetland)	0.5 (4%)	5.5 (53%)	2.5 (24%)	1.9 (19%)	10.5
<i>B. gymnorrhiza</i> (Manko Wetland)	1.9 (15%)	7.2 (55%)	3.9 (30%)	-	13

Table 6.3: Increment of *AGB*, total litterfall, tree dead mass increment, and NPP_{AG} ($Mg\ ha^{-1}\ y^{-1}$) of upstream and downstream *B. gymnorrhiza* stands, downstream *R. stylosa* stand along the Miyara River, and *K. obovata*, *R. stylosa* and *B. gymnorrhiza* plots in the Manko Wetland of Japan. The *AGB* and tree dead mass increments, and total litterfall production from 2022 to 2023 were used for the Miyara River mangrove whereas in the Manko Wetland mangrove, the mean values from 2019 to 2020 and from 2021 to 2022 were used for *K. obovata* and *R. stylosa*, and from 2021 to 2022 were used for *B. gymnorrhiza*. Here, the comparison was done within the Miyara River species stands. Letter matched with different values show significant variation. Proportion of the components (%) to the NPP_{AG} is shown in parenthesis.

Plots	<i>AGB</i> increment	Total litterfall production	Tree dead mass increment	NPP_{AG} ($Mg\ ha^{-1}\ y^{-1}$)
<i>B. gymnorrhiza</i> (upstream, Miyara River))	5.4 ± 8 ^a (24%)	12.7 ± 0.5 ^a (54%)	5.1 ± 5 ^a (22%)	23.2 ± 6 ^a
<i>B. gymnorrhiza</i> (downstream, Miyara River)	10.4 ± 5 ^a (41%)	14.1 ± 0.8 ^{ab} (55%)	0.9 ± 1.2 ^a (4%)	25.3 ± 3 ^a
<i>R. stylosa</i> (downstream, Miyara River)	11.7 ± 9 ^a (42%)	15.2 ± 0.7 ^b (54%)	1.1 ± 2.1 ^a (4%)	28 ± 7 ^a
<i>K. obovata</i> (Manko Wetland)	2 (18%)	9 (76%)	0.7 (6%)	11.7
<i>R. stylosa</i> (Manko Wetland)	10.5 (45%)	12 (51%)	1 (4%)	23.6
<i>B. gymnorrhiza</i> (Manko Wetland)	13 (56%)	9.6 (41%)	0.8 (3%)	23.3

Table 6.4: $\Delta BGB_{\text{coarse-living}}$, $\Delta BGB_{\text{coarse-dead}}$, fine root production, NPP_{BG} ($\text{Mg ha}^{-1} \text{y}^{-1}$) of upstream and downstream *B. gymnorrhiza* plots, downstream *R. stylosa* plots in Miyara river mangrove, and *K. obovata*, *R. stylosa* and *B. gymnorrhiza* plots in Manko Wetland of Japan. The $\Delta BGB_{\text{coarse-living}}$, $\Delta BGB_{\text{coarse-dead}}$, fine root production and NPP_{BG} from 2022 to 2023 were used for the Miyara River mangrove whereas mean values from 2019 to 2020 and from 2021 to 2022 were used for *K. obovata* and *R. stylosa*, and values from 2021 to 2022 were used for *B. gymnorrhiza* to show the mean increment in the Manko Wetland mangrove. Here, the comparison was done within the Miyara River species stands. Letter matched with different values show significant variation. Proportion of the components (%) to the NPP_{BG} is shown in parenthesis.

Plots	$\Delta BGB_{\text{coarse-living}}$ in $\text{Mg ha}^{-1} \text{y}^{-1}$	$\Delta BGB_{\text{coarse-dead}}$ in $\text{Mg ha}^{-1} \text{y}^{-1}$	Fine root production in $\text{Mg ha}^{-1} \text{y}^{-1}$	NPP_{BG} ($\text{Mg ha}^{-1} \text{y}^{-1}$)
<i>B. gymnorrhiza</i> (upstream, Miyara River))	4.5 ± 3^a (46%)	2.5 ± 4^a (26%)	2.8 ± 1^a (28%)	9.8 ± 6^a
<i>B. gymnorrhiza</i> (downstream, Miyara River)	4.5 ± 1^a (45%)	0.4 ± 0.6^a (3%)	5.2 ± 2^a (52%)	10 ± 3^a
<i>R. stylosa</i> (downstream, Miyara River)	2.7 ± 2^a (31%)	0.3 ± 0.5^a (4%)	5.6 ± 3^a (65%)	8.6 ± 4^a
<i>K. obovata</i> (Manko Wetland)	0.6 (8%)	0.3 (3%)	6.5 (89%)	7.5
<i>R. stylosa</i> (Manko Wetland)	2.5 (52%)	0.3 (6%)	2.7 (42%)	5.6
<i>B. gymnorrhiza</i> (Manko Wetland)	5.5 (61%)	0.3 (3%)	3.3 (36%)	9.1

Table 6.5: Aboveground biomass increment (*AGB*), belowground biomass (*BGB_{coarse}*) increment, fine root production, total litterfall, tree dead mass increment, and net primary production (*NPP*) of upstream and downstream *B. gymnorrhiza* plots, downstream *R. stylosa* plots in Miyara river mangrove, and *K. obovata*, *R. stylosa* and *B. gymnorrhiza* plots in Manko Wetland of Japan. The increments from 2022 to 2023 were used for the Miyara River mangrove whereas in the Manko Wetland mangrove, the mean values from 2019 to 2020 and from 2021 to 2022 were used for *K. obovata* and *R. stylosa*, and from 2021 to 2022 were used for *B. gymnorrhiza*. Here, the comparison was done within the Miyara River species stands. Letter matched with different values show significant variation.

Plots	<i>NPP_{AG}</i> (Mg ha ⁻¹ y ⁻¹)			<i>NPP_{BG}</i> (Mg ha ⁻¹ y ⁻¹)			Total <i>NPP</i> (Mg ha ⁻¹ y ⁻¹)
	<i>AGB</i> increment	Total litterfall production	Tree dead mass increment	<i>BGB_{coarse}</i> increment		Fine root production	
				<i>BGB_{coarse}</i> biomass	<i>BGB_{coarse}</i> dead mass		
<i>B. gymnorrhiza</i> (upstream, Miyara River))	5.4 ± 8 ^a	12.7 ± 0.5 ^a	5.1 ± 5 ^a	4.5 ± 3 ^a	2.5 ± 4 ^a	2.8 ± 1 ^a	33 ± 12 ^a
<i>B. gymnorrhiza</i> (downstream, Miyara River)	10.4 ± 5 ^a	14.1 ± 0.8 ^{ab}	0.9 ± 1.2 ^a	4.5 ± 1 ^a	0.4 ± 0.6 ^a	5.2 ± 2 ^a	35.3 ± 5 ^a
<i>R. stylosa</i> (downstream, Miyara River)	11.7 ± 9 ^a	15.2 ± 0.7 ^b	1.1 ± 2.1 ^a	2.7 ± 2 ^a	0.3 ± 0.5 ^a	5.6 ± 3 ^a	36.3 ± 9 ^a
<i>K. obovata</i> (Manko Wetland)	2	9	0.7	0.6	0.3	6.5	19.3
<i>R. stylosa</i> (Manko Wetland)	10.5	12	1	2.5	0.3	2.7	29
<i>B. gymnorrhiza</i> (Manko Wetland)	13	9.6	0.8	5.5	0.3	3.3	32.4

Table 6.6: Locations, forest types, dominant species, latitude, aboveground biomass *AGB*, tree density ρ (ha^{-1}), basal area ($\text{m}^2 \text{ha}^{-1}$) and mean *H* (m) at different mangroves.

Location	Forest types	Dominant species	Latitude ($^{\circ}$)	<i>AGB</i> (Mg ha^{-1})	ρ (ha^{-1})	Basal Area ($\text{m}^2 \text{ha}^{-1}$)	<i>H</i> (m)	Reference
Miyara River (Downstream), Ishigaki	Primary	<i>R. stylosa</i>	24.35	203.4	11306	32.88	5.8	Present Study
Miyara River (Downstream), Ishigaki	Primary	<i>B. gymnorrhiza</i>	24.35	298.6	2864	53.39	6.7	Present Study
Miyara River (Upstream), Ishigaki	Primary	<i>B. gymnorrhiza</i>	24.35	261.4	4531	51	8.15	Present Study
Manko Wetland	Primary	<i>K. Obovata</i>	26.18	58.3	5800	17.6	5.1	Present Study
Manko Wetland	Primary	<i>R. stylosa</i>	26.18	243.6	18700	46	5.2	Present Study
Manko Wetland	Primary	<i>B. gymnorrhiza</i>	26.18	148.8	26300	36	3.9	Present Study
Ryukyu Islands, Japan	Primary	<i>B. gymnorrhiza</i>	26	107.1	7522	25.45	6.3	Nakasuga (1979)
Ryukyu Islands, Japan	Primary	<i>Rhizophora</i> spp.	26	185.3	9600	48.03	7.2	Nakasuga (1979)
Ishigaki Island, Japan	Primary	<i>B. gymnorrhiza</i>	24	97.6	N/R	32.9	6	Suzuki & Tagawa (1983)
Ishigaki Island, Japan	Primary	<i>R. stylosa</i>	24	108.1	N/R	22.7	6	Suzuki & Tagawa (1983)
East Sumatra, Indonesia	Concession area	<i>Bruguiera</i> spp.	1	177.9	281	14.39	19.7	Kusmana et al. (1992)
East Sumatra, Indonesia	Concession area	<i>Rhizophora</i> spp.	1	40.7	32	2.5	29.5	Kusmana et al. (1992)
Maluku Island, Indonesia	Primary	<i>R. stylosa</i>	1.20	178.2	206	13.96	22.3	Komiyama et al. (1988)
Maluku Island, Indonesia	Primary	<i>B. gymnorrhiza</i>	1.20	421.5	350	36.03	24.4	Komiyama et al. (1988)
Ranong, Thailand	Primary	<i>Rhizophora</i> spp.	9	398.8	1246	20.78	10.6	Tamai et al. (1986)
Puerto Rico	N/A	<i>Rhizophora</i> spp.	18	62.9	13600	N/R	8	Golley et al. (1962)
Panama	Primary	<i>Rhizophora</i> spp.	9	279.2	712	13.6	30-40	Golley et al. (1969)
Sungai Merbok, Malaysia	Old growth	<i>Rhizophora</i> spp.	5	314	N/R	N/R	15	Ong et al. (1981)

Table 6.7: The changed total basal area ($\text{m}^2 \text{ha}^{-1}$) of upstream and downstream *B. gymnorrhiza* and downstream *R. stylosa* stands along with the changed contribution (%) of trees of $D \leq 5$ cm and $D > 5$ cm avoiding the trees at the 7 m from the center.

Stands	Basal area		
	Total ($\text{m}^2 \text{ha}^{-1}$)	$D \leq 5$ cm	$D > 5$ cm
<i>B. gymnorrhiza</i> (upstream)	49.9	1.3%	98.7%
<i>B. gymnorrhiza</i> (downstream)	47.9	0.6%	99.4%
<i>R. stylosa</i> (downstream)	28.1	21.9%	78.1%

Table 6.8: Locations, dominant species, latitude, total belowground biomass BGB_{total} including coarse and fine roots mass, fine roots mass percentage in BGB_{total} , and root shoot ratio RSR are shown for different mangroves.

Locations	Dominant Species	Latitude ($^{\circ}$)	BGB_{total} (Mg ha $^{-1}$)	Fine roots (Mg ha $^{-1}$)	Fine roots mass to BGB_{total} (%)	Root shoot ratio (RSR)	Reference
Miyara River, Ishigaki (Downstream)	<i>R. stylosa</i>	24.35	52.3	13	21	0.52 ^a	Present study
Miyara River, Ishigaki (Downstream)	<i>B. gymnorrhiza</i>	24.35	122	11	8.6	0.35 ^b	Present study
Miyara River, Ishigaki (Upstream)	<i>B. gymnorrhiza</i>	24.35	110.5	6.4	5.7	0.35 ^b	Present study
Celestun, Yucatan, Mexico	<i>Rhizophora</i> spp	20.71	11.3	1.8	15.9	N/A	Adame et al. (2014)
Taylor River, US	<i>Rhizophora</i> spp	38.92	23.2	3.2	13.8	1.96	Castañeda-Moya et al. (2011)
Shark River, US	<i>Rhizophora</i> spp	40.19	31.9	5.8	18.2	0.35	Castañeda-Moya et al. (2011)
Trat River, Thailand	<i>R. stylosa</i>	12.24	42.9	21.9	51	N/A	Chalermchatwilai et al. (2011)
Samana Bay, Dominican Republic	<i>Rhizophora</i> spp	19.10	66	7.9	12	N/A	Sherman et al. (2003)
Southern Thailand	<i>Bruguiera</i> spp.	9.97	242.6	137.5	56.8	N/A	Komiyama et al. (1987)
Southern Thailand	<i>Rhizophora</i> spp	9.97	509.5	236.4	46.4	N/A	Komiyama et al. (1987)
Magueyes Island, Puerto Rico	<i>Rhizophora</i> spp	18	3.9	2.4	62.1	0.68	Golley et al. (1962)
Yela river, Micronesia	<i>Bruguiera</i> spp.	5.32	9.5	1.5	15.8	0.07	Cormier et al. (2015)
Yela river, Micronesia	<i>Rhizophora</i> spp	5.32	14.3	1.8	12.6	0.05	Cormier et al. (2015)
Sapwalap river, Micronesia	<i>Bruguiera</i> spp.	6.95	4.5	1.7	37.8	0.05	Cormier et al. (2015)
Sapwalap river, Micronesia	<i>Rhizophora</i> spp	6.95	13.7	2.9	21.2	0.02	Cormier et al. (2015)

Table 6.9: Comparison of BGB_{coarse} (Mg ha^{-1}) of the present study with other studies

Location	BGB_{coarse} (Mg ha^{-1})	Reference
Miyara River, Ishigaki	52.3-122	Present study
Sundarban, Bangladesh	82	Kamruzzaman et al. 2018
Hawkesbury River, Australia	35-166	Saintilan 1997
Rookery Bay and Naples bay, Florida, USA	61.85-153.95	Giraldo Sánchez 2005
Mayaguez, Puerto Rico	64.4	Golley et al. 1962
Samana Bay, Dominican Republic	67.8	Sherman et al. 2003
Manko Wetland, Japan	71.8	Khan et al. 2009
Manko Wetland, Japan	71.5	Khan and Kabir 2017
Western Australia	17.90-50.30	Alongi et al. 2000
Thailand	25.48-45.77	Poungparn et al. 2016
Thailand	84.80-509.50	Komiyama et al. 1987 and Komiyama et al. 2000
Indonesia	164.44-178.45	Komiyama et al. 1988
Brisbane River, Australia	109-127	Mackey 1993
Pacific coast, Panama	306	Golley et al. 1969

Chapter 7

7. Conclusion and recommendation

In Chapter 2, the downstream stand of the Miyara River mangrove was characterized by higher salinity and lower pH than the upstream area but the estimated mean D , AGB , and BGB_{coarse} were not significantly higher in the upstream *B. gymnorrhiza* stands than those in the downstream *B. gymnorrhiza* stands. In addition, the $H - D$ relationships also did not differ between the upstream and downstream *B. gymnorrhiza* stands. Mean D , mean H , AGB and BGB_{coarse} were lower in the *R. stylosa* stands than that in the *B. gymnorrhiza* stands at downstream area. In the Manko Wetland, significant difference among soil salinity and pH was observed. Higher soil N could account for higher fine root production in *K. obovata* than other two plots.

In Chapter 3, allometric models were developed using simple allometric equations based on power functions to predict the biomass of the different components of a tree for two species. The coefficients differed between the two species due to differences in height and diameter classes which affected the biomass distribution. The general view showed that the Miyara River mangrove is an old-growth mangrove forest but the mangrove in the Manko Wetland is relatively young with a low diameter (4.1) and height (3.9 m) class. The developed biomass allometric models of *B. gymnorrhiza* and *R. stylosa* will be useful to assess the biomass, nutrients and carbon cycling in this region which might be helpful for future sustainable mangrove forest management. Moreover, the findings of this study can contribute to planning for utilization and management of these species in nearby subtropical areas.

In Chapter 4, I found that all the species showed the highest total litterfall in summer including litterfall of leaves and stipules, and the lowest in winter. The litterfall of flowers and fruits peaked in July for *R. stylosa*, and in August and again in October–November for *K. obovata*. Finally, it was observed that the temperature and rainfall impacted the seasonality of litter production whenever litters were collected monthly, found that the maximum litterfall was found during high temperature and rainfall season. A strong correlation between the monthly production of litterfall with temperature and rainfall was observed in the Miyara River mangrove but not found in another site. Furthermore, the litterfall production varied between the species although no significant variation was observed in litterfall between upstream and downstream stands in the Miyara River area. The amount of litterfall was higher in the Miyara River mangrove than in the Manko Wetland, likely because the Miyara River mangrove is a naturally developed old-growth forest which showed higher diameter and height class along with higher tree density compared to the Manko Wetland, suggesting higher production of foliage.

In Chapter 5, seasonal variation in fine root production, mortality within the same species stand was clearly observed in the Miyara River mangrove but the variation was not clear in the Manko Wetland mangrove. Moreover, biomass and necromass in different sampling months in both sites showed variation whereas the very fine roots showed higher values than fine roots. The high amount of necromass indicated that a large amount of organic matter is available for decomposition that enrich production. There was significant seasonal variation in soil salinity and pH between upstream and downstream sites, and between species downstream but the correlation with fine root production was not significant in the Miyara River mangrove. Contrast to the Miyara River mangrove, seasonal variations of soil salinity, pH were not significant for any species in the Manko Wetland mangrove. Differences were found between species plots, which were however not significantly correlated with fine root production.

In Chapter 6, *NPP* was higher, although not significant, downstream than upstream in *B. gymnorrhiza* despite higher soil salinity. Insignificant difference in *NPP* was observed between the two species downstream. The *NPP* between the three species at the Manko Wetland cannot be compared although difference in soil *N* was observed. The variation in litterfall and fine root production did not impact on the total *NPP*. A similar contribution of the belowground biomass increments was observed in two study areas (6-19% in the Miyara River mangrove and 9-16% in the Manko Wetland mangrove). There was no significant variation in the belowground root production among different species or same species between upstream and downstream, although there was significant differences in the carbon allocation (biomass) to fine roots and coarse roots between the species.

Total dead mass increment of upstream *B. gymnorrhiza* was higher than that in downstream, and seems unusual, requiring further studies over multiple years to clarify the overall scenario of the increment of dead mass. At a glance, I observed that one upstream *B. gymnorrhiza* plot among the four plots, very close to the bank of the Miyara River with the highest diameter and height classes, was severely damaged during the cyclone.

In the Manko Wetland, I found comparatively lower values of the total *NPP* in the *K. obovata* plot than in the other two species plots. Very low tree density in *K. obovata* plot resulted in less biomass and litter production than the other two species.

The contribution of the components to total *NPP* was very similar in the two study areas. Shared species characters and natural habitats might be responsible for this similarity. *R. stylosa* generally grows at the edge of the rivers and produces stilt or prop roots. One of the functions of this kind of specialized root is to provide mechanical strength. This root system might be responsible for the relatively higher contribution of fine roots in *R. stylosa* than *B. gymnorrhiza*

because a part of the specialized root system enters into soil which might contribute to fine root production. The growth condition of the relatively younger *B. gymnorrhiza* in the Manko Wetland mangrove (low *D* and *H* class) than Miyara River mangrove denotes that the trees grows better in the early stage. Significantly higher fine root production for *K. obovata* than for the other two species in the Manko Wetland could potentially be related to the fact that *K. obovata* grows in the clay and muddy environment, which is favorable for fine root production, while the other two species grow in sandy environments.

Several implications for the management of mangrove forests and designing further studies were obtained. In the Miyara River mangrove, there was no clear difference in biomass carrying capacity along the tidal gradient within the *B. gymnorrhiza* stands through the analysis of $w_t-\rho$ relationship. However, it is necessary to conduct further research on the biomass carrying capacity in various mangroves because mangroves show wide variations in forest structure due to their complex environmental dynamics. Long-term observation would provide valuable information to deepen our comprehension about growth condition in both above- and belowground parts.

The present study indicates that the *NPP* of the mangrove forest near the northern limit of its geographical distribution along the Miyara River of Ishigaki Island and in the Manko Wetland of Okinawa Island contributes to global blue carbon budget because high biomass accumulation and productivity designates high carbon turnover of the species stands. It can be used as important information to the decision makers involved in mangrove forest management.

References

- Aber JD, Melillo JM, Nadelhoffer KJ, et al (1985) Fine root turnover in forest ecosystems in relation to quantity and form of nitrogen availability: a comparison of two methods. *Oecologia* 66:317–321. <https://doi.org/10.1007/BF00378292>
- Adame MF, Teutli C, Santini NS, et al (2014) Root biomass and production of mangroves surrounding a karstic oligotrophic coastal lagoon. *Wetlands* 34:479–488. <https://doi.org/10.1007/s13157-014-0514-5>
- Aiba SI, Kohyama T (1997) Crown architecture and life-history traits of 14 tree species in a warm- temperate rain forest: significance of spatial heterogeneity. *J Ecol* 85:611. <https://doi.org/10.2307/2960532>
- Aké-Castillo JA, Vázquez G, López-Portillo J (2006) Litterfall and decomposition of *Rhizophora mangle* l. in a coastal lagoon in the southern Gulf of Mexico. *Hydrobiologia* 559:101–111. <https://doi.org/10.1007/s10750-005-0959-x>
- Alemayehu F, Richard O, James KM, Wasonga O (2014) Assessment of mangrove covers change and biomass in Mida Creek, Kenya. *Open J For* 04:398–413. <https://doi.org/10.4236/ojf.2014.44045>
- Alongi DM (2011) Patterns of mangrove wood and litter production within a beach ridge-fringing reef embayment, northern great barrier reef coast. *Estuaries Coasts* 34:32–44. <https://doi.org/10.1007/s12237-010-9289-y>
- Alongi DM, Tirendi F, Clough BF (2000) Below-ground decomposition of organic matter in forests of the mangroves *Rhizophora stylosa* and *Avicennia marina* along the arid coast of Western Australia. *Aquat Bot* 68:97–122. [https://doi.org/10.1016/S0304-3770\(00\)00110-8](https://doi.org/10.1016/S0304-3770(00)00110-8)
- Atwood TB, Connolly RM, Almahasheer H, et al (2017) Global patterns in mangrove soil carbon stocks and losses. *Nat Clim Change* 7:523–528. <https://doi.org/10.1038/nclimate3326>
- Baishya R, Barik SK (2011) Estimation of tree biomass, carbon pool and net primary production of an old-growth *Pinus kesiya* Royle ex. Gordon forest in north-eastern India. *Ann For Sci* 68:727–736. <https://doi.org/10.1007/s13595-011-0089-8>
- Ball MC, Cochrane MJ, Rawson HM (1997) Growth and water use of the mangroves *Rhizophora apiculata* and *R. stylosa* in response to salinity and humidity under ambient and elevated concentrations of atmospheric CO₂. *Plant Cell Environ* 20:1158–1166. <https://doi.org/10.1046/j.1365-3040.1997.d01-144.x>
- Basuki TM, Van Laake PE, Skidmore AK, Hussin YA (2009) Allometric equations for estimating the above-ground biomass in tropical lowland Dipterocarp forests. *For Ecol Manag* 257:1684–1694. <https://doi.org/10.1016/j.foreco.2009.01.027>
- Bouillon S, Koedam N, Raman A, Dehairs F (2002) Primary producers sustaining macro-invertebrate communities in intertidal mangrove forests. *Oecologia* 130:441–448. <https://doi.org/10.1007/s004420100814>

- Brassard BW, Chen HYH, Bergeron Y (2009) Influence of environmental variability on root dynamics in northern forests. *Crit Rev Plant Sci* 28:179–197. <https://doi.org/10.1080/07352680902776572>
- Bunt JS (1995) Continental scale patterns in mangrove litter fall. *Hydrobiologia* 295:135–140
- Canham CD, Papaik MJ, Uriarte M, et al (2006) Neighborhood analyses of canopy tree competition along environmental gradients in New England forests. *Ecol Appl* 16:540–554
- Carter M (1973) Ecosystems analysis of the Big Cypress Swamp and estuaries. U Environ Prot Agency Reg IV
- Castañeda-Moya E, Twilley RR, Rivera-Monroy VH, et al (2011) Patterns of root dynamics in mangrove forests along environmental gradients in the Florida coastal everglades, USA. *Ecosystems* 14:1178–1195. <https://doi.org/10.1007/s10021-011-9473-3>
- Chalermchatwilai B, Pongparn S, Patanaponpaiboon P (2011) [No title found]. *ScienceAsia* 37:1. <https://doi.org/10.2306/scienceasia1513-1874.2011.37.001>
- Chambers JQ, Santos JD, Ribeiro RJ, Higuchi N (2001) Tree damage, allometric relationships, and above-ground net primary production in central Amazon forest. *For Ecol Manag* 152:73–84. [https://doi.org/10.1016/S0378-1127\(00\)00591-0](https://doi.org/10.1016/S0378-1127(00)00591-0)
- Chapin FS, Zavaleta ES, Eviner VT, et al (2000) Consequences of changing biodiversity. *Nature* 405:234–242. <https://doi.org/10.1038/35012241>
- Chave J, Andalo C, Brown S, et al (2005) Tree allometry and improved estimation of carbon stocks and balance in tropical forests. *Oecologia* 145:87–99. <https://doi.org/10.1007/s00442-005-0100-x>
- Clark DA, Brown S, Kicklighter DW, et al (2001) Measuring net primary production in forests: concepts and field methods. *Ecol Appl* 11:356–370. [https://doi.org/10.1890/1051-0761\(2001\)011](https://doi.org/10.1890/1051-0761(2001)011)
- Clough B (1998) Mangrove forest productivity and biomass accumulation in Hinchinbrook Channel, Australia. *Mangroves Salt Marshes* 2:191–198
- Clough BF, Dixon P, Dalhaus O (1997) Allometric relationships for estimating biomass in multi-stemmed mangrove trees. *Aust J Bot* 45:1023. <https://doi.org/10.1071/BT96075>
- Clough BF, Scott K (1989) Allometric relationships for estimating above-ground biomass in six mangrove species. *For Ecol Manag* 27:117–127. [https://doi.org/10.1016/0378-1127\(89\)90034-0](https://doi.org/10.1016/0378-1127(89)90034-0)
- Comley BWT, McGuinness KA (2005) Above- and below-ground biomass, and allometry, of four common northern Australian mangroves. *Aust J Bot* 53:431. <https://doi.org/10.1071/BT04162>
- Cormier N, Twilley RR, Ewel KC, Krauss KW (2015) Fine root productivity varies along nitrogen and phosphorus gradients in high-rainfall mangrove forests of Micronesia. *Hydrobiologia* 750:69–87. <https://doi.org/10.1007/s10750-015-2178-4>

- Cox EF, Allen JA (1999) Stand Structure and Productivity of the Introduced *Rhizophora* mangrove in Hawaii. *Estuaries* 22:276. <https://doi.org/10.2307/1352983>
- Das AK, Ramakrishnan PS (1985) Litter dynamics in khasi pine (*Pinus kesiya* Royle ex Gordon) of North-Eastern India. *For Ecol Manag* 10:135–153. [https://doi.org/10.1016/0378-1127\(85\)90018-0](https://doi.org/10.1016/0378-1127(85)90018-0)
- Dawes C, Siar K, Marlett D (1999) Mangrove structure, litter and macroalgal productivity in a northern-most forest of Florida. *Mangroves and Salt Marsh* 3:259–267
- Day JW, Conner WH, Ley-Lou F, et al (1987) The productivity and composition of mangrove forests, Laguna de Términos, Mexico. *Aquat Bot* 27:267–284. [https://doi.org/10.1016/0304-3770\(87\)90046-5](https://doi.org/10.1016/0304-3770(87)90046-5)
- Donato DC, Kauffman JB, Murdiyarso D, et al (2011) Mangroves among the most carbon-rich forests in the tropics. *Nat Geosci* 4:293–297. <https://doi.org/10.1038/ngeo1123>
- Enoki T, Ueda M, Nanki D, et al (2009) Distribution and stem growth patterns of mangrove species along the Nakara River in Iriomote Island, Southwestern Japan. *J For Res* 14:51–54. <https://doi.org/10.1007/s10310-008-0094-4>
- Enoki T, Yasuda K, Kusumoto B (2014) Aboveground net primary production and stand dynamics of mangroves along a river on Iriomote Island, southwestern Japan. *Tropics* 23:91–98. <https://doi.org/10.3759/tropics.23.91>
- Feller IC, Mckee KL, Whigham DF, O'Neill JP (2003) Nitrogen vs. phosphorus limitation across an ecotonal gradient in a mangrove forest
- Finér L, Ohashi M, Noguchi K, Hirano Y (2011) Fine root production and turnover in forest ecosystems in relation to stand and environmental characteristics. *For Ecol Manag* 262:2008–2023. <https://doi.org/10.1016/j.foreco.2011.08.042>
- Fujimoto K, Ono K, Watanabe S, et al (2021) Estimation of probable annual fine-root production and missing dead roots associated with the ingrowth core method: attempt with major mangrove species on Iriomote Island, southwestern Japan, located in the subtropics
- Giraldo Sánchez B (2005) Belowground productivity of mangrove forests in southwest Florida. Doctor of Philosophy, Louisiana State University and Agricultural and Mechanical College
- Gleason SM, Ewel KC (2002) Organic matter dynamics on the forest floor of a Micronesian mangrove forest: an investigation of species composition shifts. *Biotropica* 34:190–198. <https://doi.org/10.1111/j.1744-7429.2002.tb00530.x>
- Golley F, Odum HT, Wilson RF (1962) The structure and metabolism of a Puerto Rican red mangrove forest in May. *Ecology* 43:9–19. <https://doi.org/10.2307/1932034>
- Golley FB, McGinnis JT, Clements RG, et al (1969) The structure of tropical forests in Panama and Colombia. *BioScience* 19:693–696. <https://doi.org/10.2307/1294896>

- Gong WK, Ong JE (1990) Plant biomass and nutrient flux in a managed mangrove forest in Malaysia. *Estuar Coast Shelf Sci* 31:519–530. [https://doi.org/10.1016/0272-7714\(90\)90010-O](https://doi.org/10.1016/0272-7714(90)90010-O)
- Hardiwinoto S, Nakasuga T, Igarashi T (1989) Litter production and decomposition of a mangrove forest at Ohura Bay, Okinawa
- Hendricks JJ, Hendrick RL, Wilson CA, et al (2006) Assessing the patterns and controls of fine root dynamics: an empirical test and methodological review. *J Ecol* 94:40–57. <https://doi.org/10.1111/j.1365-2745.2005.01067.x>
- Hoque AR, Sharma S, Hagihara A (2011) Above and belowground carbon acquisition of mangrove *Kandelia obovata* trees in Manko Wetland, Okinawa, Japan
- Hossain M (2004) Biomass, litter production and selected nutrients in *Bruguiera parviflora* (Roxb.) Wight & Arn. dominated mangrove forest ecosystem at Kuala Selangor, Malaysia. Thesis Dr Philos
- Hossain M, Siddique MRH, Bose A, et al (2012) Allometry, above-ground biomass and nutrient distribution in *Ceriops decandra* (Griffith) Ding Hou dominated forest types of the Sundarbans mangrove forest, Bangladesh. *Wetl Ecol Manag* 20:539–548. <https://doi.org/10.1007/s11273-012-9274-2>
- Imam Maulana S, Wibisono Y, Utomo S (2016) Development of local allometric equation to estimate total aboveground biomass in Papua tropical forest. *Indones J For Res* 3:107–118. <https://doi.org/10.20886/ijfr.2016.3.2.107-118>
- Janssens IA, Sampson DA, Curiel-Yuste J, et al (2002) The carbon cost of fine root turnover in a Scots pine forest. *For Ecol Manag* 168:231–240. [https://doi.org/10.1016/S0378-1127\(01\)00755-1](https://doi.org/10.1016/S0378-1127(01)00755-1)
- Kairo JG, Bosire J, Langat J, et al (2009) Allometry and biomass distribution in replanted mangrove plantations at Gazi Bay, Kenya. *Aquat Conserv Mar Freshw Ecosyst* 19:104–114. <https://doi.org/10.1002/aqc.1046>
- Kamruzzaman M, Ahmed S, Paul S, et al (2018) Stand structure and carbon storage in the oligohaline zone of the Sundarbans mangrove forest, Bangladesh. *For Sci Technol* 14:23–28. <https://doi.org/10.1080/21580103.2017.1417920>
- Kamruzzaman M, Mouctar K, Sharma S, Osawa A (2019) Comparison of biomass and net primary productivity among three species in a subtropical mangrove forest at Manko Wetland, Okinawa, Japan. *Reg Stud Mar Sci* 25:100475. <https://doi.org/10.1016/j.rsma.2018.100475>
- Kamruzzaman M, Osawa A, Deshar R, et al (2017) Species composition, biomass, and net primary productivity of mangrove forest in Okukubi River, Okinawa Island, Japan. *Reg Stud Mar Sci* 12:19–27. <https://doi.org/10.1016/j.rsma.2017.03.004>
- Kamruzzaman M, Sharma S, Kamara M, Hagihara A (2013) Phenological traits of the mangrove *Rhizophora stylosa* Griff. at the northern limit of its biogeographical distribution. *Wetl Ecol Manag* 21:277–288. <https://doi.org/10.1007/s11273-013-9299-1>

- Kamruzzaman M, Sharma S, Rafiqul Hoque ATM, Hagihara A (2012) Litterfall of three subtropical mangrove species in the family Rhizophoraceae. *J Oceanogr* 68:841–850. <https://doi.org/10.1007/s10872-012-0134-8>
- Kangkuso A, Jamili J, Septiana A, et al (2016) Allometric models and aboveground biomass of *Lumnitzera racemosa* Willd. forest in Rawa Aopa Watumohai National Park, Southeast Sulawesi, Indonesia. *For Sci Technol* 12:43–50. <https://doi.org/10.1080/21580103.2015.1034191>
- Kauffman J, Donato D (2012) Protocols for the measurement, monitoring and reporting of structure, biomass and carbon stocks in mangrove forests. Center for International Forestry Research (CIFOR)
- Kauffman JB, Hernandez Trejo H, Del Carmen Jesus Garcia M, et al (2016) Carbon stocks of mangroves and losses arising from their conversion to cattle pastures in the Pantanos de Centla, Mexico. *Wetl Ecol Manag* 24:203–216. <https://doi.org/10.1007/s11273-015-9453-z>
- Kemmitt S, Wright D, Goulding K, Jones D (2006) pH regulation of carbon and nitrogen dynamics in two agricultural soils. *Soil Biol Biochem* 38:898–911. <https://doi.org/10.1016/j.soilbio.2005.08.006>
- Ketterings QM, Coe R, Van Noordwijk M, et al (2001) Reducing uncertainty in the use of allometric biomass equations for predicting above-ground tree biomass in mixed secondary forests. *For Ecol Manag* 146:199–209. [https://doi.org/10.1016/S0378-1127\(00\)00460-6](https://doi.org/10.1016/S0378-1127(00)00460-6)
- Khan MNI, Kabir ME (2017) Ecology of *Kandelia obovata* (S., L.) Yong: A Fast-Growing Mangrove in Okinawa, Japan. In: DasGupta R, Shaw R (eds) *Participatory Mangrove Management in a Changing Climate*. Springer Japan, Tokyo, pp 287–301
- Khan MNI, Suwa R, Hagihara A (2009) Biomass and aboveground net primary production in a subtropical mangrove stand of *Kandelia obovata* (S., L.) Yong at Manko Wetland, Okinawa, Japan. *Wetl Ecol Manag* 17:585–599. <https://doi.org/10.1007/s11273-009-9136-8>
- Khan MNI, Suwa R, Hagihara A (2005) Allometric relationships for estimating the aboveground phytomass and leaf area of mangrove *Kandelia candel* (L.) Druce trees in the Manko Wetland, Okinawa Island, Japan. *Trees* 19:266–272. <https://doi.org/10.1007/s00468-004-0377-0>
- Kihara Y, Dannoura M, Ohashi M (2021) Estimation of fine root production, mortality, and decomposition by using two core methods and litterbag experiments in a mangrove forest. *Ecological Research* 37(1):53–66. <https://doi.org/10.1111/1440-1703.12275>
- Kira T, Ogawa H (1971) Assessment of primary production in tropical and equatorial forests. 309–321
- Kloeppel BD, Harmon ME, Fahey TJ (2007) Estimating aboveground net primary productivity in forest-dominated ecosystems. In: Fahey TJ, Knapp AK (eds) *Principles and Standards for Measuring Primary Production*. Oxford University Press, pp 63–81

- Koch MS (1997) *Rhizophora mangle* L. Seedling Development into the Sapling Stage across Resource and Stress Gradients in Subtropical Florida ¹. *Biotropica* 29:427–439. <https://doi.org/10.1111/j.1744-7429.1997.tb00037.x>
- Komiyama A, Havanond S, Srisawatt W, et al (2000) Top/root biomass ratio of a secondary mangrove (*Ceriops tagal* (Perr.) C.B. Rob.) forest. *For Ecol Manag* 139:127–134. [https://doi.org/10.1016/S0378-1127\(99\)00339-4](https://doi.org/10.1016/S0378-1127(99)00339-4)
- Komiyama A, Jintana V, Sangtiew T, Kato S (2002) A common allometric equation for predicting stem weight of mangroves growing in secondary forests. *Ecol Res* 17:415–418. <https://doi.org/10.1046/j.1440-1703.2002.00500.x>
- Komiyama A, Moriya H, Prawiroatmodjo S, et al (1988) Primary productivity of mangrove forest. *Minist Educ Sci Cult Jpn* 97–117
- Komiyama A, Ogino K, Aksornkoae S, Sabhasri S (1987) Root biomass of a mangrove forest in southern Thailand. 1. Estimation by the trench method and the zonal structure of root biomass. *J Trop Ecol* 3:97–108. <https://doi.org/10.1017/S0266467400001826>
- Komiyama A, Ong JE, Pongparn S (2008) Allometry, biomass, and productivity of mangrove forests: A review. *Aquat Bot* 89:128–137. <https://doi.org/10.1016/j.aquabot.2007.12.006>
- Komiyama A, Pongparn S, Kato S (2005) Common allometric equations for estimating the tree weight of mangroves. *J Trop Ecol* 21:471–477. <https://doi.org/10.1017/S0266467405002476>
- Kusmana C, Sabiham S, Abe K, Watanabe H (1992) An estimation of above-ground tree biomass of a mangrove forest in east Sumatra, Indonesia. *Tropics* 1:243–257. <https://doi.org/10.3759/tropics.1.243>
- Leach GJ, Burgin S (1985) Litter production and seasonality of mangroves in Papua New Guinea. *Aquat Bot* 23:215–224. [https://doi.org/10.1016/0304-3770\(85\)90067-1](https://doi.org/10.1016/0304-3770(85)90067-1)
- Lee SY (1989) Litter production and turnover of the mangrove *Kandelia candel* (L.) druce in a Hong Kong tidal shrimp pond. *Estuar Coast Shelf Sci* 29:75–87. [https://doi.org/10.1016/0272-7714\(89\)90074-7](https://doi.org/10.1016/0272-7714(89)90074-7)
- Liu Y, Xu M, Li G, et al (2021) Changes of aboveground and belowground biomass allocation in four dominant grassland species across a precipitation gradient. *Front Plant Sci* 12:650802. <https://doi.org/10.3389/fpls.2021.650802>
- Lovelock CE (2008) Soil Respiration and Belowground Carbon Allocation in Mangrove Forests. *Ecosystems* 11:342–354. <https://doi.org/10.1007/s10021-008-9125-4>
- Lovelock CE, Atwood T, Baldock J, et al (2017) Assessing the risk of carbon dioxide emissions from blue carbon ecosystems. *Front Ecol Environ* 15:257–265. <https://doi.org/10.1002/fee.1491>
- Lucak M (2012) Measuring Roots. In: Mancuso (ed.), *Measuring Roots*. Springer-Verlag Berlin Heidelberg, pp 363–373

- Luo T, Li W, Zhu H (2002) Estimated biomass and productivity of natural vegetation on the Tibetan plateau. *Ecol Appl* 12:980–997. [https://doi.org/10.1890/1051-0761\(2002\)012\[0980:EBAPON\]2.0.CO;2](https://doi.org/10.1890/1051-0761(2002)012[0980:EBAPON]2.0.CO;2)
- Mackey A (1993) Biomass of the mangrove *Avicennia marina* (Forsk.) Vierh. Near Brisbane, South-eastern Queensland. *Mar Freshw Res* 44:721. <https://doi.org/10.1071/MF9930721>
- McKee KL (2001) Root proliferation in decaying roots and old root channels: a nutrient conservation mechanism in oligotrophic mangrove forests? *J Ecol* 89:876–887. <https://doi.org/10.1046/j.0022-0477.2001.00606.x>
- McKee KL, Cahoon DR, Feller IC (2007) Caribbean mangroves adjust to rising sea level through biotic controls on change in soil elevation. *Glob Ecol Biogeogr* 16:545–556. <https://doi.org/10.1111/j.1466-8238.2007.00317.x>
- McKee KL, Faulkner PL (2000) Restoration of Biogeochemical Function in Mangrove Forests. *Restor Ecol* 8:247–259. <https://doi.org/10.1046/j.1526-100x.2000.80036.x>
- McLeod E, Chmura GL, Bouillon S, et al (2011) A blueprint for blue carbon: toward an improved understanding of the role of vegetated coastal habitats in sequestering CO₂. *Front Ecol Environ* 9:552–560. <https://doi.org/10.1890/110004>
- Mfilinge PL, Meziane T, Bachok Z, Tsuchiya M (2005) Litter dynamics and particulate organic matter outwelling from a subtropical mangrove in Okinawa Island, South Japan. *Estuar Coast Shelf Sci* 63:301–313. <https://doi.org/10.1016/j.ecss.2004.11.022>
- Middleton BA, McKee KL (2001) Degradation of mangrove tissues and implications for peat formation in Belizean island forests. *J Ecol* 89:818–828. <https://doi.org/10.1046/j.0022-0477.2001.00602.x>
- Minagawa M (2000) Japan: Mangrove areas and their utilization
- Mooney HA (ed) (1996) Functional roles of biodiversity: a global perspective. Wiley, Chichester
- Mugasha WA, Bollandås OM, Eid T (2013) Relationships between diameter and height of trees in natural tropical forest in Tanzania. *South For J For Sci* 75:221–237. <https://doi.org/10.2989/20702620.2013.824672>
- Nadelhoffer KJ (2000) The potential effects of nitrogen deposition on fine-root production in forest ecosystems. *New Phytol* 147:131–139. <https://doi.org/10.1046/j.1469-8137.2000.00677.x>
- Nadelhoffer KJ, Aber JD, Melillo JM (1985) Fine roots, net primary production, and soil nitrogen availability: a new hypothesis. *Ecology* 66:1377–1390. <https://doi.org/10.2307/1939190>
- Návar J (2009) Allometric equations for tree species and carbon stocks for forests of northwestern Mexico. *For Ecol Manag* 257:427–434. <https://doi.org/10.1016/j.foreco.2008.09.028>
- Nelson BW, Mesquita R, Pereira JLG, et al (1999) Allometric regressions for improved estimate of secondary forest biomass in the central Amazon. *For Ecol Manag* 117:149–167. [https://doi.org/10.1016/S0378-1127\(98\)00475-7](https://doi.org/10.1016/S0378-1127(98)00475-7)

- Ngomanda A, Engone Obiang NL, Lebamba J, et al (2014) Site-specific versus pantropical allometric equations: Which option to estimate the biomass of a moist central African forest? *For Ecol Manag* 312:1–9. <https://doi.org/10.1016/j.foreco.2013.10.029>
- Ogawa H, Yoda K, Ogino K, Kira T (1965) Comparative ecological studies on three main types of forest vegetation in Thailand. II. Plant biomass. *Nature and Life in South East Asia* 4:
- O’Grady AP, Worledge D, Battaglia M (2006) Above- and below-ground relationships, with particular reference to fine roots, in a young *Eucalyptus globulus* (Labill.) stand in southern Tasmania. *Trees* 20:531–538. <https://doi.org/10.1007/s00468-006-0055-5>
- Ohtsuka T, Negishi M, Sugita K, et al (2013) Carbon cycling and sequestration in a Japanese red pine (*Pinus densiflora*) forest on lava flow of Mt. Fuji. *Ecol Res* 28:855–867. <https://doi.org/10.1007/s11284-013-1067-4>
- Ong J, Gong W, Wong C (1981) Ecological monitoring of the Sungai Merbok estuarine mangrove ecosystem. *Sch Biol Sci Univ Sains Malays Penang*
- Ong JE, Gong WK, Wong CH (2004) Allometry and partitioning of the mangrove, *Rhizophora apiculata*. *For Ecol Manag* 188:395–408. <https://doi.org/10.1016/j.foreco.2003.08.002>
- Osawa A, Aizawa R (2012) A new approach to estimate fine root production, mortality, and decomposition using litter bag experiments and soil core techniques. *Plant Soil* 355:167–181. <https://doi.org/10.1007/s11104-011-1090-6>
- Ostertag R (2001) Effects of nitrogen and phosphorus availability on fine-root dynamics in Hawaiian montane forests. 82:
- Parresol B (1999) Assessing tree and stand biomass: a review with examples and critical comparisons. *Forest Science* 45:573–593
- Peichl M, Arain MA (2007) Allometry and partitioning of above- and belowground tree biomass in an age-sequence of white pine forests. *For Ecol Manag* 253:68–80. <https://doi.org/10.1016/j.foreco.2007.07.003>
- Picard N, Rutishauser E, Ploton P, et al (2015) Should tree biomass allometry be restricted to power models? *For Ecol Manag* 353:156–163. <https://doi.org/10.1016/j.foreco.2015.05.035>
- Poungparn S, Charoenphonphakdi T, Sangteian T, Patanaponpaiboon P (2016) Fine root production in three zones of secondary mangrove forest in eastern Thailand. *Trees* 30:467–474. <https://doi.org/10.1007/s00468-015-1220-5>
- Poungparn S, Komiyama A, Sangteian T, et al (2012) High primary productivity under submerged soil raises the net ecosystem productivity of a secondary mangrove forest in eastern Thailand. *J Trop Ecol* 28:303–306
- Putz F, Chan H (1986) Tree growth, dynamics, and productivity in a mature mangrove forest in Malaysia. *Forest Ecology and Management* 17:211–230

- Ramos E Silva CA, Oliveira SR, Rêgo RDP, Mozeto AA (2007) Dynamics of phosphorus and nitrogen through litter fall and decomposition in a tropical mangrove forest. *Mar Environ Res* 64:524–534. <https://doi.org/10.1016/j.marenvres.2007.04.007>
- Ross MS, Ruiz PL, Telesnicki GJ, Meeder JF (2001) Estimating aboveground biomass and production in mangrove communities of Biscayne National Park, Florida (USA). *Wetl Ecol Manag* 9:27–37. <https://doi.org/10.1023/A:1008411103288>
- Ruess RW, Hendrick RL, Burton AJ, et al (2003) Coupling fine root dynamics with ecosystem carbon cycling in black spruce forests of interior Alaska. *Ecol Monogr* 73:643–662. <https://doi.org/10.1890/02-4032>
- Ryser P (1996) The importance of tissue density for growth and life span of leaves and roots: a comparison of five ecologically contrasting grasses. *Funct Ecol* 10:717. <https://doi.org/10.2307/2390506>
- Saenger P, Snedaker SC (1993) Pantropical trends in mangrove above-ground biomass and annual litterfall. *Oecologia* 96:293–299. <https://doi.org/10.1007/BF00317496>
- Saintilan N (1997) Above- and below-ground biomasses of two species of mangrove on the Hawkesbury River estuary, New South Wales. *Mar Freshw Res* 48:147. <https://doi.org/10.1071/MF96079>
- Santantonio D, Grace J (1987) Estimating fine root production and turnover from biomass and decomposition data: a compartment flow model. *Can J For Res* 17:900–908
- Scheer MB, Gatti G, Wisniewski C, et al (2009) Patterns of litter production in a secondary alluvial Atlantic Rain Forest in southern Brazil. *Rev Bras Botânica* 32:805–817. <https://doi.org/10.1590/S0100-84042009000400018>
- Schmidt M, Kiviste A, Von Gadow K (2011) A spatially explicit height–diameter model for Scots pine in Estonia. *Eur J For Res* 130:303–315. <https://doi.org/10.1007/s10342-010-0434-8>
- Sherman RE, Fahey TJ, Martinez P (2003) Spatial patterns of biomass and aboveground net primary productivity in a mangrove ecosystem in the Dominican Republic. *Ecosystems* 6:384–398. <https://doi.org/10.1007/s10021-002-0191-8>
- Shvidenko AZ, Schepashchenko DG, Vaganov EA, Nilsson S (2008) Net primary production of forest ecosystems of Russia: A new estimate. *Dokl Earth Sci* 421:1009–1012. <https://doi.org/10.1134/S1028334X08060330>
- Smith TJ, Whelan KRT (2006) Development of allometric relations for three mangrove species in South Florida for use in the Greater Everglades Ecosystem restoration. *Wetl Ecol Manag* 14:409–419. <https://doi.org/10.1007/s11273-005-6243-z>
- Smithwick EAH, Lucash MS, McCormack ML, Sivandran G (2014) Improving the representation of roots in terrestrial models. *Ecol Model* 291:193–204. <https://doi.org/10.1016/j.ecolmodel.2014.07.023>
- Sofawi AB (2017) Nutrient variability in mangrove soil: anthropogenic, seasonal and depth variation factors. *Appl Ecol Environ Res* 15:1983–1998. https://doi.org/10.15666/aeer/1504_19831998

- Srisunont C, Jaiyen T, Tenrung M, Likitchaikul M (2017) Nutrient accumulation by litterfall in mangrove forest at Klong Khone, Thailand. *Thammasat Int J Science Technol* 22:9–17
- Steinke TD, Ward CJ, Rajh A (1995) Forest structure and biomass of mangroves in the Mgeni estuary, South Africa
- Suwa R, Analuddin K, Khan MdNI, Hagihara A (2008) Structure and productivity along a tree height gradient in a *Kandelia obovata* mangrove forest in the Manko Wetland, Okinawa Island, Japan. *Wetl Ecol Manag* 16:331–343. <https://doi.org/10.1007/s11273-007-9071-5>
- Suwa R, Deshar R, Hagihara A (2009) Forest structure of a subtropical mangrove along a river inferred from potential tree height and biomass. *Aquat Bot* 91:99–104. <https://doi.org/10.1016/j.aquabot.2009.03.001>
- Suzuki E, Tagawa H (1983) Biomass of a mangrove forest and a sedge marsh on Ishigaki Island, South Japan. *Japanese Journal of Ecology* 33:231–234
- Tam NFY, Wong YS, Lan CY, Chen GZ (1995) Community structure and standing crop biomass of a mangrove forest in Futian Nature Reserve, Shenzhen, China
- Tateno R, Hishi T, Takeda H (2004) Above- and belowground biomass and net primary production in a cool-temperate deciduous forest in relation to topographical changes in soil nitrogen. *For Ecol Manag* 193:297–306. <https://doi.org/10.1016/j.foreco.2003.11.011>
- Tripathi BM, Stegen JC, Kim M, et al (2018) Soil pH mediates the balance between stochastic and deterministic assembly of bacteria. *ISME J* 12:1072–1083. <https://doi.org/10.1038/s41396-018-0082-4>
- Trumbore SE, Gaudinski JB (2003) The secret lives of roots. *Science* 302:1344–1345. <https://doi.org/10.1126/science.1091841>
- Twilley RR, Pozo M, Garcia VH, et al (1997) Litter dynamics in riverine mangrove forests in the Guayas River estuary, Ecuador. *Oecologia* 111:109–122. <https://doi.org/10.1007/s004420050214>
- UNEP (2014) The Importance of mangroves to People. In: van Bochove J, Sullivan E, Nakamura T (eds) A call to action. In: United Nations Environment Programme World Conservation Monitoring Centre, Cambridge. p 128
- Valverde-Barrantes OJ, Raich JW, Russell AE (2007) Fine-root mass, growth and nitrogen content for six tropical tree species. *Plant Soil* 290:357–370. <https://doi.org/10.1007/s11104-006-9168-2>
- Van Do T, Sato T, Saito S, Kozan O (2015) Fine-root production and litterfall: main contributions to net primary production in an old-growth evergreen broad-leaved forest in southwestern Japan. *Ecol Res* 30:921–930. <https://doi.org/10.1007/s11284-015-1295-x>
- Wafar S, Untawale AG, Wafar M (1997) Litter fall and energy flux in a mangrove ecosystem. *Estuar Coast Shelf Sci* 44:111–124. <https://doi.org/10.1006/ecss.1996.0152>

- Wang C, Chen Z, Yin H, et al (2018) The responses of forest fine root biomass/necromass ratio to environmental factors depend on mycorrhizal type and latitudinal region. *J Geophys Res Biogeosciences* 123:1769–1788. <https://doi.org/10.1029/2017JG004308>
- Wang S, Zhou L, Chen J, et al (2011) Relationships between net primary productivity and stand age for several forest types and their influence on China's carbon balance. *J Environ Manage* 92:1651–1662. <https://doi.org/10.1016/j.jenvman.2011.01.024>
- Wang'ondu VW, Bosire JO, Kairo JG, et al (2014) Litter fall dynamics of restored mangroves (*Rhizophora mucronata* lamk. and *Sonneratia alba* sm.) in Kenya. *Restor Ecol* 22:824–831. <https://doi.org/10.1111/rec.12149>
- Warren JM, Hanson PJ, Iversen CM, et al (2015) Root structural and functional dynamics in terrestrial biosphere models – evaluation and recommendations. *New Phytol* 205:59–78. <https://doi.org/10.1111/nph.13034>
- Winterdahl M, Erlandsson M, Futter MN, et al (2014) Intra-annual variability of organic carbon concentrations in running waters: Drivers along a climatic gradient. *Glob Biogeochem Cycles* 28:451–464. <https://doi.org/10.1002/2013GB004770>
- Yashiro Y, Lee N-YM, Ohtsuka T, et al (2010) Biometric-based estimation of net ecosystem production in a mature Japanese cedar (*Cryptomeria japonica*) plantation beneath a flux tower. *J Plant Res* 123:463–472. <https://doi.org/10.1007/s10265-010-0323-8>
- Yoshikai M, Nakamura T, Bautista D, et al (2022) Field Measurement and Prediction of Drag in a Planted *Rhizophora* Mangrove Forest. *J Geophys Res Oceans* 127:e2021JC018320. <https://doi.org/10.1029/2021JC018320>
- Zak DR, Pregitzer KS (1998) Integration of ecophysiological and biogeochemical approaches to ecosystem dynamics. In: Pace ML, Groffman PM (eds) *Successes, Limitations, and Frontiers in Ecosystem Science*. Springer New York, New York, NY, pp 372–403
- Zar JH (2010) *Biostatistical analysis*, 5th ed. Prentice-Hall/Pearson, Upper Saddle River, N.J
- Zhang H, Yuan W, Dong W, Liu S (2014) Seasonal patterns of litterfall in forest ecosystem worldwide. *Ecol Complex* 20:240–247. <https://doi.org/10.1016/j.ecocom.2014.01.003>
- Zhou Y, Su J, Janssens IA, et al (2014) Fine root and litterfall dynamics of three Korean pine (*Pinus koraiensis*) forests along an altitudinal gradient. *Plant Soil* 374:19–32. <https://doi.org/10.1007/s11104-013-1816-8>

Appendix

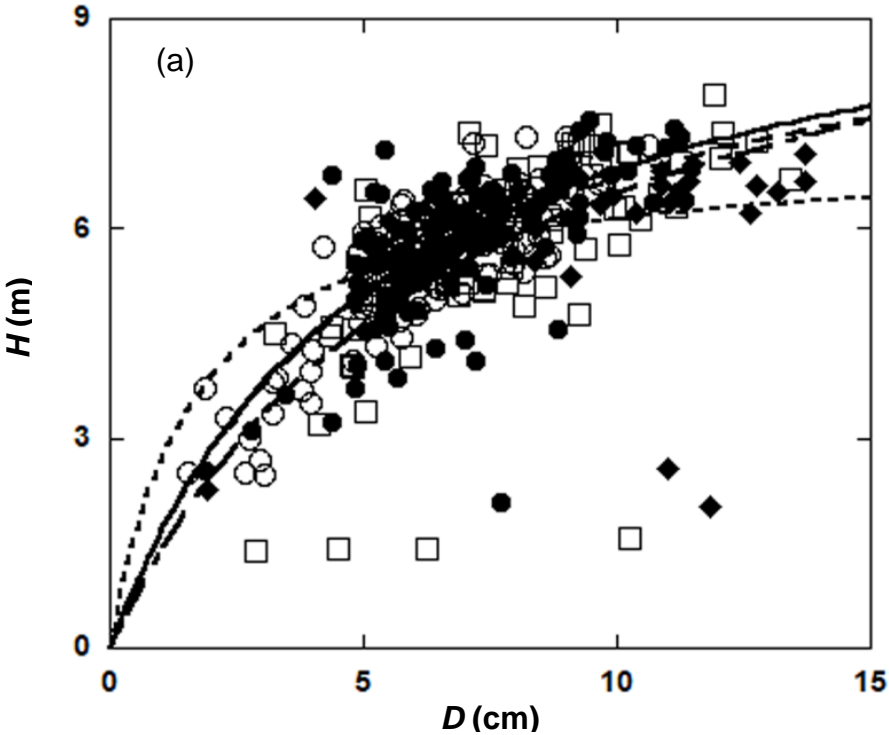


Fig. S3.1 (a)

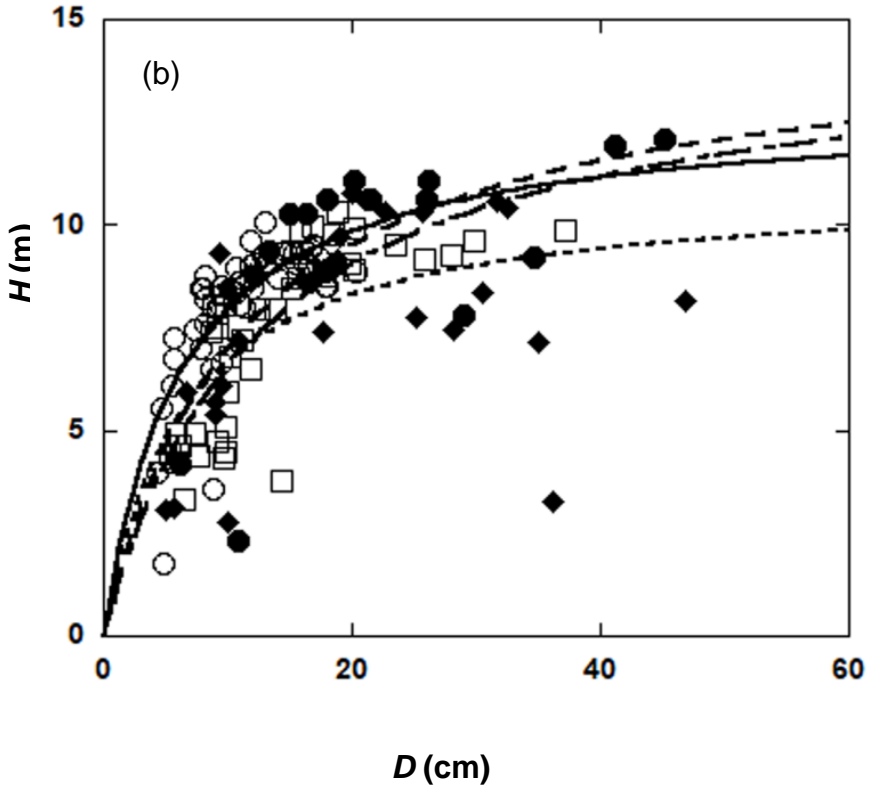


Fig. S3.1 (b)

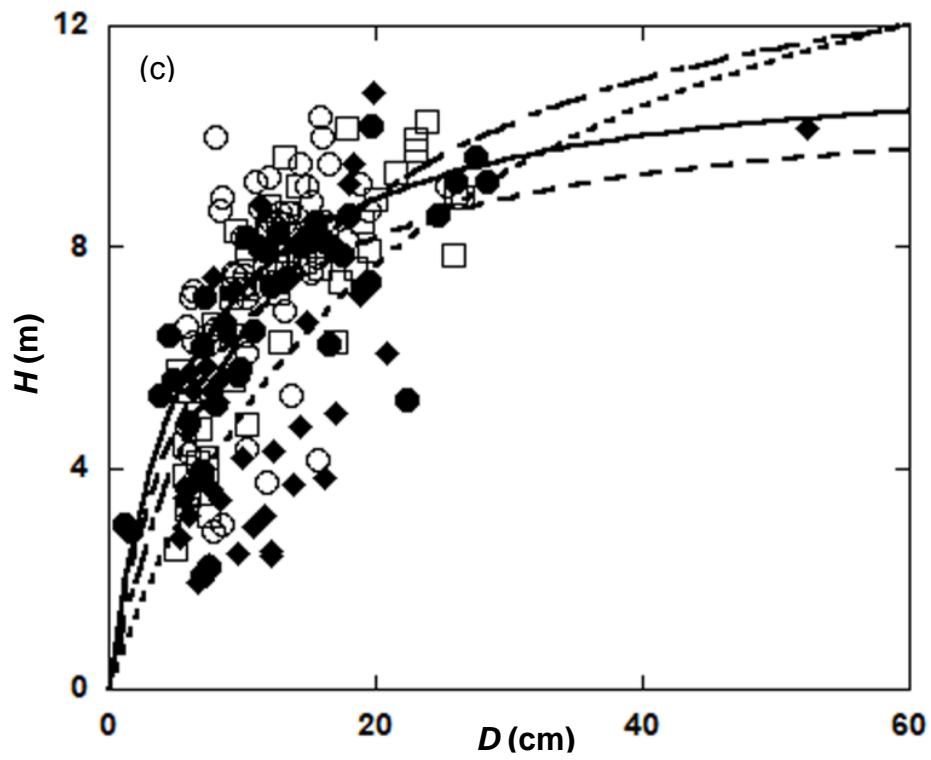


Fig. S3.1 (c)

Fig. S3.1 (a-c): The stem diameter D - height H relationships of a) *R. stylosa* plots, b) downstream *B. gymnorhiza* plots and c) upstream *B. gymnorhiza* plots, respectively wherever each line represents a regression result for each plot based on Eq. 7.



Fig. S4.2

Fig. S3.2: One of the *R. stylosa* plots near the edge of the river. Some of the *R. stylosa* trees were severely damaged.

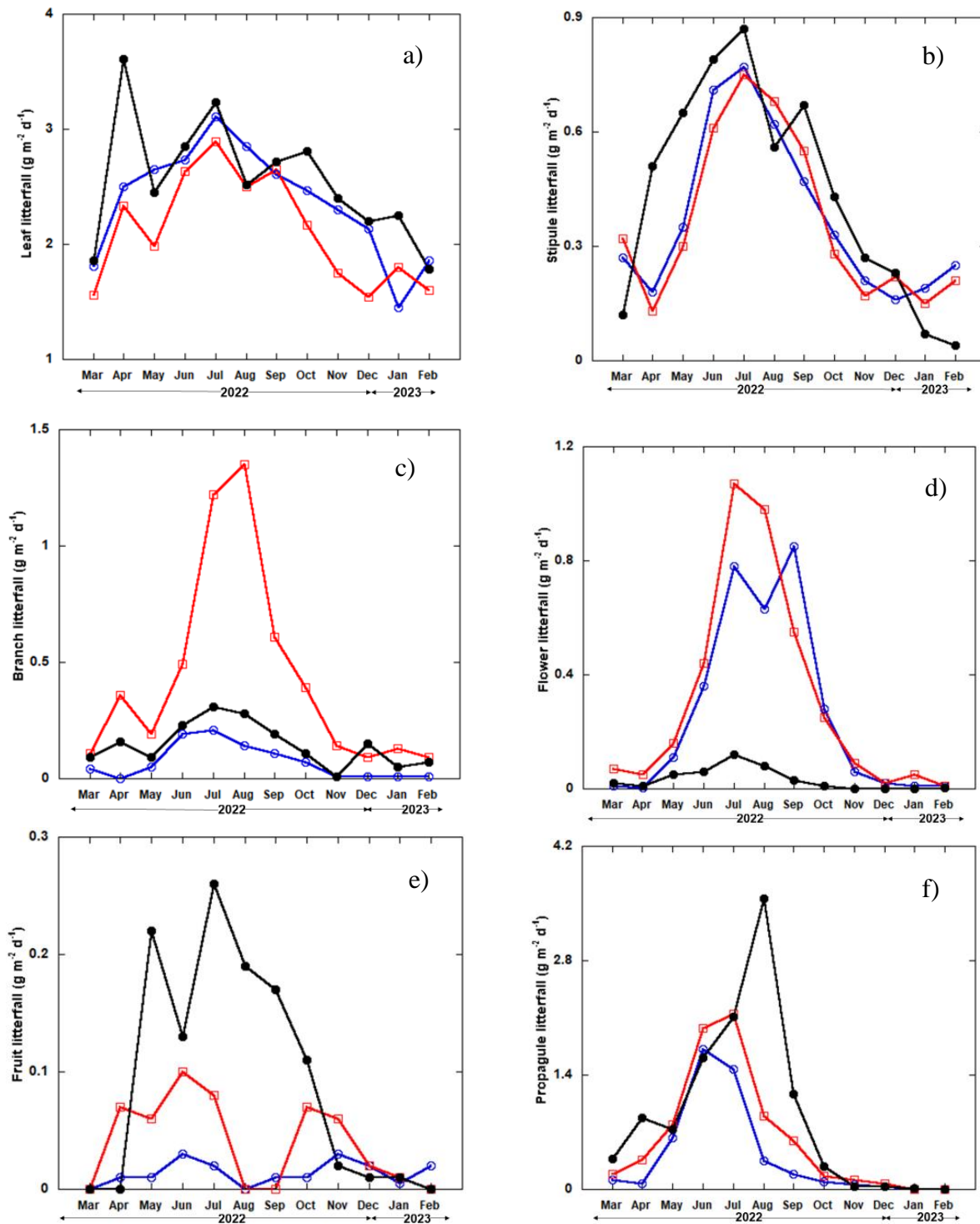


Fig. S4.2: Daily litterfall of a) leaves, b) stipules, c) branches, d) flowers, e) fruits and f) propagules along the Miyara river mangrove. Here blue, red and black lines represent upstream *B. gymnorrhiza*, downstream *B. gymnorrhiza* and downstream *R. stylosa* stands, respectively. Litterfall were collected every 26th and 27th of each month from March 2022 to February 2023.

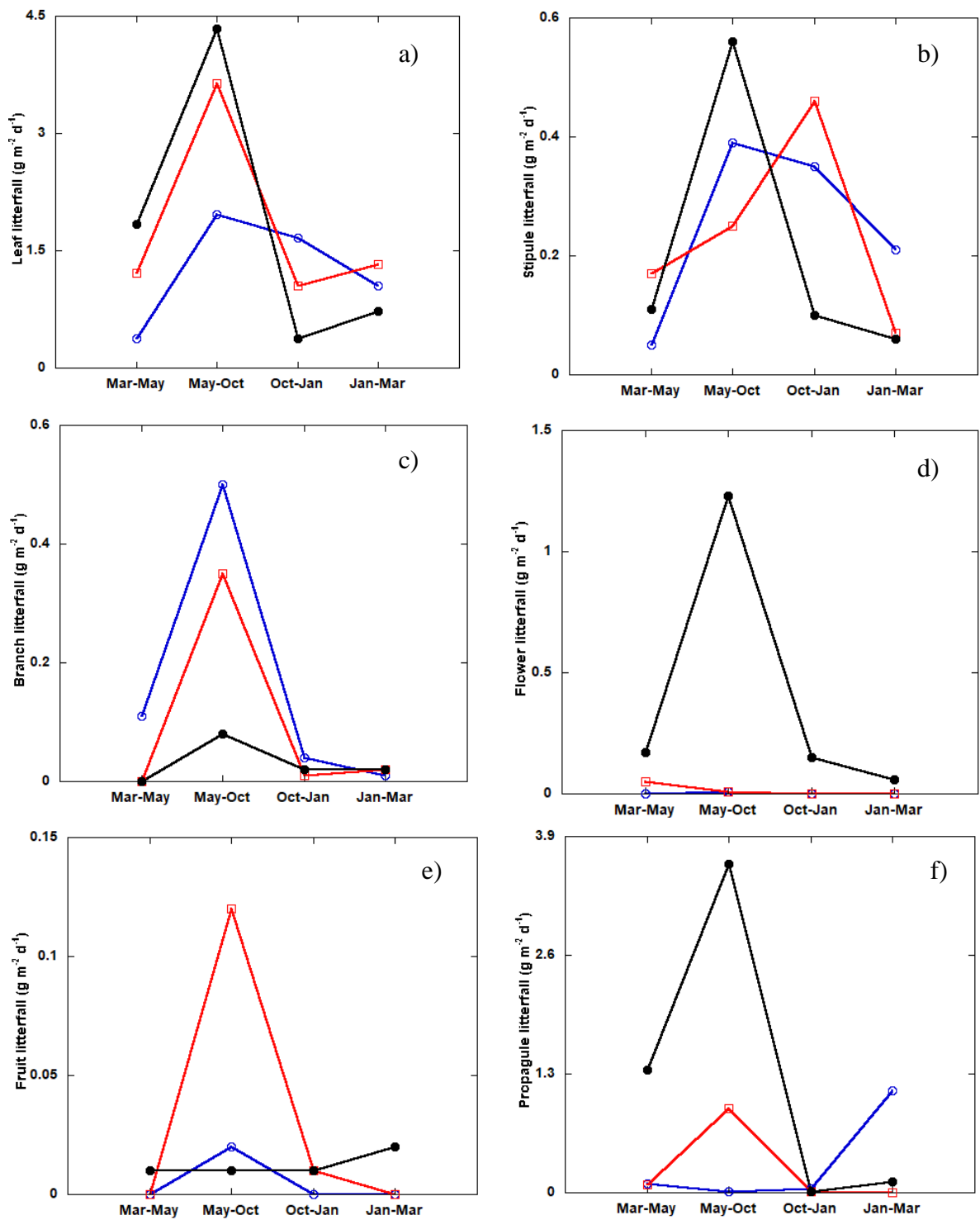


Fig. S4.3: Daily litterfall of a) leaves, b) stipules, c) branches, d) flowers, e) fruits and f) propagules in the Manko Wetland. Here blue, red and black lines represent *K. obovata*, *R. stylosa* and *B. gymnorhiza* plots, respectively. Litterfall were collected on May 18, October 10 in 2019 and January 24 and March 26 in 2020.

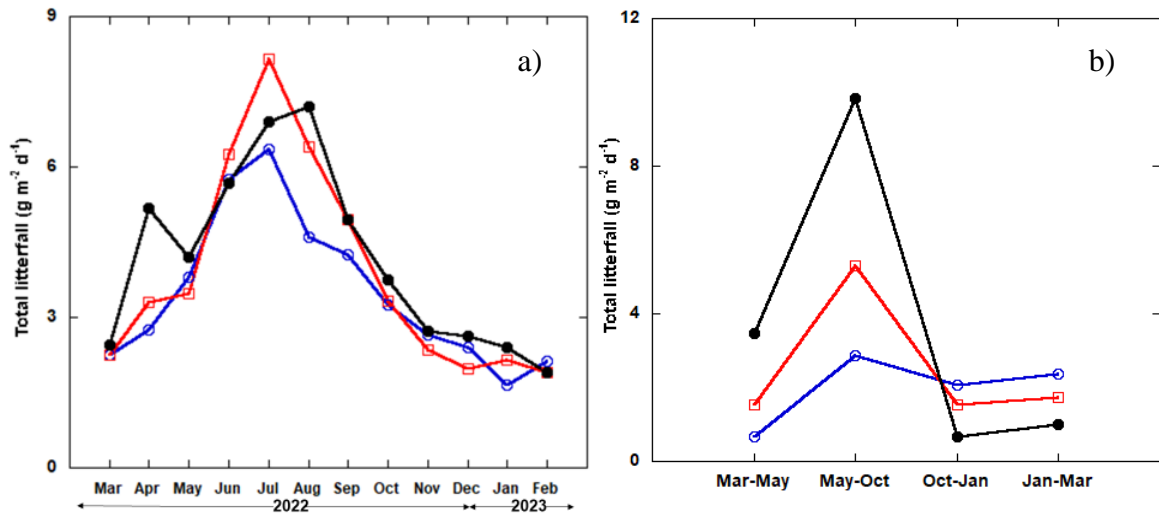


Fig. S4.4: Daily total litterfall a) along the Miyara river mangrove and b) in the Manko Wetland mangrove. Here blue, red and black lines represent in a) upstream *B. gymnorrhiza*, downstream *B. gymnorrhiza* and downstream *R. stylosa* stands, respectively and b) *K. obovata*, *R. stylosa* and *B. gymnorrhiza* plots, respectively.

Table S5.1: Total fine root production ($\text{Mg ha}^{-1} \text{y}^{-1}$) and mortality ($\text{Mg ha}^{-1} \text{y}^{-1}$) of three species in the Miyara River mangrove and three species in the Manko Wetland using sequential core method.

Plot	Location	Total fine root production	Total fine root mortality
		($\text{Mg ha}^{-1} \text{y}^{-1}$)	($\text{Mg ha}^{-1} \text{y}^{-1}$)
<i>B. gymnorrhiza</i> (upstream)	Miyara river, Ishigaki	2.8	1.3
<i>B. gymnorrhiza</i> (downstream)	Miyara river, Ishigaki	5.2	2.5
<i>R. stylosa</i> (downstream)	Miyara river, Ishigaki	5.6	2.9
<i>K. obovata</i>	Manko Wetland, Okinawa	6.5	5.4
<i>R. stylosa</i>	Manko Wetland, Okinawa	2.7	1.3
<i>B. gymnorrhiza</i>	Manko Wetland, Okinawa	3.3	1.1

Table S5.2: Total fine root production, mortality, and decomposition of three species ($\text{Mg ha}^{-1} \text{y}^{-1}$) in the Manko Wetland mangrove. Here, ingrowth core method was used to extract fine root samples.

	Plots		
	<i>K. obovata</i>	<i>R. stylosa</i>	<i>B. gymnorrhiza</i>
Production ($\text{Mg ha}^{-1} \text{y}^{-1}$)	6.07	3.60	4.92
Mortality ($\text{Mg ha}^{-1} \text{y}^{-1}$)	4.24	2.23	2.97
Decomposition ($\text{Mg ha}^{-1} \text{y}^{-1}$)	0.28	0.11	0.19

Acknowledgments

I am very grateful and thankful to my Ph.D. supervisor Associate professor Masako Dannoura for her continuous support, comments and suggestions during preparing the dissertation and for making this research possible. I would like to acknowledge Prof. Daniel Epron who helped me by providing valuable comments and suggestions on arranging the dissertation. I am also very much thankful to my previous supervisor Associate prof. Naoki Okada for his valuable suggestions and comments and for making my field survey possible. Thanks to Rempei Suwa for his presence and suggestions during the field survey. His assistance during the field in Miyara River mangrove increased my ability to understand the ecological significance of this research. A part of this research was financially supported by the Japan International Cooperation Agency (JICA) and Japan Science and Technology Agency (JST) as a part of the project “Comprehensive Assessment and Conservation of Blue Carbon Ecosystems and their Services in the Coral Triangle (BlueCARES)” under the Science and Technology Research Partnership for Sustainable Development Program (SATREPS) and so I am grateful to these authorities. Also, I am grateful to JST through the e-ASIA Joint Research Program for financially supporting the Project “Enhancing Climate Change Resilience of Socio-Ecological Systems in the Coral Triangle and Its Surrounding Areas (EnSES)”. I would also like to thank the personnel of Japan International Research Centre for Agricultural Sciences (JIRCAS) for their support during data collection and the members of the Forest Utilization Laboratory of Graduate School of Agriculture under Kyoto University, Japan for their valuable contribution through comments during seminar. Finally, I am thankful to the professors of Division of Forest and Biomaterials Science for the evaluation of my Ph.D. dissertation.